Exploring the properties of a newly described rotifer-specific biopolymer escpecially in relation to neurotoxic aggregates

Evelin Dobóczky-Balázs

PhD Thesis

Department of Psychiatry

Albert Szent-Györgyi Clinical Center

Faculty of Medicine

University of Szeged,

Supervisor: Zsolt László Datki, PhD

Doctoral School of Clinical Medicine

Szeged

2023

Publications

I. **Balazs E,** Galik-Olah Z, Galik B, Bozso Z, Kalman J, Datki Z, Neurodegeneration-related beta-amyloid as autocatabolism-attenuator in a micro-in vivo system, IBRO Reports, 2020. https://doi.org/10.1016/j.ibror.2020.10.002, MTMT: 31639846, **IF: 0.5**

II. Datki Z, Acs E, **Balazs E**, Sovany T, Csoka I, Zsuga K, Kalman J, Galik-Olah Z. Exogenic production of bioactive filamentous biopolymer by monogonant rotifers, Ecotoxicol Environ Saf 2021. https://doi.org/10.1016/j.ecoenv.2020.111666, MTMT: 31776926, **IF: 7.129**

III. **Balazs E,** Galik-Olah Z, Galik B, Somogyvari F, Kalman J, Datki Z, External modulation of Rotimer exudate secretion in monogonant rotifers, Ecotoxicol Environ Saf 2021. https://doi.org/10.1016/j.ecoenv.2021.112399, MTMT: 32059771, **IF: 7.129**

IV. Datki Zs, **Balazs E**, Galik B, Sinka R, Zeitler L, Bozso Zs, Kalman J, Hortobagyi T, Galik-Olah Z, The interacting rotifer-biopolymers are anti- and disaggregating agents for human-type beta-amyloid *in vitro*, International Journal of Biological Macromolecules, 2022. https://doi.org/10.1016/j.ijbiomac.2021.12.184, MTMT: 32591465, **IF: 8.025**

The cumulative impact factor of the publications directly related to Thesis: 22.783

Abbreviations

AO → acridine orange

ASC → Average Size of Conglomerates

ASIP → Average Size of Inductor Particles

AVOs → acidic vesicular organelles

Aβ → beta-amyloid

Aβ42 → beta-amyloid 1-42

BisANS → 4,4′-dianilino-1,1′-binaphthyl-5,5′-disulfonic acid dipotassium salt

BSA → bovine serum albumin

CA → Covered Area

cAMP → cyclic adenosine monophosphate

CCA → conglomerate covered area

ConA → Concanamycin A

D0 → Day 0

D20 → Day 20

D25 → Day 25

DMSO → dimethyl sulfoxide

DW → distilled water

ED → *Euchlanis dilatata*

ED-RIC → *Euchlanis dilatata* Rotimer-Inductor Conglomerate

EDTA → ethylenediaminetetraacetic acid

EGTA → ethylene glycol-bis(β-aminoethyl ether)-N,N,N′ ,N′ -tetraacetic acid tetrasodium salt

EtOH → etanol

FI → fluorescence intensity

FROS → functionally reversible organ shrinkage

FROSi → FROS index

FTIR → Fourier Transform Infrared Spectroscopy

H-Aβ → human-beta-amyloid

LB → *Lecane bulla*;

LB-RIC → *Lecane bulla* Rotimer-Inductor Conglomerate

LFC → longest filament of conglomerate

MeOH → methanol

NaN_3 → sodium azide

NaOH → sodium hydroxide

NFI% → percentage of normalized fluorescence intensity

NIH → National Institutes of Health

NR → Number of Rotifers

PI → propidium-iodide

RIC → Rotimer-Inductor Conglomerate

RPC → RIC-producing capacity

RPCi → RPC index

S.E.M. → standard error of the mean

S-Aβ42 → scrambled isoform of Aβ

SDS → sodium dodecyl sulfate

SEM → scanning electron microscope

ThT → Thioflavin T

TPEN → N,N,N′ ,N′ -Tetrakis(2-pyridylmethyl)ethylenediami

1. Introduction

Neurodegenerative disorders, such as Alzheimer's disease (AD), could be regarded as phenotypes secondary to the progressive functional impairment of proteomes [1–3]. The molecular basis of brain aging can be described as an accelerated accumulation accompanied by reduced clearance and degradation of misfolded proteins [4]. There is a direct correlation between protein aggregation and age-related pathologies. Intramolecular domains arranged in a β-sheet conformation are highly resistant to enzymatic action [4,5]. The various neurotoxic aggregates, share common features, with their accumulation and aggregation facilitating neurodegeneration, where the aggregation is caused by an abnormal conformational change in related molecules [6]. These dysfunctions occur either extra- or intracellularly [7,8]. Misfolded peptide and protein aggregates can be partially digested by several endogenous enzymes, such as insulin-degrading enzyme (IDE) [9], neprilysin (NEP) [10], endothelin-converting enzyme [11], angiotensin-converting enzyme [12], plasmin [13] and metalloproteinases [7]; beta-myloids, such as Aβs, are central molecules in aging-associated diseases, representing an initial point in the development of dementias. Several types of cell-toxic aggregates are known depending on different cognitive diseases [14], such as Alzheimer's disease (AD), characterized by human-type beta-amyloid 1-42 (H-Aβ) deposits in the brain [15]. Studies with various exogenous Aβ isoforms can be well-known models of Alzheimer's disease, with several case studies using *in vitro* and *in vivo* systems to explore precise effects. Studies are available using human neuroblastoma cells [16,17], rodents, primates, and invertebrates [18–20].

The rotifer is one of the most commonly used microinvertebrate animal models; these animals are excellent models of ecotoxicology, aging, pharmaceutical, or longevity-related research [21–24]. The rotifers are validated models of toxicity screening related to environmental parameters and chemical agents [25]. Rotifers can be grouped into bdelloid and monogonant classes; the two groups differ in morphology and reproduction. Both types are found in the marine environment or freshwater lakes [23]. Rotifers are eutelic multicellular animals of microscopic size, providing a significant part of aquatic biomass [26]. Although their bodies consist of approximately 950-1000 cells, they have complex organ systems, including gastro-intestinal tract, reproductive organs, nervous system, or secretory glands. These organisms are small and multicellular animals with well-defined anatomical features, having a ciliated head, ovaries, masticatory organ (mastax), muscles, digestive, nervous and secretory systems, tactile and tactile and photosensitive organs [27,28] They are promising scientific models due to their optimal culturing requirements [29,30], short lifespan and specific measurable phenotypic

features and viability markers [31]. Despite these facts, only one publication deals with the effects of Aβ on bdelloid rotifers, e.g., *Philodina* species by Poeggeler et al., [17]. A relevant example of this is the phenomenon that some rotifers can exceedingly metabolize (catabolize) the extremly resistant peptide- or protein aggregates (well-known neurotoxins), such as alpha-synuclein, scrapie prions and beta-amyloid (Aβ) under starvation conditions. In an exceptional way, the human-type aggregates are potential nutrient sources to bdelloid rotifers [21]. These animals can use conglomerates and aggregates as an energy source, by their phylogenetically selected ability (**Fig. 1**).

Figure 1. Exceptional in vivo catabolism of neurodegeneration-related aggregate by rotifers [21].

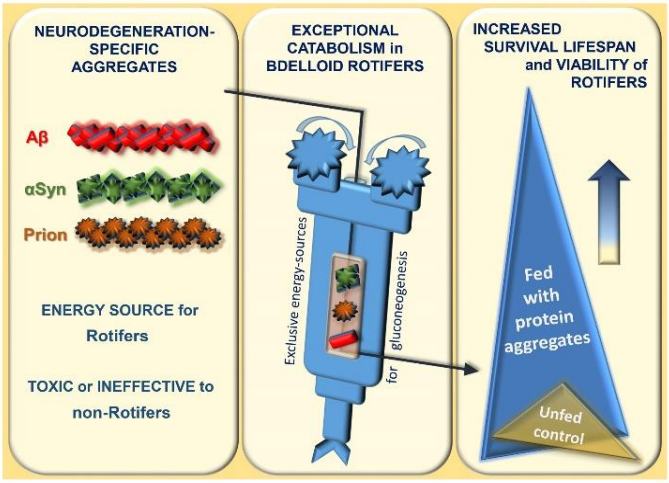

Research related to the association of rotifers and aggregates is a relatively new field; there is no relevant data on Aβ-induced signaling and regulation in these *micro-in vivo* animals. Bdelloids, such as *Philodina or Adineta* species, have high tolerance to normal environmental changes due to their capability of adaptive phenotypic plasticity [29,32,33] Rotifers highly tolerate natural environmental changes; moreover, they are able to survive life-incompatible conditions by halting activities, such as reducing metabolism by suspending active life or egg production [34–36]. The direct connection between anatomical changes (e.g., organ shrinkage) and autophagy has been proved in rotifers [29,37]. Benefiting from these evolutionally developed anatomic and physiologic abilities [38]. Among these evolutionarily conservative organisms, rotifers make up most of the natural biomass; furthermore, their use as modern *micro-in vivo* models has been demonstrated in many interdisciplinary fields, such as neurobiology, drug toxicology, and especially metabolic biochemistry. Due to their specific anatomy and physiology, rotifers have outstanding advantages for breeding and are easy to work with [23]. These creatures are highly resistant to physical environmental changes and successfully adapt to the different types and amounts of nutrients in their natural habitat. The natural decomposition of organic matter is a process that results in the formation of precipitates and aggregates that are potential nutrients for them [39]. The metabolic utilization of all available sources of organic matter is also their special feature. [40].

One of the definitive proofs of the adaptability of these microinvertebrates is their ability to secrete biopolymers [41]. Biopolymers are produced exclusively by living organisms, and these chemical substances are composed of repetitive units that create higher-order molecular structures. They can be grouped based on their chemical structure: polypeptides, polynucleotides, polysaccharides, peptidoglycans, proteoglycans, glycoproteins, and the mixed types of these groups [42,43]. The structural formation of polymers always requires cross-linkers, such as metal ions, e.g., calcium [44]. The earliest known adhesive biopolymer is described by Aristotle, called byssus, produced by a marine mollusk, *Pinna nobilis*. This substance is barely studied in biochemistry, material science, biomedicines, and biomimetics. The variety of biopolymers is shown by the fact that different animals are able to secrete versions with other functions depending on their lifestyle and environment. The adhesive capability depends on the various types of attachment which can be permanent, transitory, temporary, and instantaneous [45]. Their enzyme resistance or sensitivity strongly correlates with their basic structure, for example, polypeptides can be degraded by proteases, such as trypsin or proteinase K [46]. Due to the favorable properties of these natural materials, such as antimicrobial [47,48] or hypoglycemic activities [49], they are used in multiple fields for pharmaceutical [50], medical [51], or industrial purposes [52,53]. As the eco-friendly approach becomes dominant in industrial developments, the relevance of biopolymers gains more importance due to their biodegradable, renewable and environmentally friendly nature [54]. These natural agents are applied in environmental protection, agriculture, food-, pharmaco- and energetic industries [50].

Since biopolymers are also involved in degradation processes in the natural habitat [55]; therefore, they may influence the conglomeration and aggregation processes. Several biopolymers can affect the polymerization or precipitation of different types of organic materials and molecules [56]. Thus, it is worth studying the prevention and possible inhibition of peptide and protein aggregation processes. Beneficial effects of these exudates have also been studied in medicine. A representative example for this technical translation is the gold nanoparticles, coated with dextrin or chitosan, which can inhibit insulin amyloid fibrillation in a complex form [57]. These biopolymer-coated artificial particles interact with insulin monomers and prevent the formation of dimers and oligomers. In addition, the polysaccharide β-D-glucan and carboxymethylated derivatives could also block platelet aggregation [58]. In addition to various compounds, numerous proteins complexes (e.g., heat shock types) can attenuate the aggregation of different monomers [59]. Because biopolymers are biocompatible, biodegradable and have low immunogenicity, they are promising theoretical sources in

biomedicine [60], even in neurobiology. There are several natural molecules (e.g., collagen, gelatin, heparin or chitosan) that are the bases of artificial products available in clinical application [61]. Furthermore, many plant-based biopolymers (e.g., cellulose) can also be used as medical engineering constructs due to their excellent physical and biochemical properties. These agents are suitable as therapeutic molecules in drug and gene delivery [62].

Biopolymers are scientific hotspots for which researchers have been recently gaining more academic interest [51]. The investigation of the function, nature, and applicability of biopolymers is a significant branch of biology nowadays [63]. The list of these natural and multifunctional materials is long; moreover, all of them have a unique characteristic, making it necessary to study them individually.

Many studies deal with biopolymers, but we found no relevant data in the literature about the secretion of monogonant or bdelloid rotifer biopolymers. At the same time, they are characterized by outstanding biological diversity, with many new properties and phenomena waiting to be explored. The goal of our research team is to learn as much as possible about the natural characteristics of these animals.

2. Specific aims

The physiological development of neurodegenerative diseases is the consequence of the accumulation of toxic aggregates in the brain. During our previous research, our group discovered a unique phenomenon, according to rotifers, as micrometazoans, which are able to metabolize various neurotoxic aggregates, including human-specific beta-amyloid, and consume them as food. Our main goal was an explorative investigation of the background of this ability.

Specific aims:

1. Further investigation of the exceptional catabolic ability of rotifers, understanding of the interaction between animals and neurotoxic beta-amyloid.
2. The theoretical interpretation of the background mechanism of the above-mentioned capability, the assumption of the existence of a special molecule that helps the degrading enzymes and modifies the aggregated structures.
3. Searching for biomolecules secreted by rotifers (consisting of approximately 1000 cells but with complex organs), finding presumed exudates.
4. Development, testing, validation, and application of methodologies and tools necessary to implement pioneering interdisciplinary experiments.
5. Explorative examination of the potentially founded biomolecules, produced in relatively large quantities, both alone (e.g., bioactivity, environmental regulation) and together with targeted human-type aggregates (molecular interactions).
6. Setting up a complex theory to explain the unique ability of rotifers regarding the catabolism of toxic aggregates.

3. Material and methods

3.1. Materials

The cultures of rotifers were kept in standard culture flasks (# 430168). The nutrient solution, standard medium content (mg/L) were: Ca^{2+} 31.05; Mg^{2+} 17.6; Na^{+} 0.9; K^{+} 0.25; Fe^{2+} 0.001; HCO_3^{-} 153.097; SO_4^{-} 3; Cl^{-} 0.8; F^{-} 0.02; H_2SiO_3 3.3 (pH=7.5) [31]. For standard food cultures: homogenized yeast (*Saccharomyces cerevisiae*; EU-standard granulated instant form, #2-01-420674/001-Z12180/HU); algae (*Chlorella vulgaris*; BioMenu, Caleido IT-Outsource Kft.; #18255), which was heat-inactivated and filtered (Whatman filter with 10 μm pore; 6728-5100).

The Aβ42 and its scrambled isoform (S-Aβ42: LKAFDIGVEYNKVGEGFAISHGV AHLDVSMFGEIGRVDVHQA) were prepared at the Department of Medical Chemistry, University of Szeged, Hungary. The concentrations of the stock solutions were 1 mg/mL in distilled water; the aggregation time was 3h (25 °C, pH 3.5); the neutralization (to pH 7.5) was performed with NaOH (1 N) [64,65]. The final concentrations of Aβ were 100 μg/mL. For *in vivo* investigations we applied Concanamycin A (ConA; 27689, 50 nM), 4,4′-dianilino-1,1′-binaphthyl-5,5′-disulfonic acid dipotassium salt (BisANS, D4162; 50 μM), propidiume-iodide (PI, 81845; 5 μM;), AO (13000; 15 μM) and NR (N4638; 50 mM) fluorophoores obtained from Sigma-Aldrich, USA.

From Sigma-Aldrich: bovine serum albumin (BSA; #A-9418); sodium spermidine (#S2626), Calcein-AM (#17783), Proteinase K (#P-6556), Potassium bromide (#221864), Triton X-100 (#X-100), dimethyl sulfoxide (DMSO; #D8418), ethylenediaminetetraacetic acid (EDTA; #E9884), ethylene glycol-bis (β-aminoethyl ether)-N,N,N′,N′-tetraacetic acid tetrasodium salt (EGTA; #E8145), N,N,N′,N′-Tetrakis(2-pyridylmethyl)ethylenediamine (TPEN; #P4413), acetic acid (#695092), SH-SY5Y human neuroblastoma cell line (#94030304), Whatman filter (pore diameter was 2 μm; #6783-2520); from Merck: ultra-powdered Carmine crystals (Natural Red 4; #2233), sodium azide (NaN_3; #822335), methanol (MeOH; #1.07018.2511), glycerol (#1.04092.1000), hydrochloric acid (HCl; #1.00317.1000), distilled water (DW; Millipore Ultrapure); Dynabeads M-270 epoxy (Life Technologies AS, #14301); from Reanal: sodium dodecyl sulphate (SDS; #24680-1-0833), sodium hydroxide (NaOH; #24578-1-01-38), urea crystals (#08072), micro-cellulose (#D-76); from Biochrom HG: trypsin (Seromed, #L2103), Collagenase II (Seromed; 252 U/mg; #L6723); from Corning or Corning-Costar: 24-well plate (#3524), 96-well plate (Nunc; #167008), Petri dish (#430167), flasks (#430168); standard plastic web (pore diameters was 15 and 50 μm); EtOH (Molar Chemicals Kft.; #02911-481-430). The glass coverslip (diameter was 12 mm, thickness: 0.15 mm; #89167-106) was

purchased from VWR International. The human type beta-amyloid 1-42 (Aβ42; #A14075) was obtained from AdooQ Bioscience LLC., USA.

From Sigma-Aldrich: ascorbic acid (#A1300000), catechin (#C-1788), glucose (#47829), taurine (#T0625), cyclic adenosine monophosphate (cAMP; #A9501), ethyl nicotinate (#E40609); from Merck: powdered Carmine crystals (Natural Red 4; #2233), glycerol (#1.04092.1000); distilled water (DW; Millipore SAS, Direct-Q 3 UV, ultrapure; type 1; Molsheim, France); different pH-calibrated media (Mettler Toledo SevenEasy pH meter, Switzerland, InLab 413; #Z654272); from Reanal: NaCl (#14064-1-38), KCl (#30080), LiCl (#12033), $CaCl_2$ (#11024), $MgCl_2$ (#232-094-6), $SrCl_2$ (#19066), ethylenediaminetetraacetic acid (EDTA; #9884), choline chloride (#11222); from KRKA Novo Mestro: Lucidril (meclofenoxate hydrochloride; #5812-67/721/1-63); from Other Pharmacy: Selegiline (#903871-2G); from Cambridge Research Biochemicals: isoguvacine (#PE7097); from Molecular Probes: Fluo-3 (cell impermeable calcium-specific fluorescent dye; #F3715); from Corning or Corning-Costar: 24-well plate (#3524), from Greiner Bio-One GmbH: specific 96 well plate (half area, #675101); Petri dish (#430167), flasks (#430168); universal plastic web (pore diameter: 50 μm); Acrodisc 13 filter, Low Protein Binding (pore diameter: 0.2 μm; #4454) from Gelman Sciences.

Materials used to study the interaction between RIC and Aβ: the applied fluorescent dyes were obtained from Sigma-Aldrich: 4,4′-dianilino-1,1′-binaphthyl-5,5′-disulfonic acid dipotassium salt (Bis-ANS, #D4162) and Thioflavin T (ThT; #T3516); from Merck: distilled water (DW; Millipore Ultrapure); from Life Technologies AS: DynaMag-2 magnet (#12321D); Dynabeads M-270 superparamagnetic epoxy beads (#14301); from Greiner: 96-well microplate with half-area (#675101, Greiner Bio-One International); from Corning: treated (#430293) and non-treated (#430591) Petri dishes; Whatman filter with 10 μm pore (#6728-5100); universal plastic web (pore diameter: 50 μm); conductibility (20 °C): 428 μS/cm.

Human-type beta-amyloid 1-42 (H-Aβ; #A14075, human Amyloid b-Peptide 1-42; #107761-42-2) was obtained from AdooQ Bioscience LLC., USA. The scrambled Aβ (S-Aβ; LKAFDIGVEYNKVGEGFAISHGVAHLDVSMFGEIGRVDVHQA) were prepared at the Department of Medical Chemistry, University of Szeged, Szeged, Hungary [64]. The peptides used for treatment were synthesized on Fmoc-Ala-Wang resin, with Nα-Fmoc-protected amino acids, using a CEM Liberty microwave peptide synthesizer (Matthews, NC, USA). The protocol for producing amyloid aggregates: the dose of the different beta-amyloid (H-Aβ and S-Aβ) stock solutions was 1 mg/mL, dissolved in DW. The aggregation time was 3 hours (3h) or 3 days (3d) alone or together with Rotimer-Inductor Conglomerate (RIC) at 24 °C (pH 3.5). The

neutralization (to pH 7.5) was performed with NaOH (1 N; [64,65]). At the end of the aggregation process the samples were vortexed (5 min; 600 rpm) and before using their stock solutions, they were ultrasonicated (Emmi-40 HC, EMAG AG, Mörfelden-Walldorf, Germany) for 10 min at 45 kHz to achieve semi-sterilization and homogenization. After 20x dilution with standard medium, the working concentration of Aβs were 50 μg/mL.

3.2. Rotifers

3.2.1. Origin of animals

During measurements were carried out on invertebrate bdelloid rotifers, *Philodina acuticornis* and *Adineta vaga* species; therefore, no specific ethical permission was needed according to the current international regulations. They come from Hungarian aquavaristics from an agricultural farm in Szarvas. The species were maintained for six years under standard laboratory conditions.

Further the experiments were performed on microinvertebrate monogonant rotifers *Euchlanis dilatata* and *Lecane bulla*; thus, according to the current international regulations, no specific ethical permission was needed. The animals were obtained from Red Cross Lake (GPS coordinates: 46° 16′ 25″ N; 20° 08′ 39″ E; early summer) in Szeged (Southern Great Plain, Hungary). They have been maintained in a standardized laboratory environment for years. The measurements were carried out in accordance with globally accepted norms: Animals (Scientific Procedures) Act, 1986, associated guidelines, EU Directive 2010/63/EU for animal experiments, and the National Institutes of Health instructions for the care and use of Laboratory animals (NIH Publ. No. 8023 from 1978). Animal studies comply with the ARRIVE guidelines. The *P. acuticornis, A. vaga, E. dilatata* and *L. bulla* are maintained as permanetly cultures in our micrometazoa-based *micro-in vivo* laboratory.

3.2.2. Identification of pieces

The species collected were *E. dilatata, Ehrenberg, 1832; L. bulla, Gosse, 1851; Lepadella patella, O. F. Muller, 1773; Colurella adriatica, Ehrenberg, 1831; Itura aurita, Ehrenberg, 1830; Trichocerca iernis, Gosse, 1887; Brachionus leydigii rotundus, Rousselet, 1907; Brachionus calyciflorus, Pallas, 1766; Cephalodella intuta, Myers, 1924; Synchaeta pectinata, Ehrenberg, 1832* which were monitored (DSLR-Nikon D5100, NEF-RAW, ISO 100, 16 MP; Nikon Corp., Japan) under inverted microscope (at 65X and 400X magnification; Leitz Labovert, Germany). Serial images were taken at every 5-μm levels yielding a total of 5-10 photographic layers per animal, which were merged into one superimposed picture (by using PS CS3 software, Adobe Systems Inc., USA) to achieve high resolution. The entities were

paralyzed with carboxygenated (5% CO_2) standard medium for 5 min during photo recordings. After the species were identified based on methods described in academic literature [66–70], species-specific information (e.g., body size in relation to age) was applied to collect relatively mature individuals (generally with an egg in their body). Rotifers were collected, harvested and isolated (using manual micropipette) to create monoclonal populations. After completing the experiments, *E. dilatata, L. bulla* and *C. intuta* were maintained as standard cultures of our laboratory.

3.2.3. Animal culturing

All tested rotifers are cultured in flasks (#430168, 25 cm^2 area) at 23°C, under diffused light, in the standard medium nutrient solution. Nutrient change takes place every second day, carefully pouring off the medium and then filling the flask with 40 ml of medium nutrient solution. Feeding is also done every other day with a mixture of algae and yeast, filtered after suspension so that particles of uniform size are obtained, of which the animals receive 140 µl. As a finishing touch, we use a light microscope (with magnification) to check the number of individuals, the size of individuals, and the substratum.

3.2.4. Harvesting of animals

The first step in isolating *E. dilatata* and *L. bulla* is to filter rotifers from flasks (more vigorous shaking). Filtration is performed with a double filter (1st filter: 500 µm Ø; 2nd filter: 80 µm Ø (pore diameter). First, soak the 2nd filter in a high-walled petri dish for a few seconds in 70 ml of clean nutrient solution. Then the filter is washed back in a high-walled petri dish with 30 ml with standard medium, using a syringe (1200 ± 50 rotifers/ 55 cm^2, 30 ml).

The process of isolating *P. acuticornis* and *A. vaga* is first picking up the substrate with a pipette, then transferring the bdelloids to a well plate. The process is followed by a 1-2 min wait for the bdelloids to adhere to the bottom of the well-plate. Afterward, the medium is removed from the well plate, and then the well is filled with a clean solution.

3.2.5. Metabolism-related *in vivo* experiments

The metabolism-related measurements in monitoring the size of the germovitellaria in the presence of glucose (1 mM) started on Day 0 (D0), providing a reference control. After twenty days (day 20; D20) of starvation and five days (day 25; D25), organ regeneration was shown. On D20, one-time feeding (600 µg/mL yeast homogenate) was applied and followed-by five days of recovery. The treatment protocol was performed on a “one house rotifer” (one animal per well) in a 96-well plate. Each fluorescence experiment contained 150 ± 30 rotifers per well. The investigated rotifer populations have sufficient individuals to ensure a similar and equal size distribution. Entities were photographed under a light inverted microscope (Leitz Labovert

FS). The two separate germovitellarium were digitally colored blue. The shrinking process with functional (egg production) regeneration capacity was named "functionally reversible organ shrinkage" (FROS). To investigate (n = 5, well) the amount of protein in the animals, BisANS was applied [71] parallelly with detecting the total amount of nucleic acid, where PI was used [72] after 10 min incubation and washing. No subtraction occurred, but marking and measurements were performed directly on the animals. Extinction/emission was 405/520 nm for BisANS and 530/620 nm for PI, measured with a microplate reader (NOVOstar, BMG, Germany). In AVOs-detection methods, we used a slightly modified version of Kang et al. [73]. The AO and the NR labellings were performed under the same conditions as the BisANS and PI applications. These two applied dyes were used in different wells, but the parameters and number of animals were the same. The extinction/emission of AO was 480/520 nm in green and 480/620 nm in red. The wavelengths of NR were 540/630 nm in red and 450/590 nm in yellow. To inhibit the autolysis-related processes, ConA was added to the wells on D0. The percentage of normalized fluorescence intensity (NFI%) was calculated from the ratio of fluorescence data divided by the number of rotifers in each well. In the experiential monitoring of FROS, each data (=36; individual one-housed rotifer/well) sums the whole (bilateral) size of the germovitellaria in one individual. The organs were circled by using a freehand tool (allowing to create irregularly shaped selections) in ImageJ program (64-bit for Windows, [74]). The scale bar was 20 μm. To demonstrate the functional recovery of the reproductive organs, the number of laid eggs was counted after the regeneration phase (from D20 to D25). The species-specific egg production without treatment was determined after five days under normal breeding conditions as a reference control.

3.3. Rotimers

3.3.1. Biopolymers and their conglomerates

3.3.1.1. Induction

Many marine species, such as the phylum of *Mollusca, Echinodermata*, or *Arthropoda*, are capable of biopolymer secretion [41]. In addition, the microinvertebrate rotifer is also suitable for biopolymer production, namely, 'Rotimer.' The first step in inducing Rotimer secretion is to harvest monogonant populations (1200 ± 85 individuals) from the culturing flasks by selective filtration of animals with a plastic web (pore size 50 μm) into surface-treated Petri dishes (55 cm^2 area). The rotifers did not feed at this time; their stomachs were empty on the second day after feeding. This precaution was necessary to avoid contamination of Rotimer solution with their faeces.

Secretion occurs only when the cilia of the rotifer are mechanically irritated with inert particles of various types and sizes. Inductors can be **a.** yeast: heat inactivated cell skeleton; **b.** BSA: heat-denatured (den-BSA; 80 °C, 20 min, solved in DW); **c.** epoxy: metal beads coated with polymers; **d.** Carmine: mechanically powdered crystals (with electric coffee grinder); **e.** urea: ultrapowdered crystals; **f.** cellulose: powdered micro-cellulose. The final (working) concentration of the administered inductors of Rotimer-secretion was 50 μg/mL, diluted from 1 mg/mL stock solution. Rotimer production capacity also varies depending on the type of inductor used **(Fig. 4)**. To monitor the nonspecific adhesion of the inducers to the well surface, the media-containing particles (without Rotimer and rotifer) were decanted from the wells. Then the passively covered area was a maximum of 1% in these blind (rotifer-free) tests. Secretion of particle-induced biopolymer resulted a 'Rotimer-Inductor Conglomerate' (RIC) in a high-density web form after 20 min incubation time (**Fig. 2K-M**; with yeast inductor).

After carefully removing the well solution, these RIC products were desiccated (dried) at room temperature (25 °C) and at 40% humidity in the dark for 30 min. We also used this high-resolution preparation method, observing the Rotimer fibers and the glue-like format (**Fig. 2L**; with epoxy inducer). Inducer particles were used in sizes below 2 μm (the Carmine was filtered with a Whatman filter) or above 50 μm (filtered with a plastic mesh), where they could not induce Rotimer secretion and RIC formation. RIC samples detected by light microscopy were photographed, and the images were converted to black-and-white graphic format (8-bit; threshold; 2.04 pixels, equivalent to 1 μm). These images were analyzed with ImageJ program (Wayne Rasband, USA), extracting data related to the conglomerate-covered area (%) and the average size (μm^2) of this complex.

The RIC analysis was used to select the best RIC-producing species using the yeast as an inductor (**Fig. 3A**) related to RIC-producing capacity (RPC); furthermore, the RPC was also applied for screening different Rotimer inductors (**Fig. 3B**) and rotifer-influencing factors (**Fig. 5**; with epoxy inductor). Yeast cell skeleton (as a natural particle) was applied as a common inductor in species-specific RIC production measurements (**Fig. 3A**). The yeast homogenate, aside from using it as an inductor, compiled two-third of the standard nutrient in the case of all species. The entities kept in Petri dishes were treated in populations during RIC production experiments (**Fig. 5A**), then they were rinsed twice by standard medium. The treated and tested animals (20 rotifers per well) were selected, and their RIC production was monitored. During repeated inductions, there were 10-minute breaks between treatment rounds (20 minutes/case). After each round, the same rotifers were carefully transferred with a micropipette to a new well to initiate the next cycle. These measurements, together with the starvation experiments, were

performed under total nutrient depletion, to attenuate the biopolymer synthesis in animals. The NaN_3 (20 μM) and spermidine (50 μM) treatments were carried out after 100x dilutions from stock solutions. During the pH (6 or 8) and salt-ion amount (0 or 1 g/L) studies, the working (final) concentrations were provided by moving the supernatant instead of the dilution. Supplemented composition of standard medium to 1 g/L dose was implemented by adding extra $NaHCO_3$. Epoxy beads were applied as an inductor in these experiments, because the RPC index (in statistics) of this agent proved to be the best (**Fig. 4**). To assess the sublethal dose of NaN_3, the swimming speed (465 ± 22 μm/sec in normal case) of rotifers was monitored as a viability marker to measure its dose-response to NaN_3.

3.3.1.2. Regulation

We examined the production of Rotimer under various environmental factors, such as temperature, pH, metal ions, and different pollutants, the two species examined during the experiment were *E. dilatata* and *L. bulla*. Every measurement was performed in standard environment (24 °C, pH = 7.5, 40% air humidity, in standard media and 12:12 hours dark-light), except for the actual parameter of interest or the optimized experiments (for *E. dilatata*: 22 °C, pH = 7.8; for *L. bulla* 25 °C, pH = 7.2). The experimentally applied animals were isolated by pouring them into Petri dishes (55 cm^2 area). In all experiments (n = 24, well; in all groups) related to rotifer-specific biopolymer, 20-22 mature (with maximal body size or with an egg inside) entities were applied in a 24-well plate (1.8 cm^2 well-area) with 1 mL working volume per well.

The influence of changing environmental parameters (temperature and pH) and the treatment with various agents (20 μM) lasted for 10 hours with a constant number of unfed animals. These RIC-influencing agents were the follows: ascorbic acid, Lucidril, DMSO, catechin, glycerol, glucose, cAMP, spermidine, ethyl nicotinate, taurine, selegiline, isoguvacine and choline. The diffrent media with various pH values (from 6.5 to 8.2) were made freshly before all relevant experiments.

The animals were let to rest (washed) in DW for 30 min before being applied in metal salts (100 mg/L) related experiments. These salts were the follows: NaCl, KCl, LiCl, $CaCl_2$, $MgCl_2$ and $SrCl_2$. These tests were carried out with a constant number of unfed rotifers after a 10-fold dilution from stock solutions. The RIC induction was initiated with mechanically ultra-powdered water insoluble Carmine crystal particles after 5 min treatment with different metal-salts.

The RIC-analysis is a slightly modified adaptation of the method applied by Datki et al. [75]. The working concentration of the Carmine inductor of Rotimer-secretion was 50 µg/mL which was diluted from stock solution (2 mg/mL). The Carmine-induced biopolymer formed RIC in a high-density web structure after 30 min incubation time. After removing the well solution by pipette, these RIC products were desiccated (dried) at room temperature (24 °C) and at 40% humidity in darkness for 60 min. The special particles were used above the size of 50 µm (filtered with standard plastic web). All manipulations were performed slowly and carefully to avoid fluid flow destroying the exudate web.

The pattern of RIC was monitored by light microscopy (Labovert FS; 65x magnification). The photos (Nikon D5100, 16 MP RAW and ISO 100) were converted in a black and white graphical format (threshold, 2.04 pixel = 1 µm, 408 pixel = 0.2 mm and 8-bit). These photos were analyzed with the ImageJ program (Wayne Rasband, USA), extracting data on the area (%) covered by the complex conglomerate of this biomolecule.

The RIC's most extended filament was detected under an inverted microscope, with 25x magnification, using a calibrated square grid, parallel layering, and plate holes. The longest straight thread with two anchor points in the web of the RIC (in all relevant wells) was measured (in mm).

The relative change in the calcium ion level in the rotifer medium was detected using a plate reader-based fluorescence technique. The external $CaCl_2$ concentration in the current media was 5 mg/L (45 µM), supplemented with 205 mg/L NaCl; therefore, the total salt concentration was equivalent with the standard medium. In these measurements, the cell-impermeant and calcium-specific Fluo-3 (stock solution: 1 mg/mL; working concentration: 50 µM) was used. Low $CaCl_2$ concentration provided 0.9:1 calcium: dye ratio, since without free dye surplus the potential alterations cannot be detected precisely.

The rotifer-free samples (0.15 mL) were filtered with Acrodisc 13 filter (pore diameter 0.2 µm) from the respective well-media (1 mL) of applied 24-well plates. The maximal calcium-specific signal did not decrease in the presence of Carmine in this animal-free setup. The labeling interval with Fluo-3 was 10 min at room temperature in the dark. The readings were carried out in a 96-well half-area plate, applying NOVO star micro-plate-reader (BMG Labtech, Germany). The volume was 95 µL/well, and the medium was supplemented with 5 µL Fluo-3 (1 mM stock solution). The extinction/emission was set at 500/530 nm and the number of flash/well/cycle was 30. Before the first turn, orbital shaking was applied where the shaking time was set at 3 sec and the plate-rounds were 600/min. The gain adjustment was normalized to the background of the dye-free solution. This blank was 650 relative unit, 1% of the

maximum fluorescence intensity with dye and without calcium (210 mg/L NaCl). Fluorescence intensity of the Fluo-3 increased about 14-15-fold after calcium binding (reference samples: 100% relative unit, without animals and Carmine). Standardised conditions (except for the calcium dose) were applied to both species in photometric measurements.

3.3.2. Isolation of conglomerates

In the case of the Carmine inductor used during Rotimer production, we first draw off the medium with the help of a 5 ml pipette, which is attached to the base of the petri dish wall at an angle of 45 °C. The RIC attached to the bottom of the petri dish is then picked up and homogenized with 4 ml of DW. Then the rotifers remaining in the solution are removed by filtration using a funnel. Next, filtration is carried out directly into a 2 ml eppendorf, followed by centrifugation (35000 g/12 min; 4 °C), carefully removing the supernatant and maximizing the pellet volume in 150 µl DW. When using epoxy beads, the first steps until the removal of rotifers are the same as when using the Carmine inductor mentioned above. A solution free of animals but containing RIC was then prepared at room temperature, and the exudate-coated beads were reversibly fixed using a DynaMag-2 magnet. Finally, the supernatant was removed with a micropipette, and the RIC pellet was washed once with DW and resuspended in 150 µl of water. This conglomerate solution was used for all types of measurements.

3.3.3. Storage of conglomerates

The Rotimer-Inductor Conglomerate is stored in a 500 µL eppendorf supplemented with 150 µL DW at -70 °C.

3.3.4. Biochemical investigation of Rotimers

3.3.4.1. Analysis of Rotimer with FTIR spectroscopy

The FTIR spectroscopy method [76] was used for the biochemical analysis of Rotimer in order to perform measurements, Rotimer containing RIC samples were prepared. As a first step, *E. dilatata* (n = 500 ± 30 individuals) populations were harvested into Petri dishes (55 cm^2 area). Then, the inductor (Carmine) was added to the rotifer-containing standard medium for 20 minutes. The produced RIC was mechanically homogenized by a pipette. The animals were removed by filtration using a plastic web (pore size 50 µm). The animal-free, but RIC-containing solution was then centrifuged by 4000 x g for 20 minutes (in 14 mL volume centrifuge tubes) at room temperature. The supernatant was decanted, and the pellet was used for FTIR measurements.

The concentrated RIC solution (15 µL) was dropped onto the surface of potassium bromide pastilles (200 mg, 13 mm diameter) three times, which were compressed with hydraulic press

(Specac Inc., UK). The pastilles were then desiccated for 48 hours in silica gel filled desiccator. The FTIR spectra of various samples were measured with a Thermo Nicolet Avatar 330 FTIR spectrometer (Thermo Fisher Scientific Ltd., Waltham, MA, USA) using a Transmission E. S. P. accessory applying 128 scans at a resolution of 4 nm. Data were collected with EZ OMNIC software, while spectrum analysis was performed with Spectragryph 1.2.13 (Friedrich Menges, Obersdorf, Germany) software. A strong shift of baseline was observed due to the beam scattering on the undissolved or recrystallized Carmine particles. Furthermore, due to the low signal intensities, resulted by the low sample concentrations, the presence of negative peaks was observed in the 2800-3000 cm^{-1} CH stretching region. It was also resulted by the uncompensated background signal of hydrophobic protective coating on the optical elements of the spectrometer. These artificial distortions and the uncompensated CO_2 signals in the region of 2280-2390 cm^{-1} were cut off from the spectrum prior to baseline correction. To compensate the effect of beam scattering two step baseline correction, simple linear correction, followed by a secondary adaptive correction (coarseness = 10) was applied prior to the analysis.

3.3.4.2. The Rotimer detection with scanning electron microscope (SEM)

Rotimer formations (glues and fibers) appeared undetectable under inverted light microscopy; therefore, analysis was performed with a scanning electron microscope (**Fig. 2**; SEM). For this series of experiments, the best and smallest stimulator, epoxy, was used (50 µg per mL) to induce Rotimer secretion and RIC formation in the most prolific species, *E. dilatata*. The RIC was produced on a round glass coverslip which was washed with 96% EtOH, DW and finally with standard medium before being experimented in 24-well plates (one coverslip/well/30 mature rotifer). The rotifers produced RIC for half our on the coverslip under standard conditions; then, they were carefully removed manually by a micropipette. The glass surface covered by RIC was monitored by a light microscope, then desiccated at room temperature for one h. The samples were coated with ionic gold. The preferred areas (based on their quality) were subjected to SEM (Zeiss EVO MA 10, Germany). The sample-carrier coverslip was fixed onto a stub using carbon tape. The coverslips were coated with gold using a Quorum Q150R sputter coater for two min. The fine structure of the RIC was observed and photo-documented with the SEM at different magnifications (from 846X to 40.47KX). The detections were operating at 10 kV with an 8-mm working distance, using a secondary electron detector in high vacuum mode. The white balance of SEM photographs was normalized.

3.3.4.3. Chemical influence on the integrity of RIC web

During our work, we examined the influencing role of various chemical substances on the dissolution of Rotimer *in vitro*. Before investigating the inductor-cohesive-stability of Rotimer

to reveal the structure of RIC (**Fig. 5B**; Carmine inductor, except of NaOH, where it was Epoxy), the animals were carefully removed by a micropipette. Then, the well-content was supplemented by the 10x concentration of treatment agents (enzymes, solvents, chelators, alcohols, and pH-solutions). These RIC-influencing-factors were the followings: normal supernatant media of rotifers, trypsin (1%), Proteinase K (0.5 mg/mL), Collagenase II (3 mg/mL), Triton X-100 (1%), SDS (1%), DMSO (70%), EDTA (0.1 M), EGTA (0.1 M), TPEN (0.1 M), EtOH (70%), MeOH (70%), Glycerol (70%), HCl (1 M), acetic acid (70%) and NaOH (1 M). Doses were applied at the highest level recommended by the manufacturers. All interventions were performed slowly and carefully to avoid fluid flow disruption in the RIC mesh. The disruption of the fiber (mechanical resistance against fluid flow) was measured under the microscope (25X magnification) using the removed and transferred micro-pipettor (at 45° angle, 3 mm from RIC web) of the micro-plate reader (NOVOstar, BMG, Offenburg, Germany). The RIC-stability was provoked by max. 230 µL/sec flow velocity (injected volume: 50 µL) where the fibers tore.

3.3.5. Biological investigation of Rotimers activity

3.3.5.1. *In vivo* bioactivity

Viability tests related to the bioactivity of Rotimer were first performed *in vivo*. In all viability-related experiments (Table), based on Calcein-AM (stock solution: 1 mg/mL in DMSO; final concentration was 5 µM), the labeling interval was 1h at room temperature in the dark. The viability (cell-fluorescence) and motility (movement of cells) of algae and yeast cells (**Fig. 14**) were measured in separate 24-well plates. Confluent cell population (120 ± 11 cells/well) was applied in cytoplasmic calcium detection where the fluorescence intensity (FI) of intracellularly trapped Calcein (ex. 490, em. 520; calibration/gain adjustment was 1% of the maximal relative intensity) was detected. Separate cells (4-5 cells/well) were administered in motility-related investigations. After 24h treatment with RIC (used inductor: den-BSA) and its reference controls (untreated or only den-BSA treated), the FI of intracellular calcium-specific dye and the moving action in different setups were measured, in the latter case the detection interval of cell motility was 10 min (unit: µm/min).

To test the physiologic effects of the examined RIC (containing Rotimer) in vitro, we applied the SH-SY5Y neuroblastoma cells. The viability (fluorescence) and motility (cell migration) of SH-SY5Y cells were separately measured in 96-well plates. The FI of intracellular Calcein was detected after 24h treatment with den-BSA or its RIC in a cell culture with confluent monolayer (cell number was 110 ± 8 in one well). Detection interval in cell motility assay (4-5 cells/well) took for 6h (unit: µm/h) after one-day-treatment.

3.3.5.2. *In vitro* molecular interactions

A further biological activity-related study of the molecular interaction of RIC and H-Aβ was carried out under in vitro conditions. During this investigation, the inductor (epoxy-metal beads; 200 μL vortexed stock solution with a dose of 6 mg/mL concentration) of Rotimer secretion was added to the rotifer-containing standard medium (30 mL in Petri dishes) for 2 hours. Based on the manufacturer's product description of the Dynabeads M-270, 1 mg of these beads can bind approximately 10 ± 2 μg of ligands (in this case the Rotimer); however, 6 mg of beads from one induction can theoretically bind about 50-60 μg Rotimer onto their surface if they are widely covered. Calculating with this amount of biopolymer, the working concentration of Aβs was determined to be 50 μg/mL. The RIC production by rotifers were monitored under light microscope (at 63x magnification; Leitz Labovert FS, Wetzlar, Germany).

During the investigation, we first used a stagogram-based optical method. Then, after a short time (5 min) of incubation, the interaction between mixed monogonant-specific RIC (6 mg Rotimer-coated epoxy beads per mL) and three hours (3h) or three days (3d) Aβ aggregates was investigated. The beads were isolated with a magnet, in the previously described way. After discarding the supernatant, the pellet was washed and resuspended in 150 μL DW. Drops (n = 10) with 1 μL volume were put onto nontreated hydrophobic plastic surface of Petri dish, then they were dried for 1h at 40% humidity.

The formed stagograms of the drops (**Fig. 15**) were detected by light microscopy and were photographed (Nikon D5600, 25 MP, RAW/NEF, 14 bit; Nikon Corp., Kanagawa, Japan). The digital pictures were converted in a black and white graphical format with greyscale (threshold; 2.46 pixel = 1 μm; 8-bit). Maximum measured area of the drops was 1.68 mm^2. These images (total area of this complex) were analyzed with ImageJ program (Wayne Rasband, USA) and the related extracting data of the conglomerate-covered area (%) and the average size (μm^2) were presented.

Other methods were Bis-ANS- and ThT-based fluorescent assays. The amyloid-sensitive Bis-ANS and ThT dyes were applied in fluorescent-based in vitro (animal-free) experiments (n = 12 wells/sample type) including investigations on: quick molecular interaction (**Fig. 16**) and on anti-aggregation (**Fig. 17A**) or disaggregation (**Fig. 17B**). The final dose of the dyes was 50 μM. In these interaction-specific experiments, the 3h or 3d Aβ aggregates (final concentration 50 μg/mL) were mixed with RIC (6 mg epoxy beads/mL), similarly to the stagogram protocol, where the incubation time was only 5 min. The free Aβ-containing supernatants and the RIC-Aβ pellets were measured separately. Bis-ANS was used for 3h samples, while ThT was preferred in the case of 3d ones. In the anti-aggregation study, the H-Aβ-stock solution (1

mg/mL) and the concentrated RIC (120 mg epoxy/mL) were incubated together during the whole aggregating period (3d). The H-Aβ and RIC stock solutions were also incubated together for 12h in the case of disaggregation experiments and the measurements were also performed. In these cases, the Rotimer containing RIC-Aβ mixes were not separated to pellet and supernatant, their fluorescent intensity was together recorded by applying the fluorescent dyes alternately. The dose ratio of Aβs and the theoretically calculated Rotimer was 1:1 in each study.

Samples containing the investigated molecules were measured with a BMG NOVOstar micro-plate reader (BMG Labtech, Ortenberg, Germany) at ex/em: 405/520 nm on Bis-ANS and 450/480 nm on ThT, using a 96-well plate with half well area (100 μL/well). The number of laser flashes per well was 30 and the orbital shaking (3 sec and 600 rpm) was applied before each detection. Calibration/gain adjustment was 1% of the maximal relative intensity, where the blank of the relevant fluorescent dye was about 650. The labelling time of the samples with the dyes took 5 min before starting detection.

3.3.6. Rotimer-related depletion

The potential role of Rotimer against Aβ42 aggregates was investigated in four different species (**Fig. 22**; *E. dilatata; L. bulla; C. intuta; S. pectinata).* Concentration of Aβ42 stock solution was 1 mg/mL (DW) with 3h (25 °C, pH 3.5) aggregation period. Neutralization (to pH 7.5) of this solution was performed with NaOH (1 N). After 10-fold dilution with standard medium, the final (working) concentrations were 100 μg/mL. After harvesting, 30 ± 2 mature rotifers per well (n = 24 well/species in 96 well-plate) were treated in 0.2 mL volume. The treatment period was 5 days in standard conditions (24 °C; 40% air humidity; standard media). The depletion protocol was performed before the Aβ42 was administered and this protocol was in line with the one applied in **Fig. 5A**-treatment (Every Aβ42-treated group had its own untreated control, which was the reference (100%) in every case. Two parameters of viability were measured, namely the number of rotifers alive and the intracellular esterase activity (indicated by relative fluorescence intensity of Calcein-AM). The populations were observed under light microscope (63X) combined with digital camera (Nikon D5100). The protocol of Calcein-AM measurements was the same with the one applied in **Fig. 14.**

3.4. Statistics

The error bars show the standard error of the mean (S.E.M.). Next, the one-way ANOVA was applied for statistical analysis, followed by the Bonferroni *post hoc test*. The homogeneity and normality of the data were checked, and they were found suitable for ANOVA followed by

Bonferroni post hoc test. The different levels of significance are indicated as follows: $p^{*, \#} \leq 0.05$, $p^{**, ¤¤} \leq 0.01$, $p^{***, ###, ¤¤¤} \leq 0.001$ and $p^{****} \leq 0.0001$ (all marks are defined in the given figure legend).

4. Results

4.1. The Rotimer-Inductor Conglomerate

4.1.1. Production

The rotifer-specific biopolymer, namely Rotimer, was first described in the literature by our research group. This exudatum was observed in six (**Fig. 2A-F**) different monogonants: *E. dilatata, L. bulla, L. patella, I. aurita, C. adriatica* and *T. iernis*. All animals studied are often found in lakes or other natural bodies of water. Rotimer is a special biomolecule complex that is vital for the survival of the animals that produce it (water purification, egg laying, and food trapping). After constant laboratory cultivation, *E. dilatata* and *L. bulla* proved to have the six investigated species' most intensive RIC production capacity (RPC). Representative photo (**Fig. 2K**) about RIC formation produced by *E. dilatata* was taken.

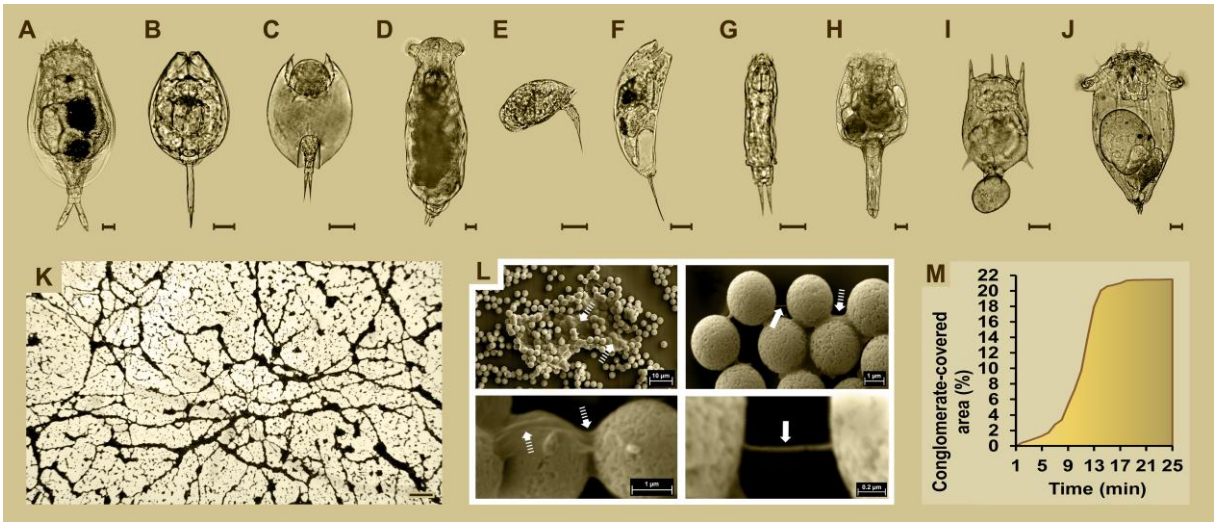

Figure 2. Presentation of the rotifers and the rotifer-specific biopolymer (Rotimer). *The representative photos of monogonant rotifer species (A-F) are shown. The species used in experiments related to Rotimer-related biomaterial (scale bar: 20 µm): E. dilatata, A; L. bulla, B; L. patella, C; I. aurita, D; C. adriatica, E; T. iernis, F; C. intuta, G; B. leydigii rotundus, H; B. calyciflorus, I; S. pectinata, J. The representative figure shows the network structure of the "Rotimer-Inductor Conglomerate" (RIC) formed by E. dilatata, K (scale bar: 200 µm). The SEM photos (L) show different occurrences of Rotimer after epoxy induction (scale bar: 0.2 and 1 µm). Regular arrows indicate the filamentous form, while dashed arrows indicate the glue-like structure. The kinetics of RIC production (M) was measured by the saturation (%) of the area covered by RIC as a function of time (minutes).*

We observed RIC formations in the original medium of wild-type animals collected from their natural habitat, meaning they can produce Rotimer in nature. Secreted Rotimer alone was not detectable by light microscopy; therefore, its existence could only be proven by adhesion to particles, as we did not detect the refraction of Rotimer between two inductor particles (1000X magnification). To try to optically visualize this biopolymer, different types of dyes (Trypan blue, Light green SF, Methylene blue, Acridine orange, Orange G, Neutral red, Fuchsine, Coomassie brilliant blue R-250 or G-250, Ponceau S, Bromophenol blue, Congo red, Luxol fast blue and Methyl red) were tested, diluted in DW or EtOH, but no success was gained in labelling them. The filaments drawn by *E. dilatata* monogonants are fragile (33 ± 3 nm in cross-section) and can only be observed only by SEM. Secretion of Rotimer could be mechanically induced by approximately 2.5 to 50 μm diameter particles, respectively in *E. dilatata.* No RIC production was observed above or below this range. Biopolymers are secreted very quickly (4 μm/sec) and bind to the surface of the inducers. The secreted exogenic Rotimer (**Fig. 2L**) can either be filamentous (arrow) or gluelike (dashed arrow). In addition to the size, the induction of Rotimer production does not depend on the quality properties of the particles; they must only have a chemical charge. Therefore, the coverage of the area covered by the conglomerate increased exponentially as time progressed, which is also well exemplified in the kinetics of RIC production by *E. dilatata* (**Fig. 2M**). The saturation of the confluent layer on the given surface took 18-20 minutes in standard medium. In the case of bdelloids, similarly to monogonants, we experienced filamentous formations; we observed the coating with nutrient particles and the adhesion of their eggs to the bottom of the flask. The existence and presence of the Rotimer are visually indicated by the formation of RIC, which is viscoelastic, filamentous, floating in liquid (3D form), and can be destroyed with water jets. Rotifers can find the web-formation from a relatively high distance in their dimensions by directional approaching; therefore, it is assumed that the fiber has a specific surface, which can be recognized by them. One of the most extended filaments produced was 1.3 mm (floating in the aqueous medium between two connected ends).

Rotimer was secreted by six different rotifers (**Fig. 3A**) and this product was investigated to assess which species could be the most effective producers under yeast induction. Representative photos from RIC show how rotifers create webs of different shapes. Furthermore, Rotimer inducers of various sizes were tested on the species *B. leydigii rotundus, C. intuta, S. pectinata,* and *B. calyciflorus*, but no production of structured filamentous material was found. During the quantitative characterization of the RIC, we observed the average size of the conglomerates and the percentage of the covered area. *E. dilatata* showed a significantly

high value in both cases, so this species became the best RIC-forming type. The next step was to find out whether there were other nontoxic inductors which might have been more effective than yeast (**Fig. 3B**). The potential candidates were tested and the average particle size (μm^2; excluding the adhesive Rotimer) were also determined: den-BSA, 165; epoxy, 7.5; Carmine, 50; urea, 83; cellulose, 75; as opposed to the reference yeast, 45.

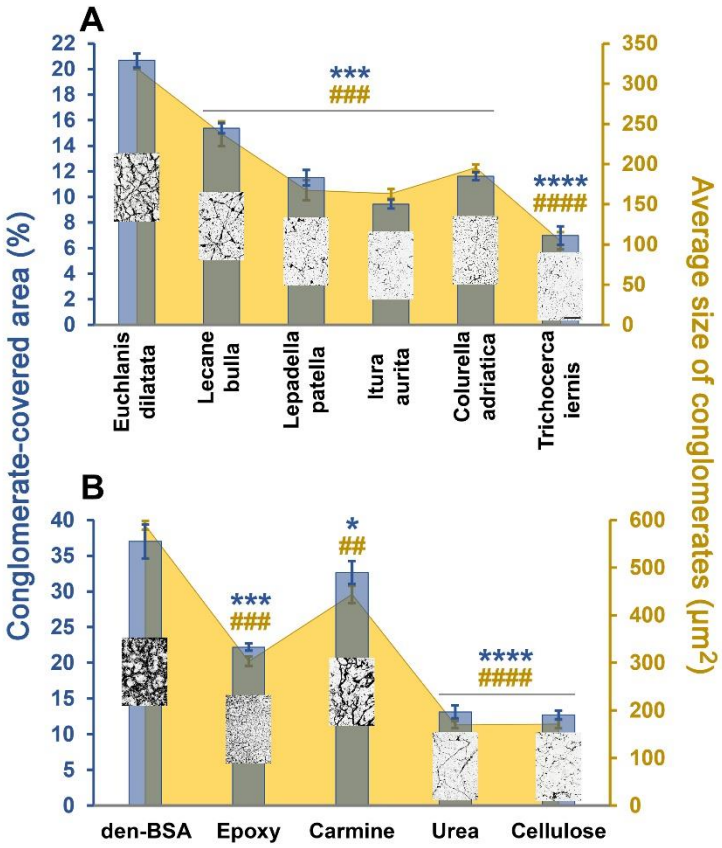

Figure 3. Rotifer- and inductor-specific production of RIC. *Monogonants with different RIC-producing capacity (A) and the impacts of inductors on the web format (B) are presented by the conglomerate-covered area (%; blue) and the average size of RIC (μm^2; yellow). The species-specific webs of RIC are shown by the representative photos on each column (scale bars: 500 µm). The Rotimer-inductors were investigated on the most productive E. dilatata (B), where the indikative pictures of the inductor-specific RIC fibers are presented on the columns (scale bars: 0.5 mm). The investigated agents were denatured bovine serum albumin (denBSA), epoxy beads, Carmine, urea, and cellulose. The error bars represent S.E.M. One-way ANOVA with Bonferroni post hoc test was used for statistical analysis, the levels of significance are p***, ### ≤ 0.001 (*, significant difference from E. dilatata (A) and from denatured-BSA (B) in conglomerate covered area; # significant difference from E. dilatata and from denatured-BSA (B) in average size of conglomerate). The black line above the bars means they are all equally important.*

Most tested inducer types could induce Rotimer secretion, which manifests in RIC formation. The result of this is shown in the representative photos. The induction process is not specific to the particle but depends only on chemical charge and size. The den-BSA-Rotimer mesh showed the highest formation value regarding the average size of conglomerates and the area covered by conglomerates. The Carmine and the epoxy beads were also applied in further experiments. The urea and cellulose were able to induce RIC production; however, their efficiency was much lower than that of the other inductors.

The particles showed differences in size, but these parameters alone were insufficient for a comprehensive characterization. We developed the RPC index to solve this task. This quantified index will be higher if there are fewer animals, and the particle size of the given inducer is small and the conglomerates formed are large. According to the RPC index (RPC_i), the epoxy was the most effective inductor, the second one was Carmine and the third one was den-BSA (**Fig. 4**). The most adequate type of inductor was chosen, considering its chemical and biological properties, and RPC_i in the relevant experiments.

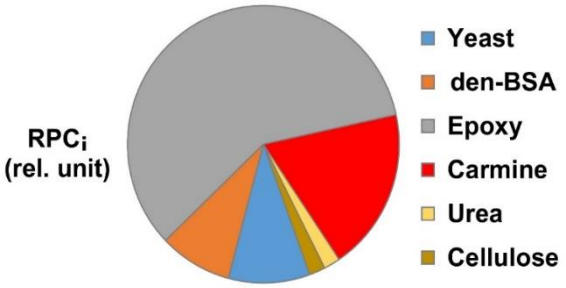

Figure 4. RIC-producing capacity index (RPC_i)

4.1.2. Analysis

The Rotimer-Inductor Conglomerate web seemed to be a very complex formation and it is characteristic to some monogonants, we wanted to test how the different environmental factors influence its production (**Fig. 5A**). Since yeast is part of the rotifers' diet, it was also optimal as an inducer. After successive inductions, depletion of endogenous Rotimer sources was observed in *E. dilatata*. After the third round of stimulation, the size of the conglomerates did not change significantly, but the proportion of the area covered by the conglomerate decreased. Differences between both measured parameters were found in the first-second rounds and third-fourth rounds. Presumably, the animals ran out of resources for production and selection, and there was not enough time for production. Active synthesis of Rotimer is required for RIC formation, which is an energetically active process.

After starvation, we observed a second mode of depletion of Rotimer secretion due to the lack of nutrients (**Fig. 5A**). The empirical parameters of the conglomerates did not change after three days of starvation, but the area covered was significantly reduced. Changes in the monitored parameters were observed between the RIC production after the first-second day of starvation and the third-fourth day. Since food was unavailable for the animals, they presumably used the endogenous Rotimer substrate as an energy source. The regeneration time of RIC production capacity was 30 ± 4 min in E. dilatata entities exhausted from starvation. In the presence of cellulose, carmine, urea, and Epoxy beads, there was no RIC production in the depleted rotifers for longer than 6 hours. Rotimer production in rotifers is relatively fast and highly nutrient-dependent.

To measure the properties of the viability marker of Rotimer secretion, the highest sublethal dose of NaN_3 in *E. dilatata* was monitored, which had no toxic effect on them. The NaN_3 was applied with the purpose of revealing how the partial mitochondrial dysfunction may influence Rotimer secretion. Based on the current literature, we used the swimming speed as an adequate reference viability marker of monogonants [26,77–79]. The swimming speed of control animals was 465 ± 22 μm/sec in the setup and the RIC production was also manifested by this kind of speed. At substance concentrations between 50 and 500 μM, a slowing of the animals' swimming speed was observed, so we chose 20 μM from now on. The sodium azide dose negatively affected biopolymer formation, demonstrating the sublethal viability marker properties of rotimer secretion. This inhibitor of mitochondrial terminal oxidation significantly reduced the average size of conglomerates and the proportion of the conglomerate-covered area. In contrast with NaN_3, spermidine had positive effects on all parameters. These data suggest that RIC production is an energy-intensive process. Surprisingly, the lower temperature (10 °C) did not decrease the monitored parameters compared to its controls, while the higher temperature (35 °C) was able to stimulate production. Similarly, to RIC production, higher temperatures favored monogonants. Immediately after the isolation of *E. dilatata* entities, increasing (1 g/L) or decreasing (DW) salt concentration had no immediate effect on RIC production compared to the standard medium (**Fig. 5A**); however, when these animals were left to rest (washed) in completely ion-free medium for half an hour, the RPC disappeared. The salinization of coastal freshwater raises serious concerns on the protection of their ecosystems [80]. High salinity induces oxidative stress, having a negative impact on lipid metabolism in another monogonant rotifer, *Brachionus koreanus*, demonstrated by Lee et al. [81]. In contrast to the comprehensive data on the salt sensitivity of monogonants, we found that extreme osmolarity has no adverse effect on the monitored parameters. The lower pH (6) did not reduce the aforementioned parameters, while the higher pH (8) positively affected RIC production.The pH 6 represented the lower pH range of most natural waters found in the United States and across Europe [82], where monogonants are found, such as *Brachionus* species which were cultured at different pH (from 6.2 to 9.8). The maximum population densities were reached at pH 8 [83]. During this study, one of the measured parameters was the average size of the conglomerate. Still, during another experiment, we extended the examination of the parameters with a higher resolution (yarn length), which is described in the regulation section.

Upon further investigation, we saw how RIC could maintain its integrity in the presence of various chemical agents (**Fig. 5B)**. The structure-retaining stability of the Rotimer-adherent

particles was demonstrated. Although epoxy appeared to be the best inducer, it is unsuitable in combination with enzymes or ionic molecules due to its specific charges, which can inactivate the applied agents. In the present experiments, carmine was used as an inducer except in NaOH because it dissolved these crystals, so we added epoxy. It was pointed out that RIC integrity was lost in two-day-old rotifer medium or the presence of trypsin, proteinase K or DMSO during the measurement, which suggests that a protein-type substance may partially or fully form the Rotimer. The RIC retained its original integrity with Triton X-100, collagenase II, glycerol, SDS, or NaOH. Triton X-100 (a nonpolar detergent) showed a high level of stabilization. Furthermore, RIC aggregated spectacularly under the influence of EGTA, EDTA, TPEN, MeOH, EtOH, HCl, or acetic acid without solubilization. We hypothesize that hydration and metal ions may be required to maintain Rotimer integrity. It is challenging to examine the components and structure of Rotimer, as we currently cannot separate the biopolymer from the specific inducer.

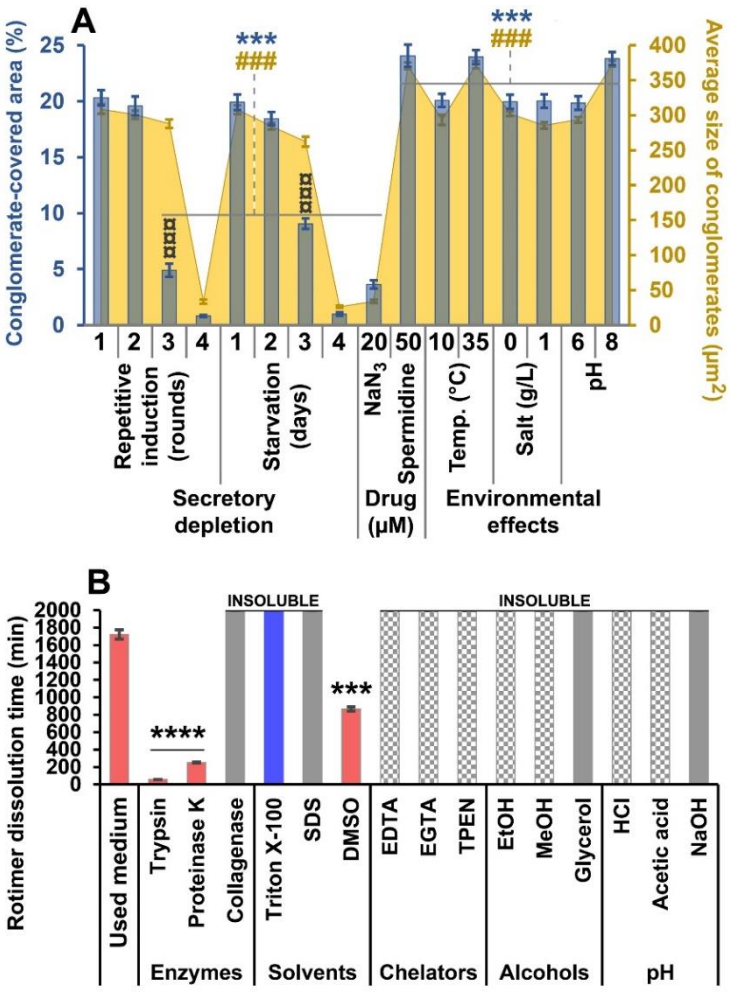

Figure 5. Rotimer production and integrity-influencing factors: in vivo secretion and dissolution. *The effects of different conditions on E. dilatata Rotimer producing activity (A) were monitored by 'Rotimer-Inductor Conglomerate' (RIC)-covered area (%; blue) and average size of RIC (μm²; yellow). The tested conditions were different secretory emptying methods: repeated carmine induction (circles) or during fasting (days). The applied drugs were the toxic NaN_3 and beneficial spermidine. The investigated environmental conditions were the temperature (4 °C and 30 °C), concentration of salts (0 and 1 g/mL) and various pH (6 and 8). Experiments related to rotimer dissolution were carried out using different solvents and drug*

*candidate groups (B), which were as follows: the culture medium used by rotifers (control); enzymes (collagenase II, trypsin, proteinase K); solvents (triton X-100, DMSO, SDS); chelators (TPEN, EDTA, EGTA); alcohols (glycerol, EtOH, MeOH) and pH-related chemical compounds (NaOH, HCl, acetic acid). Columns represent dissolution time (min), and their colors show the observed changes in original web quality, where red represents dissolution; the blue means the conservation in original high quality; the gray color represents the insolubility (during 2000 min), and the gray square shows the formation of massive RIC aggregates. The error bars show S.E.M. One-way ANOVA with Bonferroni post hoc test was used for statistical analysis; the levels of significance are p***,###,¤¤¤ ≤ 0.001 and p**** ≤ 0.0001 (*, significant difference between the columns above or below the upper or the lower gray lines (A) in percentage of RIC-covered area or from the standard environment (B); #, significant difference between the columns above or below the upper or the lower gray lines (A) in average size of the conglomerates; ¤, significant between the percentage of RIC-covered area and percentage of average size of the conglomerates in the relevant conditions). A black line above the bars means they are all equally important. For an interpretation of the references to colors in the figure legend, see the web version of the article.*

We wanted to get to know the structure of Rotimer in more detail, so we used the FTIR method in the presence of Carmine, a nonproteinous RIC-inductor (**Fig. 6**). The FTIR spectrum of the standard medium contains several broad peaks which may be associated with the HCO_3^- and silicic acid content.

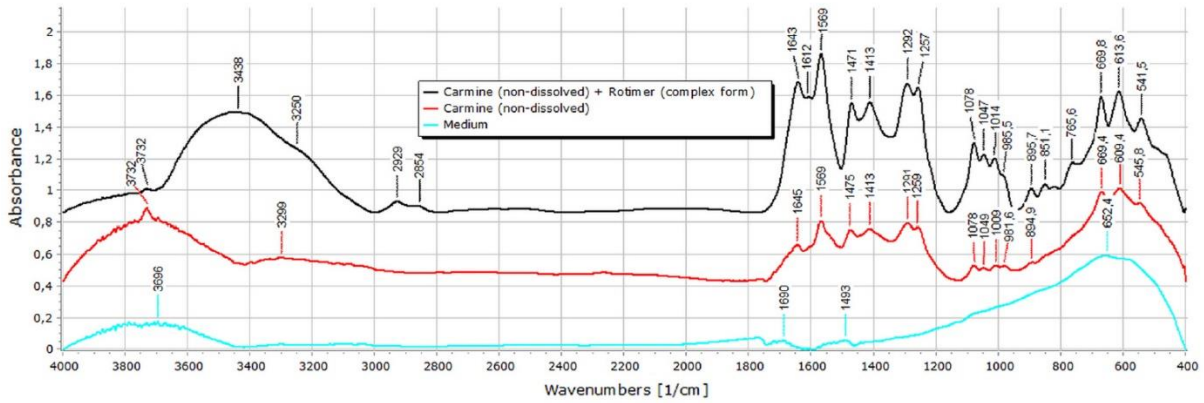

Figure 6. FTIR spectra of the medium (blue), the Carmine crystals (red) and the Carmine-Rotimer complexes (black)

The spectrum of the Carmine, as inductor molecule, contains two individual peaks in OH stretching region (3732 and 3299 cm^{-1}) belonging to the nonassociated and associated OH groups, respectively. The strong right shift of the nonassociated peak to 3438 cm^{-1} in the RIC indicates that Rotimer connects to the inductor molecules via the formation of H-bonds of those

hidroxy-groups which take no part in intramolecular relations. The appearance of a new peak 3250 cm^{-1} could be connected to the N-H stretching of amine groups of the biopolymer. The peaks associated with C=O stretching appeared at slightly lower wavenumbers than usual. The C=O stretching of aromatic carboxylic acid is visible at 1645 cm^{-1}, while the peak related to the diaromatic keto groups appeared at 1569 cm^{-1}. The unchanged position of these peaks indicates that these groups are not involved in RIC formation; their distribution is in intramolecular associations. The appearance of the new peak at the position of 1612 cm^{-1} is related to the amide II vibrations of the Rotimer backbone. The peaks at 1471 cm^{-1} and 1413 cm^{-1} belong to βOH vibrations of carboxylic and phenolic OH groups respectively, while the peak doublet at 1292 cm^{-1} and 1259 cm^{-1} may be associated with the β-hidroxy vibration of alcoholic (secondary) groups. The peak quadruplet in the 980-1080 cm^{-1} region belongs to the C-O stretching of various molecular parts. Significant differences between pure Carmine and the Carmine-Rotimer complex are observed in this region. Still, due to low signal intensity and overlapping solid peaks, the reason for the change cannot necessarily be identified.

4.1.3. Regulation

Rotimer production is sensitive to environmental factors, such as temperature, pH, metal ions, and various pollutants. These influencing factors have correspondingly different effects on rotifers; however, each species has its optimum. The *E. dilatata* preferred lower temperature (22 °C; **Fig. 7**) and higher pH (pH=7.8; **Fig. 8**) than *L. bulla* (25 °C and pH=7.2) did in our laboratory conditions. Related to the species-specific optimum, both RIC parameters (longest conglomerate strand and area covered by conglomerate) showed similarly high levels. If we moved away from this optimum, the parameters decreased, especially concerning the fiber length. In the case of *E. dilatata*, these markers produced an average 2-fold change compared to *L. bulla*.

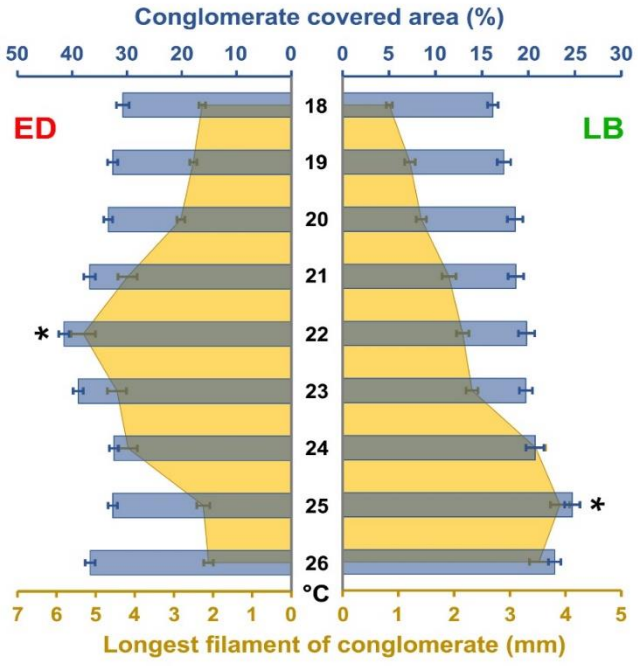

Figure 7. The effect of temperature on RIC formation*. The impacts of temperature on RIC created by E. dilatata (red; ED) and L. bulla (green; LB) are presented by the RIC-covered area (blue; %) and the longest*

filament of conglomerate (mm; yellow). The error bars represent SEM. One-way ANOVA, and Bonferroni post hoc test was applied for statistical analysis, the levels of significance are p ≤ 0.05 (* difference from all the other data, indicating the optimum, the significance is higher than or equal to 95% in both measured parameters).*

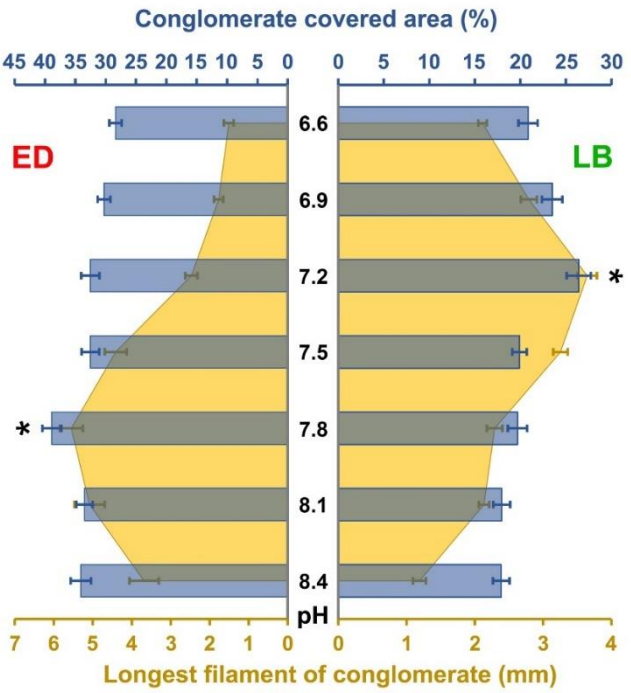

Figure 8. The effect of pH on RIC formation. *The impacts of pH on 'Rotimer-Inductor Conglomerate' (RIC) produced by E. dilatata (ED; red) and L. bulla (LB; green) are presented by the RIC-covered area (%; blue) and the longest filament of conglomerate (mm; yellow). The error bars represent SEM. One-way ANOVA, and Bonferroni post hoc test was applied for statistical analysis, the levels of significance are p* ≤ 0.05 (* difference from all measured data, indicating the optimum, the significance is higher than or equal to 95% in both measured parameters).*

Natural waters contain various metal ions which implicitly influence the flora and fauna [84]. Applying natural salts (**Fig. 9**) in artificial conditions revealed that only calcium ion is inevitable for exudate secretion. There is no RIC production in its absence. A similar phenomenon was described related to mucin biopolymers, where the sol-gel transition is pH- and calcium dependent [85]. The fact is that rotifers isolated from culture are able to produce Rotimer even in an entirely ion-free environment. Still, animals resting in DW for at least half an hour can no longer excrete the biopolymer [77]. These micro-metazoans presumably reserve a certain amount of metal ions (e.g., calcium); however, the ability to secrete secretions ceases without replacing minerals. Compared to the ion content of the standard culture medium (210 mg/L), a lower dose (100 mg/L) was used, as this level was still acceptable in terms of osmolarity. It can be stated that none of the ions proved to be toxic. The single-component treatment solutions showed significant differences from the standard and calcium-only solutions. Surprisingly, neither the magnesium, nor the strontium was able to replace the calcium, unlike in the case of some physiological process [86,87]. These facts prove that the calcium sensors or receptors of rotifers are very specific to this ion.

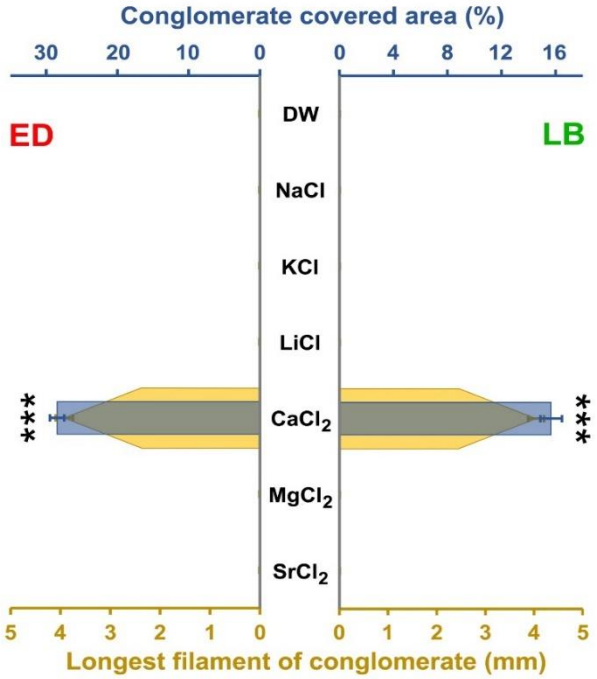

Figure 9. Metal ions-dependency of the RIC formation*. The impacts of various metal ions on 'Rotimer-Inductor Conglomerate' (RIC) produced by E. dilatata (ED; red) and L. bulla (LB; green) are presented by the RICcovered area (%; blue) and the longest fiber of conglomerate (yellow; mm). The error bars represent SEM. One-way ANOVA with Bonferroni post hoc test was used for statistical analysis, the levels of significance are p*** ≤ 0.001 (*, significant difference from all the other measured data, the significance is higher than 99.1% in related parameters).*

To accurately assess the calcium dependence of RIC production, dose-efficacy was measured (**Fig. 10**). Sodium does not affect secretion production; the various doses of calcium were supplemented with it, the same as the amount of metal ions, similar to standard media. To avoid dose dependency, it is essential to ensure a constant osmolarity in the given artificial medium. The optimal values of the two studied species differ in terms of biopolymer production. In the case of *E. dilatata*, 50 mg/L is the most favorable value, while in the case of *L. bulla*, 100 mg/L. It is worth noting that the first produces twice as much Rotimer as the latter. Results suggest that 10-20% of conglomerate formation already starts in the presence of a relatively low dose (0.1 mg/L) of calcium. A sudden increase in activity was observed for both species at a dose of 5 mg/l; furthermore, secretion production was dramatically reduced in the presence of calcium (50 mg/L) and EDTA (100 mg/L). The EDTA is a well-known chelator of different metal ions (e.g., calcium, magnesium, copper or zinc; [88] and it had no negative effect on the viability (swimming speed, µm/sec) of the animals up to the 200 mg/L dose. The inhibitory effect of non-membrane permeable calcium-specific chelator [89] on RIC production proves that this process happens extracellularly, presumably at the inlet of the intestinal tract. The calcium dependency of biopolymer-secretion and formation is not a rare phenomenon in the animal kingdom, especially in aquatic invertebrates [90,91].

Figure 10. Dose-dependent effect of calcium on RIC formation*. The impacts of different doses of calcium on RIC, produced by E. dilatata (red; ED) and L. bulla (green; LB) are presented by the RIC-covered area (blue; %) and the longest filament of conglomerate (yellow; mm). EDTA (brown; 100 mg/L) was aplied against calcium (black; 50 mg/L) in the control measurement (bottom column).*

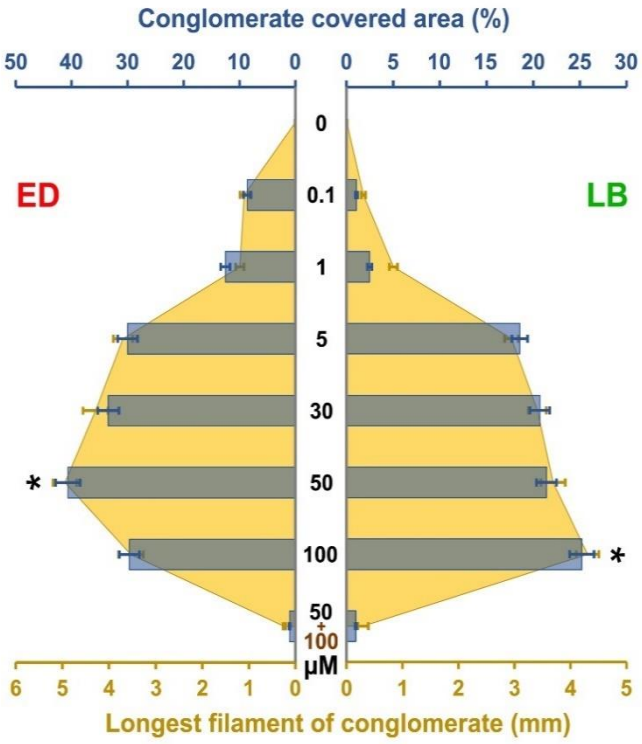

The error bars represent SEM. One-way ANOVA with Bonferroni post hoc test was applied for analysis, the levels of significance are p ≤ 0.05 (* difference from all the measured data, indicating the optimum, the significance is higher than or equal to 95% in both measured parameters).*

If exudate secretion was induced under species-specific optimal conditions in a modified culture medium (*E. dilatata*: 22 °C, pH = 7.8, calcium 50 mg/L; *L. bulla*: 25 °C, pH = 7.2, calcium 100 mg/L), both species showed significantly higher activity (**Fig. 11A**) compared to their controls (100%; standard environmental factors and media). The length of filaments and the RIC amount represents that *E. dilatata* can be better potentiated than *L. bulla*. In a parallel experiment, but also in an optimized environment (except for the amount of calcium; 5 mg/L), rotifers used calcium for RIC production and to satisfy their physiological needs. (**Fig. 11B**). It was shown by non-cell permeable Fluo-3 fluorescent dye [92] that significantly more calcium was used by the animals during RIC production than without its induction. The control measurements were performed in the same medium (with reduced calcium content), without inducer and animal. The explanation for this was an increase in the molarity ratio of the detectable dye. These data suggest that rotifers bind metal ions and extract them from their environment. The same process can be observed in the case of marine corals [93,94].

The rotimer presumably integrates calcium ions during its formation. This phenomenon may even be important in the global processes of marine and freshwater sediments. Our studies show that biopolymer production is essential for the life and survival of rotifers.

Figure 11. RIC amount (A) and calcium integration (B) under a species-specific optimized environment. *The determining factors were optimized for species in the E. dilatata (red; ED) and L. bulla (green; LB) populations. The percentage of the relative units of the exudate indicators (A) was presented in the form of the longest filament of conglomerate (LFC) and by the conglomerate-covered area (CCA). The changes in specific calcium uptake from the media (B) were detected in the presence or absence of RIC.*

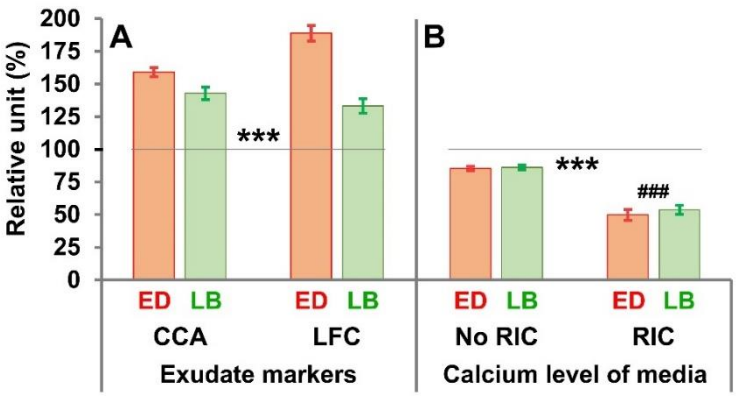

*The error bars represent SEM. One-way ANOVA with Bonferroni post hoc test was used for statistical analysis, the levels of significance are p***,### ≤ 0.001 (*, significant difference from the standard culturing, which was the 100% indicated by the black line; #, significant difference from the 'No RIC' columns).*

Numerous environmental pollutant chemicals may come from industrial sources or inadequately handled communal waste in human habitat [95]. The short-term (a few hours) effects of the tested agents (ascorbic acid, DMSO, catechin, glycerin, Lucidril, glucose, cAMP, spermidine, ethyl nicotinate, taurine, selegiline, isoguvacin, and choline) was very different; however, both species responded to them in the same way (**Fig. 12**). In some cases, the amount of RIC remained average; however, the length of the threads became significantly shorter (glycerin, isoguvacin, taurine) compared to the control. In the group of tested substances, there were two chemicals (choline and ethyl nicotinate) whose effect resulted in a decrease in the amount of relatively longer yarns. In the last variation of the pattern related to the exudate indicator (glucose and Lucidril), a high proportion of the covered area was detected, with longer fibers than the control.

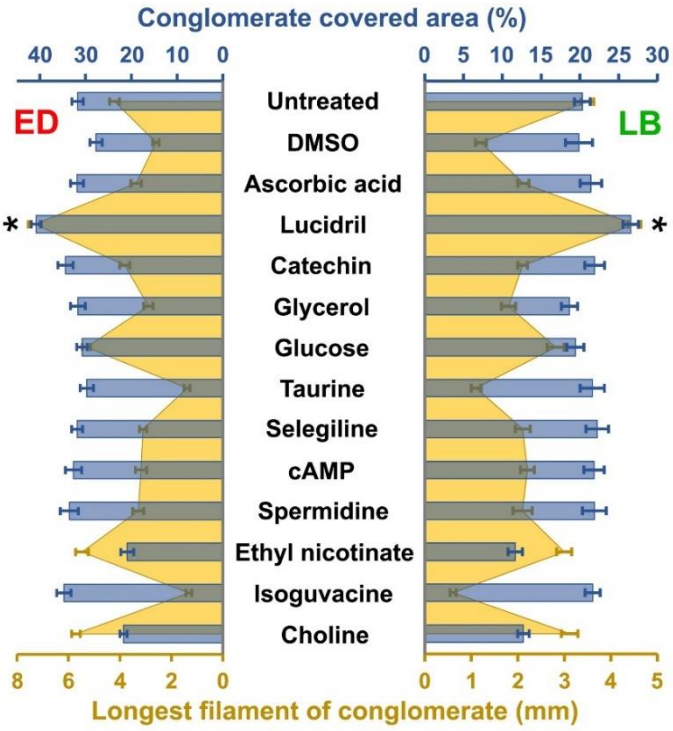

Figure 12. Chemical agents-dependency of the RIC formation*. The impacts of various chemicals on 'Rotimer-Inductor Conglomerate' (RIC) produced by E. dilatata (ED; red) and L. bulla (LB; green) are presented by the RIC-covered area (%; blue) and the longest filament of conglomerate (mm; yellow). The error bars represent SEM. One-way ANOVA, with Bonferroni post hoc test was applied for analysis, the levels of significance are p* ≤ 0.05 (* difference from all the measured data, indicating the optimum, the significance is higher than or equal to 95% in both measured parameters).*

The two examined species *E. dilatata* and *L. bulla*, show different reactions to environmental factors (temperature, pH) compared to each other (**Fig. 13**), except for the presence of calcium and the modulating effect of various drugs (Lucidril).

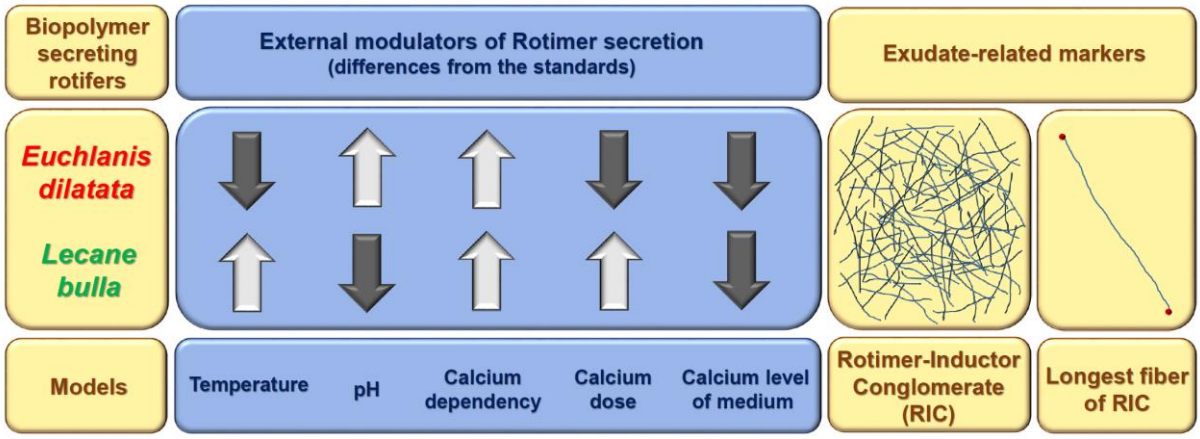

Figure 13. External modulators of Rotimer secretion summary table

4.1.4. Bioactivity

The physiological effects of Rotimer produced by *E. dilatata* were investigated on three different cell types **(Fig. 14**). We used Den-BSA as an inducer, also found in the standard medium of classical cell culture; therefore, it had a no different physiological effect on the cells in the system. The average movement of the cells was well measurable (algae: 87 ± 18 µm/min; neuroblastoma: 64 ± 19 µm/h; yeast: 150 ± 39 µm/min) in untreated controls. Passive (diffusion-based) and active (cell movement) motility occurred in yeasts and algae, while only dynamic localization was detectable in human neuroblastoma. RIC only slightly reduced the viability of the tested cells, where the extent of the damaging effect did not reach the LD50; on the contrary, it inhibited their motility in all cell types.

Figure 14. Bioactivities of monogonant-secreted Rotimer. *The specific effect of E. dilatata-formed RIC on different types of cell motility and viability is presented. The percentage of bioactivity on viability and motility of algae (Chlorella vulgaris; green), yeast (Saccharomyces cerevisiae; yellow) and human neuroblastoma cells (SH-SY5Y; blue) was monitored in the presence*

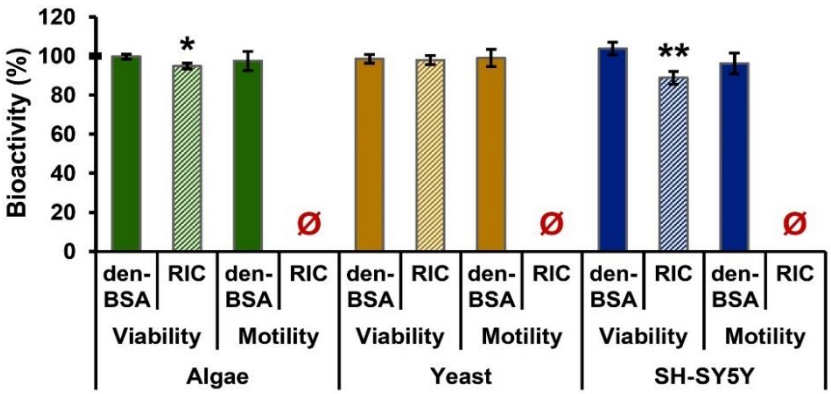

of untreated control (100%) and denatured bovine serum albumin (den-BSA; full columns; reference control) or 'Rotimer-Inductor Conglomerate' (RIC; stripped columns). The untreated control was 100% marked with bold line on the y-axis. The error bars represent S.E.M. One-way ANOVA with Bonferroni post hoc test was used for statistical analysis; the levels of significance are p ≤ 0.05 and p** ≤ 0.01 (*, significant difference from untreated control group).*

4.1.5. Conglomerate-aggregate interactions

During the interaction between the RIC and the aggregates, we investigated the binding between the biopolymer-containing conglomerates and H-Aβ neurotoxic aggregates, respectively, to reveal the effects of the RIC complex on H-Aβ aggregation itself. The measurements could not be carried out with Rotimer without inductor material (epoxy-metal beads), because according to our current knowledge and empirical experience, there is no method available to remove the mentioned biomolecule from the inductor without any structural changes (e.g., chemical, such as racemization in alkaline solution). The organizing conditions and the binding of aggregates were measured directly or indirectly with optical imaging methods, but the detailed investigation of physico-chemical properties was beyond the scope of this paper. In the first step, the quick interaction (minutes) between the natural polymers of rotifers and the artificial H-Aβ was investigated, applying two different methods. The connection between H-Aβ and *E. dilatata/L. bulla*-RIC (ED/LB-RIC) was investigated by stagogram analysis (**Fig. 15**) which is a simple, but widely accepted method to visualize e.g. the aggregation capacity of different molecular composition of samples, based on their optical diversity [96,97]. This is a very sensitive crystallizing process using the covered (%) area and average size (μm^2) parameters of particles. These indicators can be applied properly during the image analysis, based on the number and size of the conglomerate unit; moreover, the dried drops can be qualitatively differentiated. Different treatment groups were measured and compared with relevant controls. In this case, the active ingredient was RIC (epoxy beads with Rotimer). The Aβs were aggregated for 3 hours (3h) and three days (3d) before mixing it with the RIC. We measured the inductor itself, H-Aβ and ED/LB-RIC alone, and the conglomerates of H-Aβ with the ED/LB-RIC respectively using the stagogram based optical assay (**Fig. 15**). The solutions of fresh (0 min) H-Aβ and S-Aβ (with random sequence of amino acids) were not presented on the stagogram figure, because they showed transparent crystallizing patterns; therefore, the border lines of the dessicated samples could not be identified.

Figure 15. Stagogram-optical imaging and exploration of RIC and aggregated H-Aβ interactions*. ED, E. dilatata; LB, L. bulla; RIC, Rotimer-Inductor Conglomerate; H-Aβ, human-type beta-amyloid 1-42; the scale bar represents 0.5 mm. The error bars represent SEM. One-way ANOVA with Bonferroni post hoc test was used for statistical analysis, the levels of significance are p¤¤¤¤ ≤ 0.001 or p****,#### ≤ 0.0001 (*, significant difference from all other groups; #, significant difference from those treated with the same ED-RIC;¤, significant difference from LB-RIC belonging to the same group).*

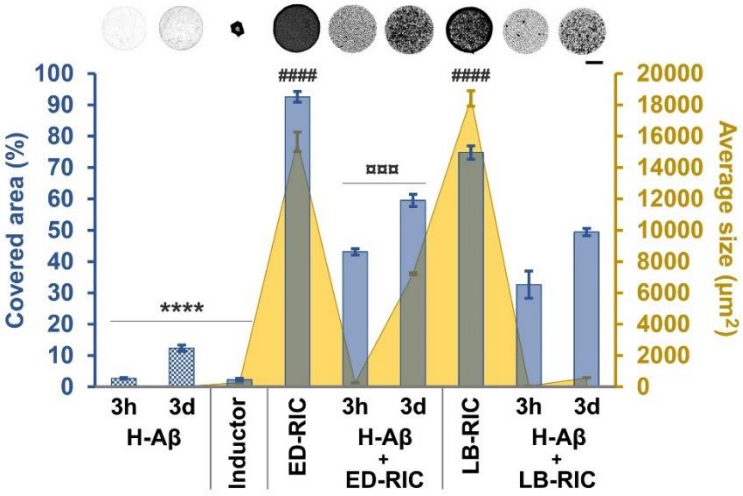

The crystallized droplets of the groups differed in both density and structural phenotype. This is a closed and exactly defined chemical environment with few components; however, it is a well controllable *in vitro* system. The profile of the different samples shows the interactions between the components during the crystallization process. The presence, absence, or variations in their amounts are the determining factors. According to the optical indicators of the stagogram, the parameters of H-Aβ, conglomerate, and inducer were visibly different. The more aggregated (3d) H-Aβ showed a denser pattern compared to the few hours-incubated ones (3h). Both RIC groups of the two tested animal groups presented outstanding density in the empiric analysis of stagograms; moreover, they provided a maximal reference to the further analysis of the other samples. After the removal of the free/unbound H-Aβ, it can be noted that the biopolymers of the two species bind to aggregates and the optical density of relevant stagograms derived from RIC alone was decreasing in the presence of H-Aβ in the conglomerate. The density of ED-RIC-H-Aβ conglomerate is higher compared to LB-RIC-H-Aβ conglomerates. Based on the results, it can be declared that are possible molecular interactions between Rotimer and Aβs, particularly with H-Aβ form. The relations between RIC and H-Aβ of both rotifer species showed similar tendencies, however, we also noticed that the samples originated from *L. bulla* the pictures were significantly brighter.

In addition to the optical analysis, the fast interactions between the investigated molecules were also analyzed using fluorescence methods. For measuring the indicator fluorescent signals two adequate dyes were applied, the Bis-ANS and the ThT. According to the literature, these molecules have different binding affinity to the various types of aggregates [98]. These

functional indicators can label the oligomeric and fibrillar forms of Aβs, marking the entire conformational spectrum of H-Aβs. The Bis-ANS is more sensitive to the oligomers [99], while the ThT is for the fibrils [100,101]. Based on the previous Aβ characterizations [21,64], it can be stated that the 3h and 3d aggregating periods are well-reflected the larger quantity of the oligomers or fibrils in the relevant samples. The H-Aβ (3h) with lower organization contains oligomers in higher proportions and they were measured by Bis-ANS, while the considered fibrillar ones with longer incubation time (3d) were detected by ThT (**Fig.16**). In anti- (**Fig. 17A**) and disaggregating **(Fig. 17B**) measurements all samples were detected with both fluorophores.

The results of the interaction studies (**Fig. 16**) can be classified into three units: 1. H-Aβ-types alone; 2. inductor, various RIC-versions and the inductor-Aβ interactions as relevant controls; 3. the interactions between the species-specific RIC and the different H-Aβs (specified in amino acid sequence and levels of aggregation). Based on the followed-up aggregates, there are three categories: 1. with Aβs alone; 2. Free Aβs in the supernatant; 3. binding Aβs to the RIC-types. The given types of H-Aβ aggregates showed elevated fluorescence intensities in the presence of both Bis-ANS and ThT, in contrast with S-Aβ, which gives higher signal intensity rather together with Bis-ANS. The S-Aβ with random sequence presented lower aggregating organization. The measurements of the Aβs alone were the reference point for the further experiments.

The fluorescence intensity of the inducer particles and ED/LB-RIC combinations was also examined and used as a background control to determine non-specific binding. Based on the results obtained, it can be stated that there was minimal binding between the above-mentioned reference controls and the fluorescent dyes used during the relatively short incubation time. However, with the same parameters, the binding of Aβ to RIC was significantly measurable. Here, the inductor itself was not a disturbing factor. After the removal of the non-bounded (free) Aβs with supernatant, the aggregates binding to RIC was labelled. The H-Aβ interacted with the conglomerates of both rotifer species and relatively high fluorescent signal was shown, while the S-Aβ gave more lower value similarly to the background control. The data derived from this reference amyloid type, made us to conclude that there is sequence specificity in H-Aβ-binding to biopolymers. The H-Aβ samples with lower (3h) or higher (3d) conformational organization were significantly bound to tested Rotimer coatings, but it showed higher affinity to the biopolymer secreted by *E. dilatata* than the one by *L. bulla*.

After proving the special interaction between Rotimer and H-Aβ, the effects of the investigated biopolymer on aggregation processes were tested using the Bis-ANS and ThT measurement,

which can detect the aggregation status of Aβs. The controls show similar fluorescence intensity to the previously measured ones (**Fig. 16**); therefore, in this case, they are not presented again. For measuring the anti-aggregating effects of RIC-types (**Fig. 17A**) Aβs with various aggregation times (0h, 3h and 3d) were applied. Under the co-incubation, the inductor alone could not inhibit the aggregation of H-Aβ; however, the initial signal of Bis-ANS significantly decreased in the 3d sample, while the ThT signal increased. These results referred to the time-dependent high aggregation level of H-Aβ; moreover, these processes are parallel with the relevant literature [102,103]. In contrast with the above mentioned, the H-Aβ (3h, 3d) + RIC related ThT signals were decreased in samples of both relevant species, while the Bis-ANS fluorescence remained in the reference (0 min) level. The materials from *E. dilatata* were more effective in anti-aggregation processes, than the ones derived from *L. bulla* using the same experimental time. The 3d group was the less efficient. In the LB-RIC and H-Aβ/3d combination the ThT gives an elevated level; thus, unlike the other samples, here was no clear conclusion about the aggregation level of H-Aβ.

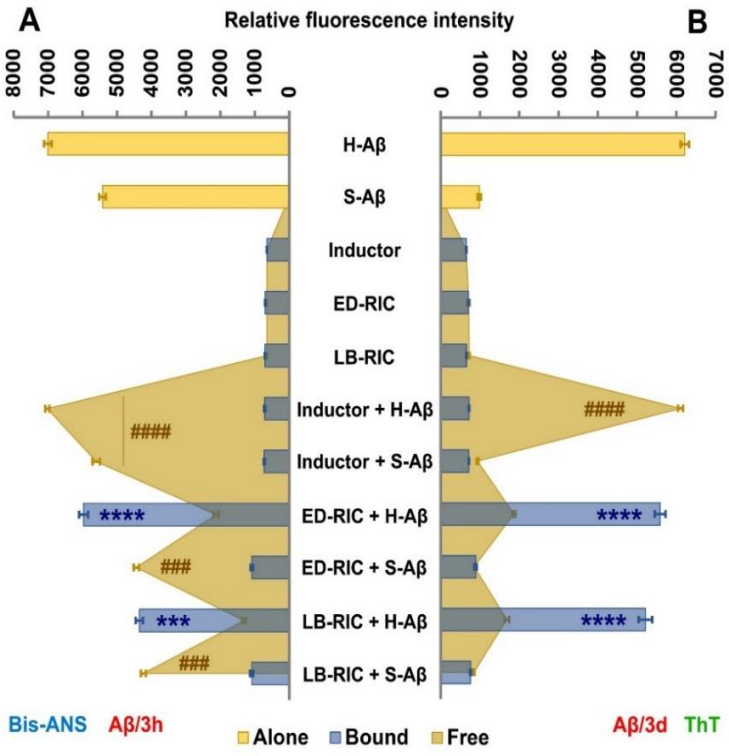

Figure 16. Quick and sequence-based interaction of E. dilatata- and L. bulla-type RIC with H-Aβ aggregates (3 h; 3d). *ED, E. dilatata; LB, L. bulla; RIC, 'Rotimer-Inductor Conglomerate'; H-Aβ, human beta-amyloid 1-42. The error bars represent SEM. One-way ANOVA with Bonferroni post hoc test was applied for statistical analysis, the levels of significance are p***,### ≤ 0.001 or p****,#### ≤ 0.0001 (* difference from all bound-type groups; #, difference from all other free-type inductor, RIC and RIC + H-Aβ groups).*

By the next experiments, it has been revealed, that the presence of inductor alone during further 12h had no impact on the condition of 3d-preaggregated H-Aβ (**Fig. 17B**). In these cases, the Bis-ANS and ThT signal ranges are similar with the previously presented graphs (**Fig. 17A**). In contrast, the control Bis-ANS and ThT values were differed significantly from the RIC-containing ones from the same category at the end of disaggregating processes. During co-

incubation, the RIC of both monogonant species increased the level of bis-ANS-sensitive oligomers and decreased the amount of ThT-specific fibrillar forms. Based on the characteristics of the two fluorophores, we may assume that the presence of Rotimer in the samples have disaggregation effect against the H-Aβ. Similar to the previous measurements, the biopolymer of *E. dilatata* was more effective and gave more understandable results about the state of the neurotoxic aggregates.

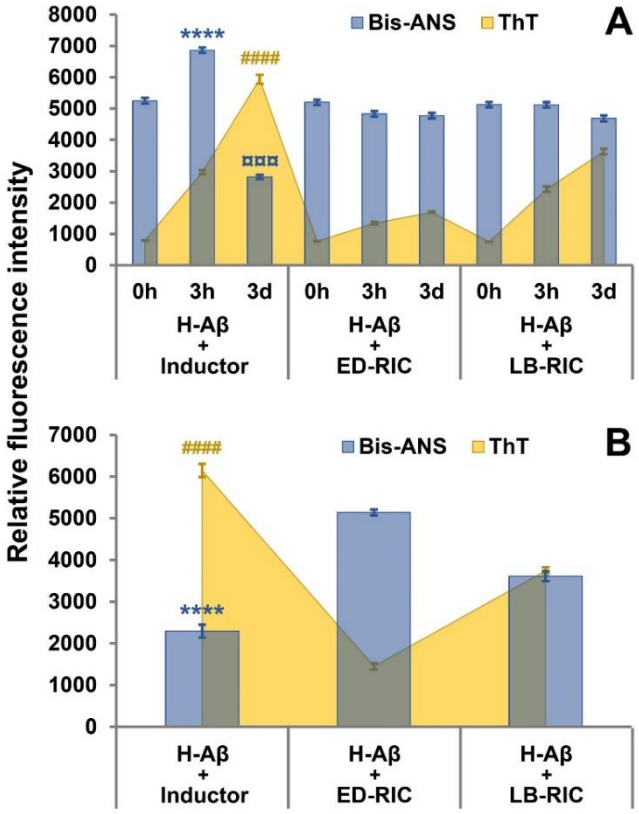

Figure 17. Anti-aggregating (A) and disaggregating (B) effects of E. dilatata- and L. bulla-specific RIC against H-Aβ aggregates (3 h; 3d). *ED, E. dilatata; LB, L. bulla; RIC, Rotimer-Inductor Conglomerate; H-Aβ, human-type amyloid beta 1-42. The error bars represent SEM. One-way ANOVA with Bonferroni post hoc test was applied for statistical analysis, the levels of significance are p¤¤¤¤ ≤ 0.001 or p****, #### ≤ 0.0001 (* difference from all other Bis-ANS groups; #, difference from all other ThT groups; ¤, significant difference from RIC-containing 3d Bis-ANS group).*

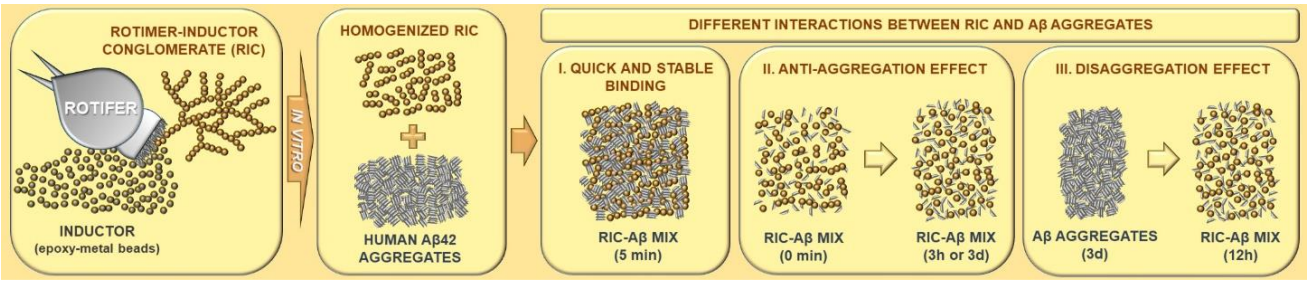

Figure 18. Interactions between rotifer-RIC and human-type Aβ aggregates

4.2. Rotifers and beta-amyloid relations

4.2.1. Autocatabolism

The Aβ42 is a well-known neurotoxin, which is prone to form highly resistant aggregates in an aquatic environment [104]. The bdelloid rotifers can catabolize these aggregates, with no

physiological damage [21]. Our aims were to reveal the special role of Aβ42 in autocatabolism-related processes during a 25-day period (**Fig. 19**). To identify the sequence specificity of this pathological molecule, we used its coded version as a control. The molecular weight of S-Aβ42 was the same as that of the wild-type form, with a different sequence of amino acids [21,105].

Figure 19. Schematic illustration of the functionally reversible organ shrinkage in a rotifer system *(starting day, D0: Day 0; organ shrinkage period with one-time drug treatment in glucose supplemented environment, D20: Day 20; organ regeneration period with one-time standard feeding, D25: Day 25).*

On D0, the reference germovitellaria of *P. acuticornis* (**Fig. 20A**) or *A. vaga* (**Fig. 20D**) can be seen. Their size and fine structure decreased after 20 days of glucose-supplemented starvation (**Figures 20B** and **20E**). On the 20th day, the animals were fed only once, guaranteeing the usual nutrients for the regeneration phase. Their internal organs were then reconstructed and showed similar characteristics (**Figures 20C** and **20F**) to the reference organs. These data may also indicate that organ shrinkage is reversible and significantly dependent on food availability. To connect the autocatabolism-related processes with starvation-induced organ shrinkage [106], we applied ConA [107] during the experiments. The amounts of nucleic acid and proteins were detected parallelly with AVOs. In conclusion, we can state that the total protein amount decreased on the 20th day, indicating that the animals catabolize them for survival. The ConA-administration inhibited these processes. The amounts of nucleic acid did not show any changes in either species (**Fig. 20G**). In line with the adequate investigations, we detected significant increase in autocatabolism-related vesicular acidification [108] in relevant species on D20 compared to the untreated reference values of D0. The ConA treatment hindered the observed alterations. On day 25, there was no change in either NR or AO. The decrease in the amount of proteins (in connection with the constant nucleic acid content) and the occurrence of AVOs during starvation show a good correlation with the tendencies of organ shrinkage. These phenomena are appropriate empirical and physiological markers of autolytic metabolism in the rotifers.

Figure 20. Functionally reversible organ shrinkage (FROS) in P. acuticornis and A. vaga rotifers*. The germovitellaria (pseudo-colored in blue; scale bar: 20 μm) of P. acuticornis (PA, A–C) and A. vaga (AV, D-F) was detected on D0 (A and D), D20 (B and E) and/or D25 (C and F). The FROS-related differences are presented (G) with the nucleic acid- (red), protein- (green), and AVOs amount in PA*

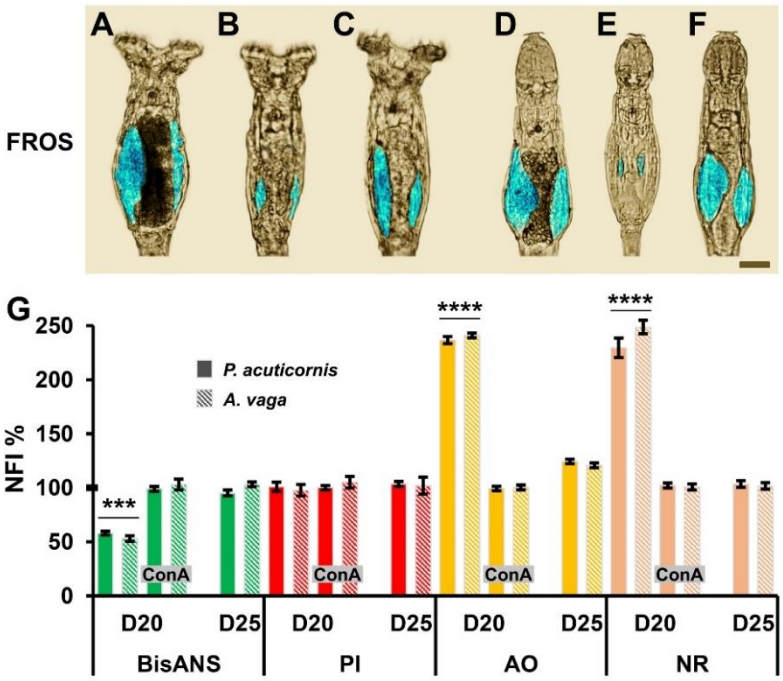

*(full columns) and AV (striped columns) species. The D0 means 100 %. ConA was applied parallelly with all investigations. The error bars represent SEM. One-way ANOVA with Bonferroni post hoc test was applied for statistical analysis, the levels of significance: p*** ≤ 0.001; p**** ≤ 0.0001 (* difference from all groups).*

Aβs are stigmatized in the scientific literature as negative and multifaceted agents. In FROS-related measurements the ConA, Aβ42 or S-Aβ42 were added to the treatment solution on D0 (**Fig. 21A**); therefore, these data served as references to the upcoming ones. For both rotifer species, organ shrinkage was less pronounced on D20 than in adequately untreated controls. In the Aβ42-treated groups, significantly greater regeneration was observed on D25 than in the other D25 groups. These measurements indicate that the aggregate with a natural structure also has a specific modulating effect. Furthermore, organ shrinkage was less in the Aβ42-treated groups than in the S-Aβ42 counterparts. The same phenomenon was also observed at the end of regeneration when the animals recovered significantly in the presence of Aβ42. These data showed that the attenuation of shrinkage via modulation is likely sequence-specific, since the order of amino acid is the only difference between the two types of Aβs [109]. On D20, the ConA inhibited the FROS in rotifer species in a food-free but glucose-containing environment. We have no professional knowledge that the treated animals consumed ConA itself as food, but the individuals remained in good shape. On the 25th day, this active ingredient did not affect the observed phenomenon.

In the acronym FROS, in addition to the reversibility of organ shrinkage ('R'), the 'F' stands for functionality, which refers to the remaining reproductive capacity of rotifers. The parameter measured on the 25th day was the number of eggs laid, which was compared with the reference values (**Fig. 21B**). In all groups, the number of eggs was low on D20 due to the minimal calorie intake. When Aβs was applied, the number of eggs was significantly increased in both rotifer species compared to ConA and control species; furthermore, Aβ42-treated animals laid especially more eggs than S-Aβ42-treated animals.

The integration of egg number data into time-dependent organ size changes resulted in a special formula, namely the FROS index, which is the indicator unit of current treatments. This index shows a linear correlation with the degree of autocatabolism. FROSi was positively lower in both species in the experiment affected by the respective agents compared to the controls (**Fig. 21C**). In contrast with their scrambled version, the FROS index of the natural aggregates showed that Aβ42 could be a food source for micrometazoans and a potential regulator of their systemic metabolism. However, *Philodina* and *Adineta* species showed the same changes; therefore, these effects of Aβ42 are non-species specific.

Figure 21. The effect of aggregated Aβ42 on the functionally reversible organ shrinkage (FROS). *The FROS was assessed in both P. acuticornis (PA) and A. vaga (AV) with using ConA, Aβ42 or S-Aβ42. The reproductive organ (germovitellaria) was monitored on days: D0, D20 and D25. (A) The organ-size during FROS (A) and the number of eggs on D20 and D25 (B) are presented. The D0 means 100 %. The error bars represent SEM. One-way ANOVA with Bonferroni post hoc test was applied for analysis, the levels of significance are p*, # ≤ 0.05, p¤¤ ≤ 0.01 and p***, ###, ¤¤¤≤ 0.001 (* difference from the same untreated control groups of the given species; #, difference from the same S-Aβ42-treated groups of the given species; ¤, difference from the D0 and D25 groups of the given species). FROS index (FROSi; relative unit) is presented (C) in untreated control, ConA, Aβ42 and S-Aβ42 groups.*

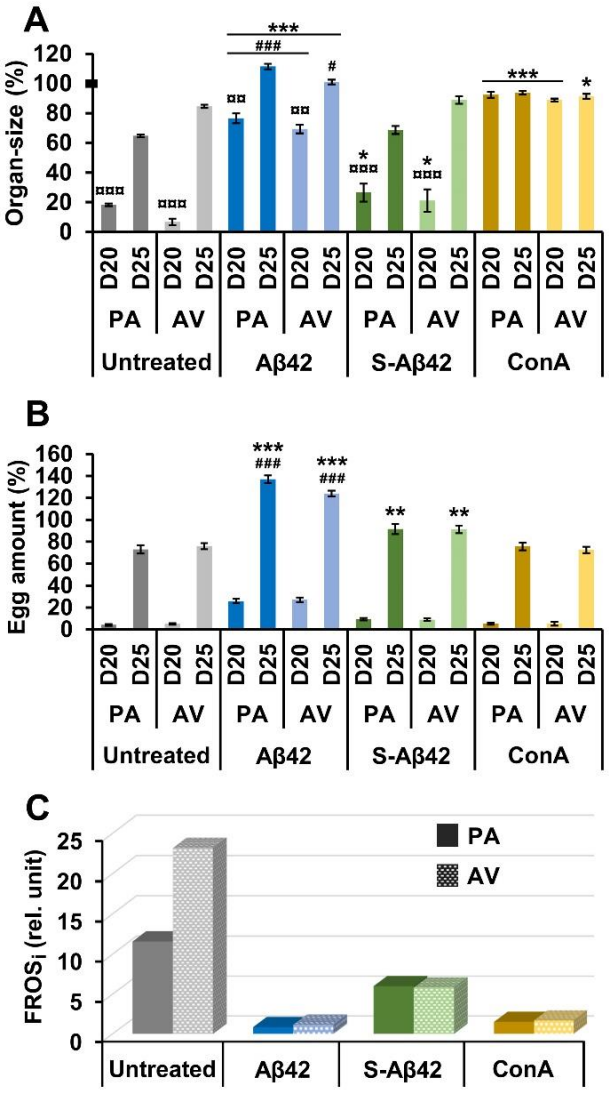

4.2.2. Depletion

We examined the Aβ-related toxicity in the presence of Rotimer (**Fig. 22**). The natural nutrient of rotifers includes conglomerated and slowly aggregated organic masses in their original habitat. Investigating the harmful Aβ42 on rotifers is an interdisciplinary approach in toxicology-related life sciences. Four species were treated with Aβ42 aggregates; only two secreted Rotimer (*E. dilatata*; *L. bulla*). Rotimer depletion was used in exudating animals to

investigate the role of this biopolymer in Aβ sensitivity and toxicity. We found that *E. dilatata* and *L. bulla* are not sensitive to Aβ42 aggregates in their healthy state, where the esterase activity and the number of living rotifers are the same as those of the species-specific untreated controls (100%). After *in vivo* biopolymer depletion, the animals lost their resistance against neurotoxic aggregates; the measured parameters were significantly reduced compared to their controls. A similar phenomenon (significant decrease) was also observed in those animals (*S. pectinata; C. intuta*) that did not secrete exogenous biopolymer. The esterase activity on the cell membrane integrity of the individuals, while the number of living rotifers is the *in vivo* characteristics of the studied populations. The number of rotifers alive refers to the *in vivo* characteristics of the studied populations, while the esterase activity indicates the cellular membrane integrity of the individuals.

Figure 22. The impacts of monogonant-secreted Rotimer on viability in beta-amyloid 1–42 (Aβ42)-treated populations are shown. *Four species were investigated: E. dilatata (ED); L. bulla (LB); C. intuta (CI) and S. pectinata (SP). The number of animals alive (colored orange) and the relative fluorescence intensity of the esterase activity (colored green) were measured, and their data were presented. The species-specific untreated control was the reference 100% (data not shown). The full columns show the Aβ42-treated normal (N) groups, while the stripped ones represent the Aβ42-administered or Rotimer-depleted (D) ones. The error bars represent S.E.M. One-way ANOVA with Bonferroni post hoc test was used for statistical analysis; the level of significance is p**** ≤ 0.0001 (*, significant difference from untreated species-specific control group). Above the columns, the black significance line represents treatments of the same quality.*

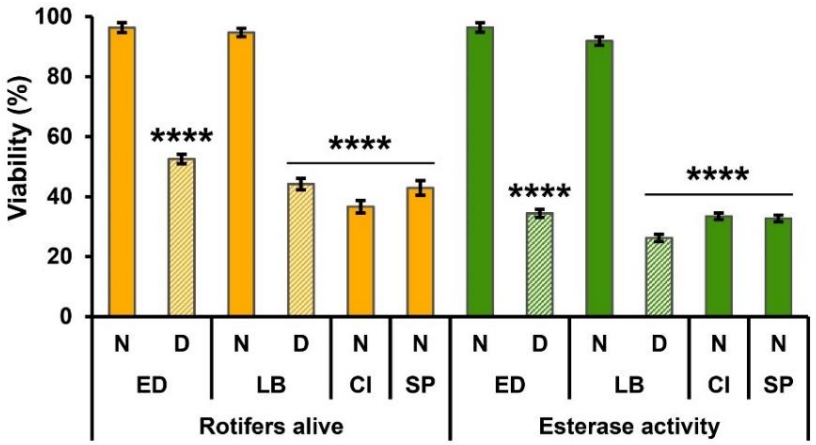

5. Discussion

Rotifers, as micrometazoans, are widely accepted ecological indicators and experimental animal models of aging, lifespan, toxicology, space exploration and pharmacology research. In addition, they have been gaining more relevance related to the *micro-in vivo* OMICS (genomics, transcriptomics, proteomics, glycomics) methodologies and environmentally friendly industrial technologies (e.g., water cleaning by exudates). Bdelloid rotifers (e.g., *P. acuticornis*) can catabolize neurotoxic aggregates *in vivo*, as these microinvertebrates are also able to use neurotoxic aggregates as an exclusive source of energy and organic matter, thereby extending their lifespan [22].

Living organisms produce biopolymers from specific monomers; therefore, they can be classified based on their basic chemical structures: polypeptides, polysaccharides, polynucleotides, and combined forms [63]. As natural and degradable organic materials, biopolymers can be used in all scientific fields, from nature conservation technologies to industrial nutrient production, for the delivery of genes and drugs, or the production of nanoparticles in translational biomedicine.

Our team has recently discovered and published the fact for the first time that rotifers are also capable of producing special biopolymers [75]. Due to its novelty, this family of rotifer-specific biopolymers, namely ‘rotimers’, is not yet known in detail. The induction of Rotimer secretion only occurs when the cilia of the rotifers are mechanically irritated with inert particles of different types and sizes (e.g., epoxy beads or Carmine). The resulting product is Rotimer-Inductor Conglomerate (RIC). The capacity of biopolymer production varies depending on the type of inductor used, and the RIC-producing ability of animals depends on viability. In addition, it is significantly modified according to physiological-, drug-and environmental effects. This filamentous, film-, and glue-like viscoelastic secretion has been observed in several monogonant and bdelloid species and are used by these small creatures to clean the medium (antiseptic and filtration effect), from food capture to egg placement (adhesive property).

Furthermore, we were also interested in how RIC can maintain its integrity in the presence of various chemicals. The result shows that the *E. dilatata*-produced conglomerate is affected by protein disruptors. This protein-type material may entirely or partially compose the Rotimer; however, it is resistant to several chemical influences. Based on the results of the FTIR analysis performed during Rotimer's biochemical test indicate strong H-bond-based interactions between the inductor Carmine crystals and the Rotimer, which exhibits a peptide-like nature.

However, separating peaks related to Rotimer alone was impossible due to the substantial overlap of the Carmine-Rotimer signals. The exact molecular identification of the Rotimer structure will require further investigation.

Various environmental factors (e.g., temperature, pH, metal ions, and chemicals) affect the production of Rotimer. RIC production is a preferable experimental indicator to follow up on this filamentous biopolymer secretion. Lucidril [110,111] may be highlighted for its holistic stimulating effect as a conclusion. Based on the above-described results concerning the pollutant agents, it is unequivocal that the activity or sensitivity of *E. dilatata* is more elevated than that of *L. bulla* related to the exudate secretion. Here, the goal was not to explore the relevant agent mechanism of action on the rotifers but to demonstrate these chemicals' various and holistic effects on the external secretion of micro-metazoans. Although both investigated rotifers are monogonant, their ancient evolutionary divergence can explain many of their phenotypic and physiological differences. These related species share only calcium-dependent biopolymer production, suggesting this is a phylogenetically ancient ability. The fact that our subjects retained this ability confirms the idea that this product is a multifunctional bioactive substance that also has a significant role as a bioindicator. Extensive investigation of Rotimer has many possibilities for various practical applications in the future. The fact that natural or artificial molecules affect microscopic populations in nature relatively quickly and in different ways, such as rotifers, in this case, raises the importance of preserving the natural environmental balance.

During the bioactivity experiments, this exudate has motility-inhibition effects in different cell types (e.g., algae and yeast). The measurements have shown their diverse and promising bioactivity inhibition of cancer neuroblastoma cell proliferation. The interaction between RIC and aggregates shows that *E. dilatata*- and *L. bulla*-RIC, with proteinous exudate on their surface, specifically bind the H-Aβ, which is an efficient influencing factor in aggregation kinetics; moreover, the activity of the species-specific biopolymers may differ from each other. There could be more explanation of the different behavior of the RIC on H-Aβ-binding and aggregating processes, derived from the two different species. One interpretation could be that *L. bulla* originally produced and adhered less biopolymer to the epoxy beads than *E. dilatata*. Another possibility could be that the biopolymers may differ in the various rotifer species in structure, functionality, and efficacy. The anti-aggregation effect of LB-RIC was not increased when the number of animals was higher with longer Rotimer secretion time, or a two-fold dose of RIC was tested in the presence of standard H-Aβ amount. The interaction between the Rotimer and the neurotoxic peptide aggregates (e.g., alpha-synuclein and prions) needs further

investigations. It is well-known that during the Rotimer secretion the calcium is built-in [112] and it may provide extra ionic characteristic to this biomaterial, therefore the metal ion content of biopolymer may enhance these molecular relations. The mechanism of anti- and disaggregating ability could be like the action of beta-sheet-breaker molecules or that of some natural (LPFFD, [113]; RIIGL, [114–116]) or artificial (LPYFD, [117,118]) peptide sequences. In summary, it is important to highlight that the direct molecular effects of natural polymers on neurodegeneration-related amyloids have been barely investigated, but there are just a few cases [57]. Based on the results obtained, it is assumed that Rotimer has some breaker activity, which can dissociate H-Aβ aggregates. The rotifer-specific biomaterials, namely Rotimer, were used for that purpose for the first time. Indirect *in vivo* measurements have been done [75] with respect to the protective role of Rotimer against H-Aβ, but *in vitro* binding, anti- and disaggregating experiments have never been performed previously. Moreover, this interdisciplinary approach may open novel perspectives also in pharmacological research against Alzheimer's disease.

Although this proteinous biopolymer's molecular structure and holistic biotechnological and biochemical significance are not yet known, further physicochemical analyses will be required. Based on the universal adhesive property of Rotimer, it may prove to be a useful tool in wastewater cleaning. Similarly, to other biopolymers [119], it may have a potential industrial use.

Rotifers are highly resistant to environmental alterations and successfully adapt to different types and amounts of nutrients in their natural habitat. The decomposition of organic matter in nature is a process that results in the formation of aggregates and conglomerates, which are potential nutrients for rotifers [41]. The metabolic utilization of all these available organic material resources is their particular property [42]. Before, nobody has investigated the *in vivo* catabolism of the Aβ as a food source or potential autocatabolism-regulator for multicellular entities. We applied an organ size-based *in vivo* monitoring system, exploring the autocatabolism-related alterations evoked by Aβ42, in a glucose-supplemented starvation model. The empirically well-monitored reduction in the size of bilateral germovitellaria (reproductive organ) in starved rotifers was attenuated by Aβ42, which served as a nutrient source- and peptide sequence-specific moderator during the organ shrinkage phase and enhanced the regenerative phase, including egg reproduction. The starvation-induced shrinkage of germovitellaria, with their regeneration and reproduction capability in these animals, is an adequate physiologic and experiential marker of autocatabolism, summarized by $FROS_i$. The FROSi of natural aggregates, in contrast to their artificial scrambled version, demonstrated that

the Aβ42 is not only a food source for rotifers but also a potential regulator and moderator of their systemic metabolism. *Philodina* and *Adineta* species showed similar types of lesions; therefore, it can be stated that these effects of Aβ42 are not limited to a specific species. By applying these microscopic invertebrates, the hitherto unknown roles of Aβ42 were demonstrated, providing additional tools for exploring relations between neurotoxic aggregates and metabolism. In another experiment, after *in vivo* biopolymer-depletion, the animals lost their resistance against neurotoxic aggregates. The above results suggest that Rotimer may play an essential protective role against Aβ aggregate toxicity in rotifers.

The cosmopolitan rotifers occur in fresh or saline water, soil, and arctic/high-altitude ice sheets. Their bioactive exudate can also play a globally decisive ecological regulatory and executive function. The impact of rotifers on the environment seems surprisingly wide-ranging. Based on this fact, we aimed to understand the mechanism of Rotimer production, their anatomical, physiological, genomic, and proteomic background, as well as their evolutionary biodiversity, their ecological role in nature, and their interdisciplinary translation possibilities. To have further and long-term plans for this natural organic product, comprehensive chemical and biological exploration is inevitable and necessary. Biopolymers can be used in all scientific fields, from nature conservation technologies to industrial nutrient production, the delivery of genes and drugs, or the production of nanoparticles to tissue regeneration. Our preliminary studies with Rotimers have not by far exhausted the versatility of this newly discovered and published molecule family, the natural and innovative potentials inherent in them.

6. Conclusion

The result of our work describes a novel and bioactive rotifer-specific biopolymer, called Rotimer, derived from certain monogonants. The motility-inhibiting effect of this bio-exudate was observed in various cell types, and its protective effect against dementia-specific aggregates in rotifers. During the investigations, it was found that the production of Rotimer proved to be obligatorily calcium-dependent; moreover, this special exudate is a promising bioindicator of the natural aquatic environment.

Our research group was the first to describe the in vitro interaction between Rotimer and H-Aβ by presenting biopolymers' anti- and disaggregating effects against Alzheimer's disease-type Aβs. The obtained results reflect the relationship between RIC and H-Aβ, in addition, the stable interaction thus formed also shows Aβ sequence specificity, since there was minimal binding between RIC and S-Aβ. The conglomerate of both monogonant rotifer species (*E. dilatata and L. bulla)* molecularly interacted with H-Aβ considered oligomer or fibril type; moreover, the ED-RIC was more effective in connecting and aggregation processes. Due to its properties mentioned above this natural material needs to study in the future; moreover, this biopolymer can be a relevant molecular specimen for developing drug candidates in neurodegeneration-related research.

Summary of the main findings were the following:

1. An exceptional relationship can develop between rotifers and human-type beta-amyloid (Aβ) aggregates under laboratory conditions (e.g., using amyloid as a nutrient source).

2. As an exudate production, the secretion of rotifer-specific biopolymer (Rotimer) is an obligatory calcium-dependent process and a philogenetically ancient phenomenon in rotifers.

3. Rotimer is a proteinous biomolecule that is sensitive to proteases.

4. Rotimer is not a toxic substance for different biological models but can universally block the motility of different cell types.

5. Endogenous Rotimer has a protective effect *in vivo* against the toxicity of Aβ aggregates.

6. Aβ aggregates are not only sources of nutrients but also regulators of the rotifer's metabolism.

7. Rotimer specifically binds to Aβ aggregates *in vitro* and affects their aggregation.

8. Rotimer may contain promising molecular information for Alzheimer's disease drug discovery.

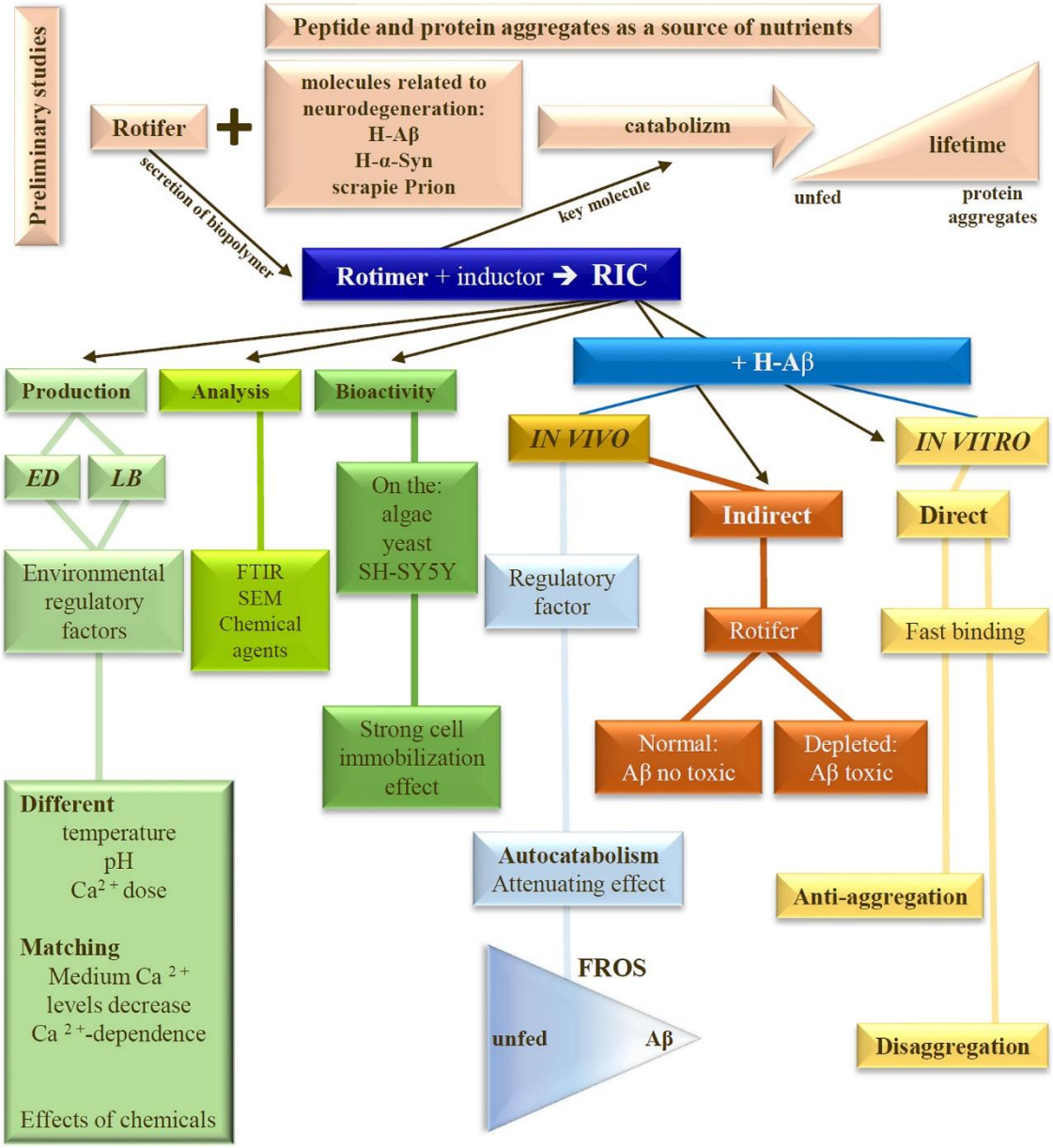
Preliminary studies
Peptide and protein aggregates as a source of nutrients
Rotifer
molecules related to neurodegeneration: H-Aβ H-α-Syn scrapie Prion
catabolizm
lifetime
unfed
protein aggregates
secretion of biopolymer
key molecule
Rotimer + inductor → RIC
+ H-Aβ
Production
Analysis
Bioactivity
IN VIVO
IN VITRO
ED
LB
On the: algae yeast SH-SY5Y
Indirect
Direct
Environmental regulatory factors
FTIR SEM Chemical agents
Regulatory factor
Rotifer
Fast binding
Strong cell immobilization effect
Normal: Aβ no toxic
Depleted: Aβ toxic
Different temperature pH Ca2+ dose
Matching Medium Ca 2+ levels decrease Ca 2+-dependence
Effects of chemicals
Autocatabolism Attenuating effect
Anti-aggregation
FROS
unfed
Aβ
Disaggregation

7. Acknowledgement

I am grateful to my supervisor, Dr. Zsolt László Datki for his mentoring, for his contribution to my every success through my PhD years and for his help for the thesis preparation. I would like to thank Professor János Kálmán, who provided me an opportunity to join the Research Group of Department of Psychiatry, University of Szeged, and Ilona Molnárné Hatvani for the laboratory assistance.
Finally, I would like to thank my parents and my husband for their steadfast support during these years.

Fundings: This project was supported by developing scientific workshops of medical-, health sciences and pharmaceutical training grant number: EFOP-3.6.3-VEKOP-16-2017-00009 (code: PÁL20042011381762038); grant number: EFOP-3.6.3-VEKOP-16-2017-00009 (code: PÁL21042117210434374); by Albert Szent-Györgyi supplementary PhD scholarship (code: PÁL22102213443610057); by New National Excellence Program (code: ÚJ22050912355186557); by the János Bolyai Research Scholarship of the Hungarian Academy of Sciences as well as TKP2021-EGA-32 of the Ministry for Innovation and Technology from the source of the National Research, Development and Innovation Found, financed under the TKP2021-EGA funding scheme.

8. References

[1] Makin S. The prion principle. Nature 2016:538:S13–S16. https://doi.org/https://doi.org/10.1038/538S13a.

[2] Wildburger NC, Esparza TJ, Leduc RD, Fellers RT, Thomas PM, Cairns NJ, et al. Diversity of Amyloid-beta Proteoforms in the Alzheimer's Disease Brain. Sci Rep 2017;7. https://doi.org/10.1038/s41598-017-10422-x.

[3] Wyss-Coray T. Ageing, neurodegeneration and brain rejuvenation. Nature 2016;539:180–6. https://doi.org/10.1038/nature20411.

[4] Morell M, Bravo R, Espargaró A, Sisquella X, Avilés FX, Fernàndez-Busquets X, et al. Inclusion bodies: Specificity in their aggregation process and amyloid-like structure. Biochim Biophys Acta - Mol Cell Res 2008;1783:1815–25. https://doi.org/10.1016/j.bbamcr.2008.06.007.

[5] Wang L, Maji SK, Sawaya MR, Eisenberg D, Riek R. Bacterial Inclusion Bodies Contain Amyloid-Like Structure 2008. https://doi.org/10.1371/journal.pbio.

[6] Chi H, Chang HY, Sang TK. Neuronal cell death mechanisms in major neurodegenerative diseases. Int J Mol Sci 2018;19. https://doi.org/10.3390/ijms19103082.

[7] Backstrom JR, Lim GP, Cullen MJ, Tökés ZA. Matrix metalloproteinase-9 (MMP-9) is synthesized in neurons of the human hippocampus and is capable of degrading the amyloid-β peptide (1-40). J Neurosci 1996;16:7910–9. https://doi.org/10.1523/jneurosci.16-24-07910.1996.

[8] Ross CA, Poirier MA. Protein aggregation and neurodegenerative disease. Nat Med 2004;10:S10. https://doi.org/10.1038/nm1066.

[9] Kurochkin I V., Goto S. Alzheimer's β-amyloid peptide specifically interacts with and is degraded by insulin degrading enzyme. FEBS Lett 1994;345:33–7. https://doi.org/10.1016/0014-5793(94)00387-4.

[10] Iwata N, Tsubuki S, Takaki Y, Watanabe K, Sekiguchi M HE et al. Identification of the major Abeta1-42-degrading catabolic pathway in brain parenchyma: suppression leads to biochemical and pathological deposition. Nat Med 2000:6:143–50. https://doi.org/https://doi.org/10.1038/72237.

[11] Eckman EA, Reed DK, Eckman CB. Degradation of the Alzheimer's Amyloid β Peptide by Endothelin-converting Enzyme. J Biol Chem 2001;276:24540–8. https://doi.org/10.1074/jbc.M007579200.

[12] Hemming ML, Selkoe DJ, Farris W. Effects of prolonged angiotensin-converting enzyme inhibitor treatment on amyloid β-protein metabolism in mouse models of Alzheimer disease. Neurobiol Dis 2007;26:273–81. https://doi.org/10.1016/j.nbd.2007.01.004.

[13] Tucker HM, Kihiko M, Caldwell JN, Wright S, Kawarabayashi T, Price D, et al. The Plasmin System Is Induced by and Degrades Amyloid-Aggregates. J Neurosci 2000:20(11):3937–3946. https://doi.org/10.1523/JNEUROSCI.20-11-03937.2000.

[14] Baranello R, Bharani K, Padmaraju V, Chopra N, Lahiri D, Greig N, et al. Amyloid-

Beta Protein Clearance and Degradation (ABCD) Pathways and their Role in Alzheimer's Disease. Curr Alzheimer Res 2015;12:32–46. https://doi.org/10.2174/1567205012666141218140953.

[15] Kumar V, Sami N, Kashav T, Islam A, Ahmad F, Hassan MI. Protein aggregation and neurodegenerative diseases: From theory to therapy. Eur J Med Chem 2016;124:1105–20. https://doi.org/10.1016/j.ejmech.2016.07.054.

[16] Datki Z, Juhász A, Gálfi M, Soós K, Papp R, Zádori D, et al. Method for measuring neurotoxicity of aggregating polypeptides with the MTT assay on differentiated neuroblastoma cells. Brain Res Bull 2003;62:223–9. https://doi.org/10.1016/j.brainresbull.2003.09.011.

[17] Poeggeler B, Durand G, Polidori A, Pappolla MA, Vega-Naredo I, Coto-Montes A, et al. Mitochondrial medicine: Neuroprotection and life extension by the new amphiphilic nitrone LPBNAH acting as a highly potent antioxidant agent. J Neurochem 2005;95:962–73. https://doi.org/10.1111/j.1471-4159.2005.03425.x.

[18] Harkany T, Timmerman W, Laskay G, To B, Sasva Âri M, Ko C, et al. Beta-Amyloid neurotoxicity is mediated by a glutamate-triggered excitotoxic cascade in rat nucleus basalis. Eur J Neurosci Eur J Neurosci 2000. https://doi.org/10.1046/j.1460-9568.2000.00164.x.

[19] Kong Y, Li K, Fu T, Wan C, Zhang D, Song H, et al. Quercetin ameliorates Aβ toxicity in Drosophila AD model by modulating cell cycle-related protein expression. Oncotarget, 2016;7. https://doi.org/10.18632/oncotarget.11963.

[20] Sharma N, Khurana N, Muthuraman A. Lower vertebrate and invertebrate models of Alzheimer's disease – A review. Eur J Pharmacol 2017;815:312–23. https://doi.org/10.1016/j.ejphar.2017.09.017.

[21] Datki Z, Olah Z, Hortobagyi T, Macsai L, Zsuga K, Fulop L, et al. Exceptional in vivo catabolism of neurodegeneration-related aggregates. Zool Lett 2018;4:1–12. https://doi.org/10.1186/s40478-018-0507-3.

[22] Datki Z, Galik-Olah Z, Bohar Z, Zadori D, Fulop F, Szatmari I, et al. Kynurenic acid and its analogs are beneficial physiologic attenuators in bdelloid rotifers. Molecules 2019;24. https://doi.org/10.3390/molecules24112171.

[23] Snell TW, Johnston RK, Gribble KE, Mark Welch DB. Rotifers as experimental tools for investigating aging. Invertebr Reprod Dev 2015;59:5–10. https://doi.org/10.1080/07924259.2014.925516.

[24] Macsai L, Olah Z, Bush AI, Galik B, Onody R, Kalman J, et al. Redox modulating factors impact longevity regulation in rotifers. J Gerontol A Biol Sci Med Sci 2018:74, 811–814. https://doi.org/10.1093/gerona/gly193/5079904.

[25] Rico-Martínez R, Arzate-Cárdenas MA, Robles-Vargas D, Pérez-Legaspi IA, Alvarado-Flores J, Santos-Medrano GE. Rotifers as Models in Toxicity Screening of Chemicals and Environmental Samples. Invertebr. - Exp. Model. Toxic. Screen., InTech; 2016. https://doi.org/10.5772/61771.

[26] Dahms HU, Hagiwara A, Lee JS. Ecotoxicology, ecophysiology, and mechanistic studies with rotifers. Aquat Toxicol 2011;101:1–12. https://doi.org/10.1016/j.aquatox.2010.09.006.

[27] Clement P, Amsellem J, Cornillac A-M, Luciani' A, Ricci' C. An ultrastructural approach to feeding behaviour in Philodina roseola and Brachionus calycyflorus (rotifers). 1980. https://doi.org/https://doi.org/10.1007/BF00019437.

[28] Hochberg R, Litvaitis MK. Functional morphology of the muscles in Philodina sp. (Rotifera: Bdelloidea). Hydrobiologia 2000;432:57–64.

[29] Marotta R, Uggetti A, Ricci C, Leasi F, Melone G. Surviving starvation: Changes accompanying starvation tolerance in a bdelloid rotifer. J Morphol 2012;273:1–7. https://doi.org/10.1002/jmor.11000.

[30] Ricci C. Culturing of some bdelloid rotifers. Hydrobiologia 1984:122: 45–51. https://doi.org/https://doi.org/10.1007/BF00007665.

[31] Olah Z, Bush AI, Aleksza D, Galik B, Ivitz E, Macsai L, et al. Novel in vivo experimental viability assays with high sensitivity and throughput capacity using a bdelloid rotifer. Ecotoxicol Environ Saf 2017;144:115–22. https://doi.org/10.1016/j.ecoenv.2017.06.005.

[32] Van Cleave HJ. Eutely or Cell Constancy in Its Relation to Body Size. Q Rev Biol 1932:Vol. 7, No. 1, pp. 59-67 (9 pages). https://doi.org/https://doi.org/10.1086/394396.

[33] Azevedo RBR, Leroi AM. A power law for cells. Proc Natl Acad Sci 2001:98 (10) 5699-5704. https://doi.org/https://doi.org/10.1073/pnas.091485998.

[34] Jönsson KI, Wojcik A. Tolerance to X-rays and heavy ions (Fe, He) in the tardigrade richtersius coronifer and the bdelloid rotifer mniobia russeola. Astrobiology 2017;17:163–7. https://doi.org/10.1089/ast.2015.1462.

[35] Kanazawa M, Nanri T, Saigusa M. Anhydrobiosis Affects Thermal Habituation in the Bdelloid Rotifer, Adineta sp. Zoolog Sci 2017;34:81–5. https://doi.org/10.2108/zs160057.

[36] Shain DH, Halldórsdóttir K, Pálsson F, Adalgeirsdóttir G, Gunnarsson A, Jónsson T, et al. Colonization of maritime glacier ice by bdelloid Rotifera. Mol Phylogenet Evol 2016;98:280–7. https://doi.org/10.1016/j.ympev.2016.02.020.

[37] Cervellione F, McGurk C, Berger Eriksen T, Van den Broeck W. Effect of starvation and refeeding on the hepatopancreas of whiteleg shrimp Penaeus vannamei (Boone) using computer-assisted image analysis. J Fish Dis 2017;40:1707–15. https://doi.org/10.1111/jfd.12639.

[38] Gilbert JJ. Non-genetic polymorphisms in rotifers: Environmental and endogenous controls, development, and features for predictable or unpredictable environments. Biol Rev 2017;92:964–92. https://doi.org/10.1111/brv.12264.

[39] Wallace RL, Snell TW. Rotifera. Ecol. Classif. North Am. Freshw. Invertebr., Elsevier Inc.; 2010, p. 173–235. https://doi.org/10.1016/B978-0-12-374855-3.00008-X.

[40] Castro BB, Antunes SC, Pereira R, Soares AMVM, Gonçalves F. Rotifer community structure in three shallow lakes: Seasonal fluctuations and explanatory factors. Hydrobiologia 2005;543:221–32. https://doi.org/10.1007/s10750-004-7453-8.

[41] Ganesan AR, Saravana Guru M, Balasubramanian B, Mohan K, Chao Liu W, Valan Arasu M, et al. Biopolymer from edible marine invertebrates: A potential functional food. J King Saud Univ - Sci 2020;32:1772–7.

https://doi.org/10.1016/j.jksus.2020.01.015.

[42] Chandra R, Rustgi R. BIODEGRADABLE POLYMERS. Prog Polym Sci 1998;23:1273–335. https://doi.org/10.1016/S0079-6700(97)00039-7.

[43] Hassan MES, Bai J, Dou D-Q. Biopolymers; definition, classification and applications. Egypt J Chem 2019;62:1725–37. https://doi.org/10.21608/EJCHEM.2019.6967.1580.

[44] Silva MA da, Bierhalz ACK, Kieckbusch TG. Alginate and pectin composite films crosslinked with Ca2+ ions: Effect of the plasticizer concentration. Carbohydr Polym 2009;77:736–42. https://doi.org/10.1016/j.carbpol.2009.02.014.

[45] Hennebert E, Gregorowicz E, Flammang P. Involvement of sulfated biopolymers in adhesive secretions produced by marine invertebrates. Biol Open 2018. https://doi.org/10.1242/bio.037358.

[46] Muhlia-Almazán A, Sánchez-Paz A, García-Carreño FL. Invertebrate trypsins: A review. J Comp Physiol B Biochem Syst Environ Physiol 2008;178:655–72. https://doi.org/10.1007/s00360-008-0263-y.

[47] Kamiya H, Sakai R, Jimbo M. Bioactive Molecules from Sea Hares. Prog Mol Subcell Biol 2006:215–239. https://doi.org/10.1007/978-3-540-30880-5_10.

[48] Azizur Rahman M. Collagen of extracellular matrix from marine invertebrates and its medical applications. Mar Drugs 2019;17. https://doi.org/10.3390/md17020118.

[49] Ruiz-Torres V, Rodríguez-Pérez C, Herranz-López M, Martín-García B, Gómez-Caravaca AM, Arráez-Román D, et al. Marine invertebrate extracts induce colon cancer cell death via ros-mediated dna oxidative damage and mitochondrial impairment. Biomolecules 2019;9. https://doi.org/10.3390/biom9120771.

[50] Yavuz B, Chambre L, Kaplan DL. Extended release formulations using silk proteins for controlled delivery of therapeutics. Expert Opin Drug Deliv 2019;16:741–56. https://doi.org/10.1080/17425247.2019.1635116.

[51] Humenik M, Pawar K, Scheibel T. Nanostructured, self-assembled spider silk materials for biomedical applications. Biol Bio-Inspired Nanomater 2019:187–221. https://doi.org/https://doi.org/10.1007/978-981-13-9791-2_6.

[52] Chen Q, Peng D. Nematode chitin and application. Adv. Exp. Med. Biol., vol. 1142, Springer New York LLC; 2019, p. 209–19. https://doi.org/10.1007/978-981-13-7318-3_10.

[53] Mohamed SAA, El-Sakhawy M, El-Sakhawy MAM. Polysaccharides, Protein and Lipid -Based Natural Edible Films in Food Packaging: A Review. Carbohydr Polym 2020;238. https://doi.org/10.1016/j.carbpol.2020.116178.

[54] Lalit R, Mayank P, Ankur K. Natural fibers and biopolymers characterization: A future potential composite material. Stroj Cas 2018;68:33–50. https://doi.org/10.2478/scjme-2018-0004.

[55] George A, Sanjay MR, Srisuk R, Parameswaranpillai J, Siengchin S. A comprehensive review on chemical properties and applications of biopolymers and their composites. Int J Biol Macromol 2020;154:329–38. https://doi.org/10.1016/j.ijbiomac.2020.03.120.

[56] Wilkinson KJ, Joz-Roland A, Buffle J. Different roles of pedogenic fulvic acids and aquagenic biopolymers on colloid aggregation and stability in freshwaters. Limnol

Oceanogr 1997;42:1714–24. https://doi.org/10.4319/lo.1997.42.8.1714.

[57] Meesaragandla B, Karanth S, Janke U, Delcea M. Biopolymer-coated gold nanoparticles inhibit human insulin amyloid fibrillation. Sci Rep 2020;10:1–14. https://doi.org/10.1038/s41598-020-64010-7.

[58] Bezerra LS, Magnani M, Castro-Gomez RJH, Cavalcante HC, Silva TAF da, Vieira RLP, et al. Modulation of vascular function and anti-aggregation effect induced by (1 → 3) (1 → 6)-β-D-glucan of Saccharomyces cerevisiae and its carboxymethylated derivative in rats. Pharmacol Reports 2017;69:448–55. https://doi.org/10.1016/j.pharep.2017.01.002.

[59] Roman SG, Chebotareva NA, Kurganov BI. Anti-aggregation activity of small heat shock proteins under crowded conditions. Int J Biol Macromol 2017;100:97–103. https://doi.org/10.1016/j.ijbiomac.2016.05.080.

[60] Nagarajan S, Radhakrishnan S, Kalkura SN, Balme S, Miele P, Bechelany M. Overview of Protein-Based Biopolymers for Biomedical Application. Macromol Chem Phys 2019;220:1–16. https://doi.org/10.1002/macp.201900126.

[61] Elzoghby AO, Samy WM, Elgindy NA. Protein-based nanocarriers as promising drug and gene delivery systems. J Control Release 2012;161:38–49. https://doi.org/10.1016/j.jconrel.2012.04.036.

[62] Nitta SK, Numata K. Biopolymer-based nanoparticles for drug/gene delivery and tissue engineering. Int J Mol Sci 2013;14:1629–54. https://doi.org/10.3390/ijms14011629.

[63] Mohan S, Oluwafemi OS, Kalarikkal N, Thomas S, Songca SP. Biopolymers – Application in Nanoscience and Nanotechnology. Recent Adv Biopolym 2016:47–72. https://doi.org/10.5772/62225.

[64] Bozso Z, Penke B, Simon D, Laczkó I, Juhász G, Szegedi V, et al. Controlled in situ preparation of Aβ(1-42) oligomers from the isopeptide “iso-Aβ(1-42)”, physicochemical and biological characterization. Peptides 2010;31:248–56. https://doi.org/10.1016/j.peptides.2009.12.001.

[65] Kalweit AN, Yang H, Colitti-Klausnitzer J, Fulóp L, Bozsó Z, Penke B, et al. Acute intracerebral treatment with amyloid-beta (1-42) alters the profile of neuronal oscillations that accompany LTP induction and results in impaired LTP in freely behaving rats. Front Behav Neurosci 2015;9:1–16. https://doi.org/10.3389/fnbeh.2015.00103.

[66] Kertész K. Budapest és környékének rotatoria-faunája. Rózsa Kálmán; 1894.

[67] Kutikova LA. Kolovratki fauna SSSR. Fauna SSSR, 1970.

[68] Voigt M, Koste W. Rotatoria 1978.

[69] Nogrady, T., Segers, H. Rotifera Vol. 6: Asplanchnidae, Gastropodidae, Lindiidae, Microcodidae, Synchaetidae, Trocoshphaeridae and Filinia. In: Dumont, H.J. (Ed.), Guides to the Identification of the Microinvertebrates of the Continental Waters of the World. Leiden, pp. 59–79.; 2002.

[70] Varga L. Rotifers I. Hungarian Academy of Sciences, Budapest. 1966.

[71] Datki Z, Olah Z, Macsai L, Pakaski M, Galik B, Mihaly G, et al. Application of BisANS fluorescent dye for developing a novel protein assay. PLoS One 2019;14.

https://doi.org/10.1371/journal.pone.0215863.

[72] Mozes E, Hunya A, Toth A, Ayaydin F, Penke B, Datki ZL. A novel application of the fluorescent dye bis-ANS for labeling neurons in acute brain slices. Brain Res Bull 2011;86:217–21. https://doi.org/10.1016/j.brainresbull.2011.07.004.

[73] Kang HM, Jeong CB, Kim MS, Lee JS, Zhou J, Lee YH, et al. The role of the p38-activated protein kinase signaling pathway-mediated autophagy in cadmium-exposed monogonont rotifer Brachious koreanus. Aquat Toxicol 2018;194:46–56. https://doi.org/10.1016/j.aquatox.2017.11.002.

[74] Collins TJ. ImageJ for microscopy. Biotechniques 2007;43:S25–30. https://doi.org/10.2144/000112517.

[75] Datki Z, Acs E, Balazs E, Sovany T, Csoka I, Zsuga K, et al. Exogenic production of bioactive filamentous biopolymer by monogonant rotifers. Ecotoxicol Environ Saf 2021;208:111666. https://doi.org/10.1016/j.ecoenv.2020.111666.

[76] Kowalczuk D, Pitucha M. Application of FTIR method for the assessment of immobilization of active substances in the matrix of biomedical materials. Materials (Basel) 2019;12. https://doi.org/10.3390/ma12182972.

[77] Chen J, Wang Z, Li G, Guo R. The swimming speed alteration of two freshwater rotifers Brachionus calyciflorus and Asplanchna brightwelli under dimethoate stress. Chemosphere 2014;95:256–60. https://doi.org/10.1016/j.chemosphere.2013.08.086.

[78] Guo R, Ren X, Ren H. A new method for analysis of the toxicity of organophosphorus pesticide, dimethoate on rotifer based on response surface methodology. J Hazard Mater 2012;237–238:270–6. https://doi.org/10.1016/j.jhazmat.2012.08.041.

[79] Dong LL, Wang HX, Ding T, Li W, Zhang G. Effects of TiO2 nanoparticles on the life-table parameters, antioxidant indices, and swimming speed of the freshwater rotifer Brachionus calyciflorus. J Exp Zool Part A Ecol Integr Physiol 2020;333:230–9. https://doi.org/10.1002/jez.2343.

[80] Venâncio C, Castro BB, Ribeiro R, Antunes SC, Abrantes N, Soares AMVM, et al. Sensitivity of freshwater species under single and multigenerational exposure to seawater intrusion. Philos Trans R Soc B Biol Sci 2019;374. https://doi.org/10.1098/rstb.2018.0252.

[81] Lee MC, Park JC, Yoon DS, Han J, Kang S, Kamizono S, et al. Aging extension and modifications of lipid metabolism in the monogonont rotifer Brachionus koreanus under chronic caloric restriction. Sci Rep 2018;8. https://doi.org/10.1038/s41598-018-20108-7.

[82] Cardwell AS, Adams WJ, Gensemer RW, Nordheim E, Santore RC, Ryan AC, et al. Chronic toxicity of aluminum, at a pH of 6, to freshwater organisms: Empirical data for the development of international regulatory standards/criteria. Environ Toxicol Chem 2018;37:36–48. https://doi.org/10.1002/etc.3901.

[83] Citarasu T, Punitha S, Selvaraj T, Albindas S, Sindhu A, Michael Babu M. Influence of physical and nutritive parameters of population and size variation in two species of rotifer. J Aqua Trop, 2014:29: 121-134.

[84] Armour MA. Protecting health from metal exposures in drinking water. Rev Environ Health 2016;31:29–31. https://doi.org/10.1515/reveh-2015-0079.

[85] Curnutt A, Smith K, Darrow E, Walters KB. Chemical and Microstructural Characterization of pH and [Ca2+] Dependent Sol-Gel Transitions in Mucin Biopolymer. Sci Rep 2020;10. https://doi.org/10.1038/s41598-020-65392-4.

[86] Saris N-EL, Mervaala E, Karppanen H, Khawaja JA, Lewenstam A. Magnesium An update on physiological, clinical and analytical aspects. Clin Chim Acta 2000;294:1–26. https://doi.org/10.1016/S0009-8981(99)00258-2.

[87] Hendrych M, Olejnickova V, Novakova M. Calcium versus strontium handling by the heart muscle. Gen Physiol Biophys 2016;35:13–23. https://doi.org/10.4149/gpb_2015026.

[88] Zaitoun MA, Lin CT. Chelating Behavior between Metal Ions and EDTA in Sol-Gel Matrix. J Phys Chem B, 1997:101(10), 1857–1860. https://doi.org/10.1021/jp963102d.

[89] George T, Brady MF. Ethylenediaminetetraacetic acid (EDTA). 2020.

[90] Wang L, Shelton RM, Cooper PR, Lawson M, Triffitt JT, Barralet JE. Evaluation of sodium alginate for bone marrow cell tissue engineering. Biomaterials 2003;24:3475–81. https://doi.org/10.1016/S0142-9612(03)00167-4.

[91] Ehrlich H. Biologically-Inspired Systems Marine Biological Materials of Invertebrate Origin, 2019, p. ISBN:978-3-319-92483-0.

[92] Zhang S, Li C, Gao J, Qiu X, Cui Z. 0 1 4 年 3 月 第 1 7 卷 第 3 期 Chin J Lung Cancer 2014;2. https://doi.org/10.3779/j.issn.1009-3419.2014.03.03.

[93] Mitterer RM. Amino Acid Composition and Metal Binding Capability of the Skeletal Protein of Corals. vol. 28. 1978.

[94] Howard L, Brown B. Heavy metals and reef corals. Oceanogr. Mar. Biol. An Annu. Rev., vol. 22, Aberdeen University Press Aberdeen, UK; 1984, p. 192–208.

[95] Bieber S, Snyder SA, Dagnino S, Rauch-Williams T, Drewes JE. Management strategies for trace organic chemicals in water – A review of international approaches. Chemosphere 2018;195:410–26. https://doi.org/10.1016/j.chemosphere.2017.12.100.

[96] Murube J. Tear crystallization test: Two centuries of history. Ocul Surf 2004;2:7–9. https://doi.org/10.1016/S1542-0124(12)70019-8.

[97] Solé A. Untersuchung über die Bewegung der Teilchen im Stagogramm und Influenzstagogramm. Kolloid-Zeitschrift 1957;151:55–62. https://doi.org/10.1007/BF01502258.

[98] Younan ND, Viles JH. A Comparison of Three Fluorophores for the Detection of Amyloid Fibers and Prefibrillar Oligomeric Assemblies. ThT (Thioflavin T); ANS (1-Anilinonaphthalene-8-sulfonic Acid); and bisANS (4,4′-Dianilino-1,1′-binaphthyl-5,5′-disulfonic Acid). Biochemistry 2015;54:4297–306. https://doi.org/10.1021/acs.biochem.5b00309.

[99] Yu M, Ryan TM, Ellis S, Bush AI, Triccas JA, Rutledge PJ, et al. Neuroprotective peptide-macrocycle conjugates reveal complex structure-activity relationships in their interactions with amyloid β. Metallomics 2014;6:1931–40. https://doi.org/10.1039/c4mt00122b.

[100] Levine H. Thioflavine T interaction with synthetic Alzheimer's disease β-amyloid

peptides: Detection of amyloid aggregation in solution. Protein Sci 1993;2:404–10. https://doi.org/10.1002/pro.5560020312.

[101] Xue C, Lin TY, Chang D, Guo Z. Thioflavin T as an amyloid dye: Fibril quantification, optimal concentration and effect on aggregation. R Soc Open Sci 2017;4. https://doi.org/10.1098/rsos.160696.

[102] Pellarin R, Caflisch A. Interpreting the Aggregation Kinetics of Amyloid Peptides. J Mol Biol 2006;360:882–92. https://doi.org/10.1016/j.jmb.2006.05.033.

[103] Sharma A, McDonald MA, Rose HB, Chernoff YO, Behrens SH, Bommarius AS. Modeling Amyloid Aggregation Kinetics: A Case Study with Sup35NM. J Phys Chem B 2021;125:4955–63. https://doi.org/10.1021/acs.jpcb.0c11250.

[104] Lin Y, Im H, Diem LT, Ham S. Characterizing the structural and thermodynamic properties of Aβ42 and Aβ40. Biochem Biophys Res Commun 2019;510:442–8. https://doi.org/10.1016/j.bbrc.2019.01.124.

[105] Bartus É, Olajos G, Schuster I, Bozsó Z, Deli MA, Veszelka S, et al. Structural optimization of foldamer-dendrimer conjugates as multivalent agents against the toxic effects of amyloid beta oligomers. Molecules 2018;23. https://doi.org/10.3390/molecules23102523.

[106] Puente C, Hendrickson RC, Jiang X. Nutrient-regulated phosphorylation of ATG13 inhibits starvation-induced autophagy. J Biol Chem 2016;291:6026–35. https://doi.org/10.1074/jbc.M115.689646.

[107] Johnson RM, Allen C, Melman SD, Waller A, Young SM, Sklar LA, et al. Identification of inhibitors of vacuolar proton-translocating ATPase pumps in yeast by high-throughput screening flow cytometry. Anal Biochem 2010;398:203–11. https://doi.org/10.1016/j.ab.2009.12.020.

[108] Tan XY, Wang X, Liu QS, Xie XQ, Li Y, Li BQ, et al. Inhibition of silkworm vacuolar-type ATPase activity by its inhibitor Bafilomycin A1 induces caspase-dependent apoptosis in an embryonic cell line of silkworm. Arch Insect Biochem Physiol 2018;99. https://doi.org/10.1002/arch.21507.

[109] Vadukul DM, Gbajumo O, Marshall KE, Serpell LC. Amyloidogenicity and toxicity of the reverse and scrambled variants of amyloid-β 1-42. FEBS Lett 2017;591:822–30. https://doi.org/10.1002/1873-3468.12590.

[110] Lazarova-Bakarova MB, Genkova-Papasova MG. Influence of nootropic drugs on the memory-impairing effect of clonidine in albino rats. Methods Find Exp Clin Pharmacol 1989;11:235–9.

[111] Verma R, Nehru B. Effect of centrophenoxine against rotenone-induced oxidative stress in an animal model of Parkinson's disease. Neurochem Int 2009;55:369–75. https://doi.org/10.1016/j.neuint.2009.04.001.

[112] Balazs E, Galik-Olah Z, Galik B, Somogyvari F, Kalman J, Datki Z. External modulation of Rotimer exudate secretion in monogonant rotifers. Ecotoxicol Environ Saf 2021;220. https://doi.org/10.1016/j.ecoenv.2021.112399.

[113] C Soto, E M Sigurdsson, L Morelli, R A Kumar, E M Castaño BF. Beta-sheet breaker peptides inhibit fibrillogenesis in a rat brain model of amyloidosis: implications for Alzheimer's therapy. Nat Med 1998:822–6. https://doi.org/10.1038/nm0798-822.

[114] Fülöp L, Zarándi M, Datki Z, Soós K, Penke B. β-Amyloid-derived pentapeptide RIIGL a inhibits Aβ 1-42 aggregation and toxicity. Biochem Biophys Res Commun 2004;324:64–9. https://doi.org/10.1016/j.bbrc.2004.09.024.

[115] Murvai Ü, Soós K, Penke B, Kellermayer MSZ. Effect of the beta-sheet-breaker peptide LPFFD on oriented network of amyloid β25-35 fibrils. J Mol Recognit 2011;24:453–60. https://doi.org/10.1002/jmr.1113.

[116] Viet MH, Ngo ST, Lam NS, Li MS. Inhibition of aggregation of amyloid peptides by beta-sheet breaker peptides and their binding affinity. J Phys Chem B 2011;115:7433–46. https://doi.org/10.1021/jp1116728.

[117] Laczkó I, Vass E, Soós K, FüLöp L, Zarándi M, Penke B. Aggregation of Aβ(1-42) in the presence of short peptides: Conformational studies. J Pept Sci 2008;14:731–41. https://doi.org/10.1002/psc.990.

[118] Datki Z, Papp R, Zádori D, Soós K, Fülöp L, Juhász A, et al. In vitro model of neurotoxicity of Aβ 1-42 and neuroprotection by a pentapeptide: Irreversible events during the first hour. Neurobiol Dis 2004;17:507–15. https://doi.org/10.1016/j.nbd.2004.08.007.

[119] Kalia S, Averous L. Biopolymers: biomedical and environmental applications. John Wiley Sons, 2011;70. https://doi.org/10.1002/9781118164792.

9. Appendix

1.sz. melléklet

Társszerzői lemondó nyilatkozat

Co-author certification

Alulírott Dr. Datki Zsolt László (felelős társszerző, levelező szerző) kijelentem, hogy Dobóczky-Balázs Evelin (pályázó) PhD értekezésének tézispontjaiban bemutatott - közösen publikált - tudományos eredmények elérésében a pályázónak meghatározó szerepe volt, ezért ezeket a téziseket más a PhD fokozat megszerzését célzó minősítési eljárásban nem használta fel, illetve nem kívánja felhasználni.

2023.02.07.

SZEGEDI TUDOMÁNYEGYETEM Pszichiátriai Klinika 34 SZEGED

.....
szerző

A pályázó tézispontjaiban érintett, közösen publikált közlemények:

I. **Balazs E**, Galik-Olah Z, Galik B, Bozso Z, Kalman J, Datki Z, *Neurodegeneration-related beta-amyloid as autocatabolism-attenuator in a micro-in vivo system*, IBRO Reports, 2020. https://doi.org/10.1016/j.ibror.2020.10.002, MTMT: 31639846, IF: -

II. Datki Z, Acs E, **Balazs E**, Sovany T, Csoka I, Zsuga K, Kalman J, Galik-Olah Z. *Exogenic production of bioactive filamentous biopolymer by monogonant rotifers*, Ecotoxicol Environ Saf 2021. https://doi.org/10.1016/j.ecoenv.2020.111666, MTMT: 31776926, IF: 7.129

III. **Balazs E**, Galik-Olah Z, Galik B, Somogyvari F, Kalman J, Datki Z, *External modulation of Rotimer exudate secretion in monogonant rotifers*, Ecotoxicol Environ Saf 2021. https://doi.org/10.1016/j.ecoenv.2021.112399, MTMT: 32059771, IF: 7.129

IV. Datki Z, **Balazs E**, Galik B, Sinka R, Zeitler L, Bozso Zs, Kalman J, Hortobagyi T, Galik-Olah Z, *The interacting rotifer-biopolymers are anti- and disaggregating agents for human-type beta-amyloid in vitro, International Journal of Biological Macromolecules*, 2022. https://doi.org/10.1016/j.ijbiomac.2021.12.184, MTMT: 32591465, IF: 8.025

I.

IBRO Reports 9 (2020) 319–323

Contents lists available at ScienceDirect

IBRO Reports

journal homepage: www.journals.elsevier.com/ibro-reports

Short Communication

Neurodegeneration-related beta-amyloid as autocatabolism-attenuator in a *micro-in vivo* system

Evelin Balazs [a], Zita Galik-Olah [a], Bence Galik [b,c], Zsolt Bozso [d], Janos Kalman [a], Zsolt Datki [a,*]

[a] Department of Psychiatry, Faculty of Medicine, University of Szeged, Szeged, Hungary
[b] Bioinformatics Research Group, Bioinformatics and Sequencing Core Facility, Szentágothai Research Centre, University of Pécs, Pécs, Hungary
[c] Department of Clinical Molecular Biology, Medical University of Bialystok, ul.Jana Kilinskiego 1, 15-089, Bialystok, Poland
[d] Department of Medical Chemistry, Faculty of Medicine, University of Szeged, Szeged, Hungary

ARTICLE INFO

Keywords:
Invertebrate
Beta-amyloid
Autocatabolism
Organ shrinkage
Metabolism
Bdelloid rotifer

Chemical compounds studied in this article:
Acridine orange (PubChem CID: 62344)
BisANS (PubChem CID: 16213473)
Concanamycin A (PubChem CID: 6438151)
NaOH (PubChem CID: 14798)
Neutral red (PubChem CID: 11105)
Propidium-iodide (PubChem CID: 104981)

ABSTRACT

Investigation of human neurodegeneration-related aggregates of beta-amyloid 1–42 (Aβ42) on bdelloid rotifers is a novel interdisciplinary approach in life sciences. We reapplied an organ size-based *in vivo* monitoring system, exploring the autocatabolism-related alterations evoked by Aβ42, in a glucose-supplemented starvation model. The experientially easy-to-follow size reduction of the bilateral reproductive organ (germovitellaria) in fasted rotifers was rescued by Aβ42, serving as a nutrient source- and peptide sequence-specific attenuator of the organ shrinkage phase and enhancer of the regenerative one including egg reproduction. Recovery of the germovitellaria was significant in comparison with the greatly shrunken form. In contrast to the well-known neurotoxic Aβ42 (except the bdelloids) with specific regulatory roles, the artificially designed scrambled version (random order of amino acids) was inefficient in autocatabolism attenuation, behaving as negative control. This native Aβ42-related modulation of the 'functionally reversible organ shrinkage' can be a potential experiential and supramolecular marker of autocatabolism *in vivo*.

1. Introduction

Rotifers are widely accepted animal models of aging-, metabolism-, starvation-, pharmacology- and *micro-in vivo* OMICS research and methodologies (Macsai et al., 2019; Snell, 2014). Bdelloids, such as *Philodina* or *Adineta* species, have high tolerance to normal environmental changes due to their capability of adaptive phenotypic plasticity (van Cleave, 1932; Azevedo and Leroi, 2001). Marotta et al. (2012) found that the organs of these animals appeared to be compressed during starvation. The germovitellaria (the combined site of the germinarium and vitellarium glands) showed significant reduction in size and in fine structure under caloric restriction. These organ tissues could also function as nutrient storage; therefore, their content is used by rotifers *via* autophagy (Mizushima and Komatsu, 2011). In acidic vesicular organelles (AVOs) detection, acidotropic dyes are applied such as acridine orange (AO) or neutral red (NR). These indicators show good correlation with each other (Morishita et al., 2017) and in some cases these fluorescent probes, without cross-linking, are more promising quantitative approaches than immunofluorescence to evaluate the late phase of autocatabolism. The vacuolar-type H^+-ATPase inhibitors (*e.g.* Concanamycin A) can hinder the catabolic processes of metabolic autophagy (Goto-Yamada et al., 2019). The direct connection between anatomical changes (*e.g.* organ shrinkage) and autophagy has been proved in rotifers (Marotta et al., 2012; Cervellione et al., 2017). Treatments with various exogenous Aβ isoforms are well-known models of Alzheimer's disease and numerous studies applying *in vitro* and *in vivo* systems to discover their exact impacts. Studies are available using human neuroblastoma cells (Datki et al., 2003; Poeggeler et al., 2005), invertebrates, rodents, and primates (Harkany et al., 2000; Kong et al., 2016; Sharma et al., 2017). Despite these facts, only one publication

Abbreviations: Aβ, beta-amyloid; AO, acridine orange; AVOs, acidic vesicular organelles; BisANS, 4,4′-dianilino-1,1′-binaphthyl-5,5′-disulfonic acid dipotassium salt; ConA, Concanamycin A; D0, Day 0; D20, Day 20; D25, Day 25; FROS, functionally reversible organ shrinkage; $FROS_i$, FROS index; NFI%, percentage of normalized fluorescence intensity; PI, propidium-iodide; S-Aβ42, scrambled isoform of Aβ; SEM, standard error of the mean.

* Corresponding author at: Department of Psychiatry, Faculty of Medicine, University of Szeged, Kalvaria sgt. 57, H-6725, Szeged, Hungary.
E-mail address: datki.zsolt@med.u-szeged.hu (Z. Datki).

https://doi.org/10.1016/j.ibror.2020.10.002
Received 25 June 2020; Accepted 2 October 2020
Available online 6 October 2020

deals with the effects of Aβ on bdelloid rotifers, *e.g. Philodina species* by Poeggeler et al. (2005). This research group administered beta-amyloid to test the potential protective effects of novel drug candidates (*e.g.*: antioxidant LPBNAH). These phylogenetically 'simple' animals are inappropriate to model higher, species-specific (*e.g.* human) physiological processes (*e.g.* neurodegeneration); nevertheless, they are suitable for demonstrating various interdisciplinary concepts (metabolic connection between non-pathogenic invertebrates and natural aggregates; Ricci and Boschetti, 2003; Ramulu et al., 2012). An adequate example for this is the phenomenon that bdelloids are able to exceedingly catabolize the highly resistant peptide- or protein aggregates (well-known neurotoxins), such as beta-amyloid (Aβ), alpha-synuclein and scrapie prions under extreme conditions (*e.g.* starvation). Investigation of neurodegeneration-related Aβ42 on rotifers is the central research topic of our team. In an exceptional way, the human-type aggregates are potential nutrient sources to bdelloid rotifers (Datki et al., 2018); however, the general foods of these animals are aggregated organic masses in their natural habitat (Fontaneto et al., 2011). Bdelloids are able to use conglomerates and aggregates as an energy source, by their phylogenetically selected ability. The rotifer-aggregates-connected research is rather a new topic, there is no relevant data about the Aβ-induced signalizations and regulations in these *micro-in vivo* entities. In this present study, our aims were to reveal the potential regulatory effects of aggregated Aβ42 in relation to the autocatabolism in rotifers.

2. Materials and methods

2.1. The invertebrate models

The experiments were performed on *Philodina acuticornis* and *Adineta vaga* species; therefore, no specific ethical permission was needed according to the current international regulations. They were obtained from a Hungarian aquavaristique, originating from an agricultural farm in Szarvas, Hungary. The species have been maintained in standard laboratory conditions for 6 years. The rotifers were cultured based on the following methods of our previous publications. The standard medium content (mg/L) were: Ca^{2+} 31.05; Mg^{2+} 17.6; Na^{+} 0.9; K^{+} 0.25; Fe^{2+} 0.001; $HCO3^{-}$ 153.097; SO4- 3; Cl- 0.8; F^{-} 0.02; H_2SiO_3 3.3 (pH = 7.5) (Olah et al., 2017). For standard food of cultures, we used homogenized baker's yeast (EU-standard granulated instant form, 2-0 1-42 0674/001-Z12180/HU) which was heat-inactivated and filtered (Whatman filter with 10 μm pore; 6728-5100).

2.2. Treatment and monitoring

The Aβ42 and its scrambled isoform (S-Aβ42: LKAFDIGVEYNKV-GEGFAISHGVAHLDVSMFGEIGRVDVHQA) were prepared at the Department of Medical Chemistry, University of Szeged, Hungary. The concentrations of the stock solutions were 1 mg/mL in distilled water; the aggregation time was 3 h (25 °C, pH 3.5); the neutralization (to pH 7.5) was performed with NaOH (1 N) (Bozso et al., 2010; Kalweit et al., 2015). The final concentrations of Aβ were 100 μg/mL. For *in vivo* investigations we applied Concanamycin A (ConA; 27689, 50 nM), 4, 4′-dianilino-1,1′-binaphthyl-5,5′-disulfonic acid dipotassium salt (BisANS, D4162; 50 μM), propidiume-iodide (PI, 81845; 5 μM;), AO (13000; 15 μM) and NR (N-4638; 50 mM) dyes obtained from Sigma-Aldrich, USA.

Monitoring the size of the germovitellaria, in the presence of glucose (1 mM), started on Day 0 (D0) providing a reference control. Following twenty days (D20) of starvation and five days (D25) later, the organ regeneration was presented. On D20, one-time feeding (600 μg/mL yeast homogenate) was applied and followed-by five days of recovery. The treatment protocol was performed on a 'one-housed rotifer' (one animal/well) setup in a 96-well plate (Costar Corning Inc., CLS3595). There were 150 ± 30 rotifer/well in all fluorescence-related experiments. Investigated rotifer populations have adequate number of individuals to provide similar and equable size distribution.

The entities were photographed (Nikon D5100 camera, Japan) under inverted microscope (Leitz Labovert FS). The two separated germovitellarium were digitally colored in blue. The process of shrinkage with functional (egg production) regeneration capability was named 'functionally reversible organ shrinkage' (FROS).

To investigate (n = 5, well) the amount of protein in the animals, BisANS was applied (Datki et al., 2019) parallelly with detecting the total amount of nucleic acid, where PI was used (Mozes et al., 2011) after 10 min incubation and washing. There was no extraction, the labelling and measurements were directly performed on the animals. The extinction/emission were 405/520 nm for BisANS and 530/620 nm for PI, measured by a microplate reader (NOVOstar, BMG, Germany).

In AVOs-detection methods, we used a slightly modified version of Kang et al. (2018). The AO and the NR labellings were performed under the same conditions as the BisANS and PI applications. These two dyes were used in different wells, but the conditions and the number of animals were the same. The extinction/emission of AO was 480/620 nm in red and 480/520 nm in green. The wavelengths of NR were 540/630 nm in red and 450/590 nm in yellow. In order to inhibit the autolysis-related processes, ConA was added to the wells on D0. The percentage of normalized fluorescence intensity (NFI%) was calculated from the ratio of fluorescence data divided by the number of rotifers in each well.

In the experiential monitoring of FROS, each data (n = 36; individual one-housed rotifer/well) sums the whole (bilateral) size of the germovitellaria in one individual. The organs were circled by using a freehand tool (allowing to create irregularly shaped selections) in ImageJ program (64-bit for Windows, (Collins, 2007). The scale bar was 20 μm.

To demonstrate the functional recovery of the reproductive organs, the number of laid eggs was counted after the regeneration phase (from D20 to D25). As a reference control, the treatment-free species-specific laid egg production was determined after 5 days in normal culturing conditions.

2.3. Statistics

Statistical analysis was performed with SPSS 23.0 (SPSS Inc, USA) using one-way ANOVA with Bonferroni *post hoc* test. The FROS index ($FROS_i$) was calculated by the following formula: $FROS_i$ = A/B*A/C*D/E (germovitellaria size on: A, D0; B, D20; C, D25; D, species-specific number of laid eggs under standard feeding; E, number of laid eggs on D25). The error bars represent the standard error of the mean (SEM). The different levels of significance are indicated as follows: $p^{*, \#} \leq 0.05$, $p^{**, ¤¤} \leq 0.01$, $p^{***, ###, ¤¤¤} \leq 0.001$ and $p^{****} \leq 0.0001$ (*, significant difference from the untreated controls; #, significant difference from the same S-Aβ42-treated groups of the given rotifer species; ¤, significant difference from the D0 and D25 groups of the given rotifer species).

3. Results and discussion

The Aβ42 is a well-known neurotoxin, which is prone to form highly-resistant aggregates in an aquatic environment (Lin et al., 2019). The bdelloid rotifers are able to catabolize these aggregates, with no physiological damage (Datki et al., 2018). Our aims were to reveal the special role of Aβ42 in autocatabolism-related processes during a 25-day period (Fig. 1). To explore the possible sequence specificity of this molecule, we applied its scrambled version as control. The molecular content and weight of S-Aβ42 were the same as that in wild-type human form, with different order of amino acids (Datki et al., 2018; Bartus et al., 2018).

On D0, the reference germovitellaria of *P. acuticornis* (Fig. 2A) or *A. vaga* (Fig. 2D) can be seen. Their size and fine structure reduced after a 20-day long glucose-supplemented (ATP-source for autolytic processes) starvation (Fig. 2B and E). On D20, the animals were fed once, providing standard nutrient for the regeneration phase. The organs were

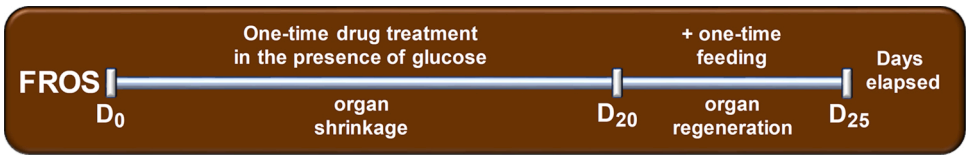

Fig. 1. Schematic protocol of the functionally reversible organ shrinkage in a micro-invertebrate system (D0 = Day 0, starting day; D20 = Day 20, organ shrinkage period with one-time drug treatment in glucose supplemented environment; D25 = Day 25, organ regeneration period with one-time standard feeding).

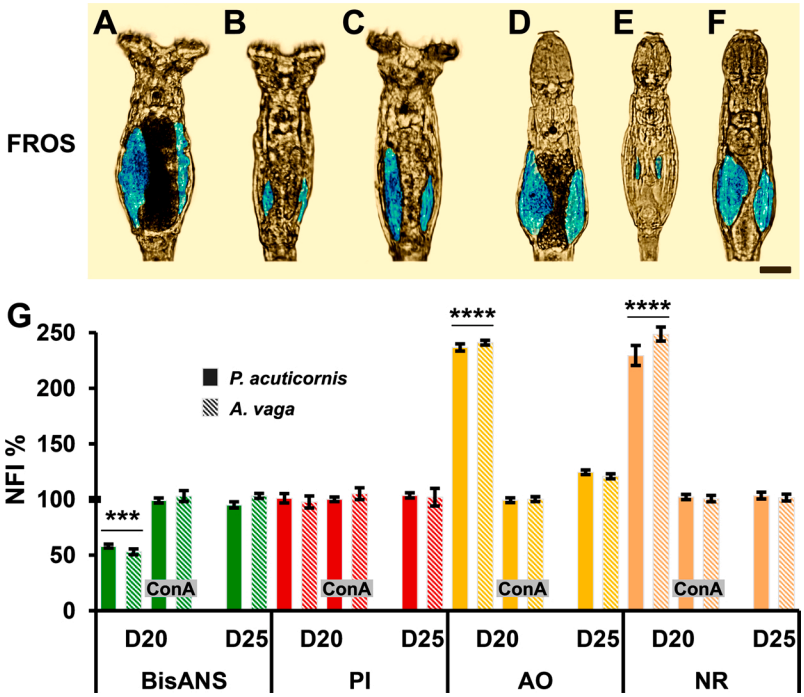

Fig. 2. Functionally reversible organ shrinkage (FROS) in *P. acuticornis* and *A. vaga* rotifers. The germovitellaria (digitally pseudo-colored in blue; scale bar: 20 μm) of *P. acuticornis* (PA; A—C) and *A. vaga* (AV; D-F) was monitored on D0 (A and D), D20 (B and E) and D25 (C and F). The FROS-related alterations are presented (G) with the protein- (green), nucleic acid- (red) and AVOs amount in PA (full columns) and AV (striped columns) rotifers. The D0 means 100 %. ConA was applied parallelly with all investigations. The error bars represent SEM. One-way ANOVA with Bonferroni *post hoc* test was used for statistical analysis, the levels of significance are $p^{***} \leq 0.001$ and $p^{****} \leq 0.0001$ (*, significant difference from all the groups) (For interpretation of the references to colour in this figure legend, the reader is referred to the web version of this article).

then rebuilt, and showed similar characteristics (Fig. 2C and F) to the reference ones. These results suggest that the organic shrinkage is reversible depending on the availability of food. To connect the autocatabolism-related processes with starvation-induced organ shrinkage (Puente et al., 2016), we applied ConA (Johnson et al., 2010) during the experiments. The amounts of protein and nucleic acid were measured parallelly with AVOs. Consequently, we found that the total protein decreased on D20, indicating that the animals catabolized it for survival. The ConA-administration inhibited these processes. The amounts of nucleic acid did not show any changes in either species (Fig. 2G). In line with the above mentioned investigations, we detected significant increase in autocatabolism-related vesicular acidification (Tan et al., 2018) in both species on D20 compared to the untreated reference values of D0. The ConA treatment hindered the observed alterations. On D25, there were no significant changes either in AO or in NR. The decrease of protein amount (associated with stable nucleic acid content) and the occurrence of AVOs under starvation show good conceptual correlation with organ shrinkage. These phenomena are adequate physiologic and experiential markers of autolytic metabolism in the aforementioned bdelloid rotifers.

The Aβs are stigmatized as negative multifunctional agents (*e.g.* in the human brain) in academic literature. Based on this concept, the core question is how Aβ42 may influence the autocatabolism-related processes in our microinvertebrate species? In FROS-related investigations the Aβ42, S-Aβ42 or ConA were added to the treatment medium on D0 (Fig. 3A); therefore, these data served as references to the upcoming ones. In both rotifer species the organ shrinkage was less pronounced on D20 compared to the given untreated controls. Significantly higher regeneration was detected on D25 in Aβ42-treated groups compared to the other ones on D25. These results indicated that the native aggregate has a potential specific modulatory effect. Decrease of organ-size was lower in Aβ42-treated groups compared to the ones influenced by S-Aβ42. The same phenomenon was observed at the end of regeneration, where the animals showed significantly higher rate of recovery in the presence of Aβ42. These data showed that the attenuation of shrinkage *via* modulation is likely sequence-specific, since the order of amino acid is the only difference between the two types of Aβs (Vadukul et al., 2017). On D20, ConA significantly inhibited the FROS in both species in a glucose-containing, but food-free environment. We have no knowledge about the treated animals eating the ConA itself, but the individuals remained alive in a good shape. On D25, the ConA had no effects on the monitored phenomenon.

In the FROS acronym, besides reversibility ('R') of organ shrinkage, 'F' stands for functionality, which refers to the remaining reproduction ability of rotifers. The measured parameter on D25 was the number of laid eggs, which was compared to the reference values (Fig. 3B). In all groups, the amount of eggs was low on D20 due to the minimal calorie intake. In the presence of Aβs, the number of eggs significantly elevated in both species compared to the control and ConA peers; moreover, the Aβ42-modulated animals laid significantly higher number of eggs than the S-Aβ42-treated ones. Integration of egg-number-data into the time-dependent organ size alterations resulted a special formula, named

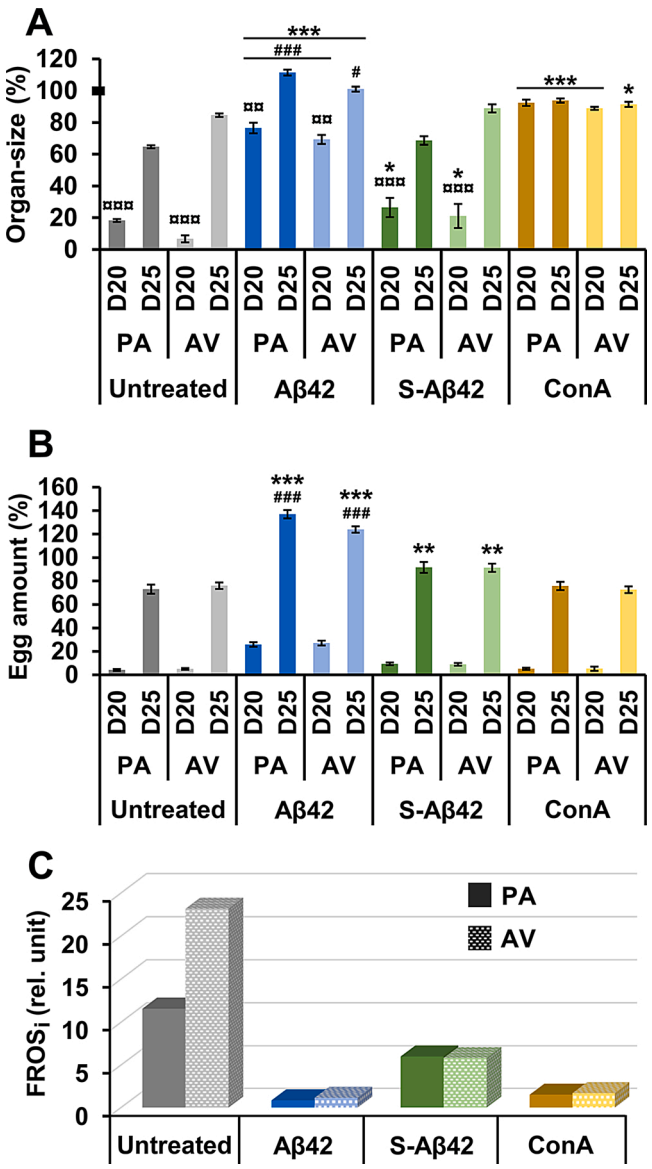

Fig. 3. Modulation of the functionally reversible organ shrinkage (FROS) by aggregated Aβ42. The FROS was assessed in both *P. acuticornis* (PA) and *A. vaga* (AV) with applying Aβ42, S-Aβ42 or ConA. The germovitellaria were monitored on D0, D20 and D25. (A) The organ-size during FROS (A) and the amount of eggs on D20 and D25 (B) are presented. The D0 means 100 %. The error bars represent SEM. One-way ANOVA with Bonferroni *post hoc* test was used for statistical analysis, the levels of significance are $p^{*,\ \#} \leq 0.05$, $p^{¤¤} \leq 0.01$ and $p^{***,\ ###,\ ¤¤¤} \leq 0.001$ (*, significant difference from the same untreated control groups of the given rotifer species; #, significant difference from the same S-Aβ42-treated groups of the given rotifer species; ¤, significant difference from the D0 and D25 groups of the given rotifer species). FROS index ($FROS_i$; relative unit) is presented (C) in untreated control, Aβ42, S-Aβ42 and ConA groups.

FROS index, which is a representative unit for the current treatment agents. This index shows a linear correlation with the level of autocatabolism. The $FROS_i$ was positively lower in all agent-influenced experiments compared to the controls in both species (Fig. 3C). The $FROS_i$ of native aggregates, in contrast to their scrambled version, demonstrated that the Aβ42 is not only a food source for rotifers, but it is also a potential regulator of their systemic metabolism. Both *Philodina* and *Adineta* species showed alterations with the same tendencies; therefore, these effects of Aβ42 are not limited to only one species.

Rotifers are extremely resistant to environmental alterations and they successfully adapt to different types and amounts of nutrients present in their natural habitat. The natural decomposition of organic materials is a process that results in the formation of precipitates and aggregates, which represent potential nutrients for rotifers (Wallace and Snell, 2010). The metabolic utilization of all these available organic material resources is their special property (Castro et al., 2005). Nobody has investigated before the *in vivo* catabolism of the Aβ as food sources or as potential autocatabolism-regulator for multicellular entities. The starvation-induced shrinkage of germovitellaria, with their regeneration and reproduction capability in these animals, is an adequate physiologic and experiential marker of autocatabolism, summarized by $FROS_i$. By applying these microinvertebrates, the hitherto unknown roles of Aβ42 were demonstrated, providing additional tools for exploring relations between neurotoxic aggregates and metabolism.

Conflicts of interest

No competing interests declared.

CRediT authorship contribution statement

Evelin Balazs: Validation, Investigation, Writing - review & editing, Project administration. **Zita Galik-Olah:** Conceptualization, Methodology, Validation, Formal analysis, Investigation, Data curation, Writing - original draft, Writing - review & editing, Supervision, Project administration. **Bence Galik:** Formal analysis, Investigation, Resources, Writing - review & editing, Funding acquisition. **Zsolt Bozso:** Investigation, Writing - review & editing, Project administration. **Janos Kalman:** Resources, Writing - review & editing, Funding acquisition. **Zsolt Datki:** Conceptualization, Methodology, Validation, Formal analysis, Investigation, Resources, Data curation, Writing - original draft, Writing - review & editing, Visualization, Supervision, Project administration.

Acknowledgements

The authors wish to thank to Anna Szentgyorgyi MA, a professional in English Foreign Language Teaching for proofreading the manuscript. This research was conducted within the project which has received funding from the European Union's Horizon 2020 research and innovation programme under the Marie Skłodowska-Curie grant agreement, Nr. 754432 and the Polish Ministry of Science and Higher Education, and from financial resources for science in 2018-2023 granted for the implementation of an international co-financed project and Developing scientific workshops of medical-, health sciences and pharmaceutical training (grant number: EFOP 3.6.3-VEKOP-16-2017-00009; Hungary).

References

Azevedo, R.B., Leroi, A.M., 2001. A power law for cells. Proc. Natl. Acad. Sci. U. S. A. 98, 5699–5704. https://doi.org/10.1073/pnas.091485998.

Bartus, É., Olajos, G., Schuster, I., Bozsó, Z., Deli, M.A., Veszelka, S., Walter, F.R., Datki, Z., Szakonyi, Z., Martinek, T.A., Fülöp, L., 2018. Structural optimization of Foldamer-Dendrimer conjugates as multivalent agents against the toxic effects of amyloid Beta oligomers. Molecules 23, 2523. https://doi.org/10.3390/molecules23102523.

Bozso, Z., Penke, B., Simon, D., Laczkó, I., Juhász, G., Szegedi, V., Kasza, A., Soós, K., Hetényi, A., Wéber, E., Tóháti, H., Csete, M., Zarándi, M., Fülöp, L., 2010. Controlled in situ preparation of A beta(1-42) oligomers from the isopeptide "iso-A beta(1-42)", physicochemical and biological characterization. Peptides 31, 248–256. https://doi.org/10.1016/j.peptides.2009.12.001.

Castro, B.B., Antunes, S.C., Pereira, R., Soares, A.M.V.M., Gonçalves, F., 2005. Rotifer community structure in three shallow lakes: seasonal fluctuations and explanatory factors. Hydrobiologia 543, 221–232. https://doi.org/10.1007/s10750-004-7453-8.

Cervellione, F., McGurk, C., Berger, Eriksen, T., Van den Broeck, W., 2017. Effect of starvation and refeeding on the hepatopancreas of whiteleg shrimp Penaeus vannamei (Boone) using computer-assisted image analysis. J. Fish Dis. 40, 1707–1715. https://doi.org/10.1111/jfd.12639.

Collins, T.J., 2007. ImageJ for microscopy. Biotechniques 43, 25–30. https://doi.org/10.2144/000112517.

Datki, Z., Juhász, A., Gálfi, M., Soós, K., Papp, R., Zádori, D., Penke, B., 2003. Method for measuring neurotoxicity of aggregating polypeptides with the MTT assay on

differentiated neuroblastoma cells. Brain Res. Bull. 62, 223–229. https://doi.org/10.1016/j.brainresbull.2003.09.011.
Datki, Z., Olah, Z., Hortobagyi, T., Macsai, L., Zsuga, K., Fulop, L., Bozso, Z., Galik, B., Acs, E., Foldi, A., Szarvas, A., Kalman, J., 2018. Exceptional in vivo catabolism of neurodegeneration-related aggregates. Acta Neuropathol. Commun. 6, 6. https://doi.org/10.1186/s40478-018-0507-3.
Datki, Z., Olah, Z., Macsai, L., Pakaski, M., Galik, B., Mihaly, G., Kalman, J., 2019. Application of BisANS fluorescent dye for developing a novel protein assay. PLoS One 14, 0215863. https://doi.org/10.1371/journal.pone.0215863.
Fontaneto, D., Westberg, M., Hortal, J., 2011. Evidence of weak habitat specialisation in microscopic animals. PLoS One 6, 23969. https://doi.org/10.1371/journal.pone.0023969.
Goto-Yamada, S., Oikawa, K., Bizan, J., Shigenobu, S., Yamaguchi, K., Mano, S., Hayashi, M., Ueda, H., Hara-Nishimura, I., Nishimura, M., Yamada, K., 2019. Sucrose starvation induces microautophagy in plant root cells. Front. Plant Sci. 10, 1604. https://doi.org/10.3389/fpls.2019.01604.
Harkany, T., Abrahám, I., Timmerman, W., Laskay, G., Tóth, B., Sasvári, M., Kónya, C., Sebens, J.B., Korf, J., Nyakas, C., Zarándi, M., Soós, K., Penke, B., Luiten, P.G., 2000. Beta-amyloid neurotoxicity is mediated by a glutamate-triggered excitotoxic cascade in rat nucleus basalis. Eur. J. Neurosci. 12, 2735–2745. https://doi.org/10.1046/j.1460-9568.2000.00164.x.
Johnson, R.M., Allen, C., Melman, S.D., Waller, A., Young, S.M., Sklar, L.A., Parra, K.J., 2010. Identification of inhibitors of vacuolar proton-translocating ATPase pumps in yeast by high-throughput screening flow cytometry. Anal. Biochem. 398, 203–211. https://doi.org/10.1016/j.ab.2009.12.020.
Kalweit, A.N., Yang, H., Colitti-Klausnitzer, J., Fülöp, L., Bozsó, Z., Penke, B., Manahan-Vaughan, D., 2015. Acute intracerebral treatment with amyloid-beta (1-42) alters the profile of neuronal oscillations that accompany LTP induction and results in impaired LTP in freely behaving rats. Front. Behav. Neurosci. 9, 103. https://doi.org/10.3389/fnbeh.2015.00103.
Kang, H.M., Jeong, C.B., Kim, M.S., Lee, J.S., Zhou, J., Lee, Y.H., Kim, D.H., Moon, E., Kweon, H.S., Lee, S.J., Lee, J.S., 2018. The role of the p38-activated protein kinase signaling pathway-mediated autophagy in cadmium-exposed monogonont rotifer Brachious koreanus. Aquat. Toxicol. 194, 46–56. https://doi.org/10.1016/j.aquatox.2017.11.002.
Kong, Y., Li, K., Fu, T., Wan, C., Zhang, D., Song, H., Zhang, Y., Liu, N., Gan, Z., Yuan, L., 2016. Quercetin ameliorates Aβ toxicity in Drosophila AD model by modulating cell cycle-related protein expression. Oncotarget 7, 67716–67731. https://doi.org/10.18632/oncotarget.11963.
Lin, Y., Im, H., Diem, L., Ham, S., 2019. Characterizing the structural and thermodynamic properties of Aβ42 and Aβ40. Biochem. Biophys. Res. Commun. 510, 442–448. https://doi.org/10.1016/j.bbrc.2019.01.124.
Macsai, L., Olah, Z., Bush, A.I., Galik, B., Onody, R., Kalman, J., Datki, Z., 2019. Redox modulating factors affect longevity regulation in rotifers. J. Gerontol. A Biol. Sci. Med. Sci. 74, 811–814. https://doi.org/10.1093/gerona/gly193.
Marotta, R., Uggetti, A., Ricci, C., Leasi, F., Melone, G., 2012. Surviving starvation: changes accompanying starvation tolerance in a bdelloid rotifer. J. Morphol. 273, 1–7. https://doi.org/10.1002/jmor.11000.
Mizushima, N., Komatsu, M., 2011. Autophagy: renovation of cells and tissues. Cell 147, 728–741. https://doi.org/10.1016/j.cell.2011.10.026.
Morishita, H., Kaizuka, T., Hama, Y., Mizushima, N., 2017. A new probe to measure autophagic flux in vitro and in vivo. Autophagy 13, 757–758. https://doi.org/10.1080/15548627.2016.1278094.
Mozes, E., Hunya, A., Toth, A., Ayaydin, F., Penke, B., Datki, Z.L., 2011. A novel application of the fluorescent dye bis-ANS for labeling neurons in acute brain slices. Brain Res. Bull. 86, 217–221. https://doi.org/10.1016/j.brainresbull.2011.07.004.
Olah, Z., Bush, A.I., Aleksza, D., Galik, B., Ivitz, E., Macsai, L., Janka, Z., Karman, Z., Kalman, J., Datki, Z., 2017. Novel in vivo experimental viability assays with high sensitivity and throughput capacity using a bdelloid rotifer. Ecotoxicol. Environ. Saf. 144, 115–122. https://doi.org/10.1016/j.ecoenv.2017.06.005.
Poeggeler, B., Durand, G., Polidori, A., Pappolla, M.A., Vega-Naredo, I., Coto-Montes, A., Böker, J., Hardeland, R., Pucci, B., 2005. Mitochondrial medicine: neuroprotection and life extension by the new amphiphilic nitrone LPBNAH acting as a highly potent antioxidant agent. J. Neurochem. 95, 62–73. https://doi.org/10.1111/j.1471-4159.2005.03425.x.
Puente, C., Hendrickson, R.C., Jiang, X., 2016. Nutrient-regulated phosphorylation of ATG13 inhibits starvation-induced autophagy. J. Biol. Chem. 291, 6026–6035. https://doi.org/10.1074/jbc.M115.689646.
Ramulu, H.G., Raoult, D., Pontarotti, P., 2012. The rhizome of life: what about metazoa? Front. Cell. Infect. Microbiol. 2, 50. https://doi.org/10.3389/fcimb.2012.00050.
Ricci, C., Boschetti, C., 2003. Bdelloid rotifers as model system to study developmental biology in space. Adv. Space Biol. Med. 9, 25–39. https://doi.org/10.1016/s1569-2574(03)09002-6.
Sharma, N., Khurana, N., Muthuraman, A., 2017. Lower vertebrate and invertebrate models of Alzheimer's disease - a review. Eur. J. Pharmacol. 815, 312–323. https://doi.org/10.1016/j.ejphar.2017.09.017.
Snell, T.W., 2014. Rotifers as models for the biology of aging. Int. Rev. Hydrobiol. 99, 84–95. https://doi.org/10.1002/iroh.201301707.
Tan, X.Y., Wang, X., Liu, Q.S., Xie, X.Q., Li, Y., Li, B.Q., Li, Z.Q., Xia, Q.Y., Zhao, P., 2018. Inhibition of silkworm vacuolar-type ATPase activity by its inhibitor Bafilomycin A1 induces caspase-dependent apoptosis in an embryonic cell line of silkworm. Arch. Insect Biochem. Physiol. 99, 21507. https://doi.org/10.1002/arch.21507.
Vadukul, D.M., Gbajumo, O., Marshall, K.E., Serpell, L.C., 2017. Amyloidogenicity and toxicity of the reverse and scrambled variants of amyloid-β 1-42. FEBS Lett. 591, 822–830. https://doi.org/10.1002/1873-3468.12590.
van Cleave, H.J., 1932. Eutely or cell constancy in its relation to body size. Q. Rev. Biol. 7, 59–67.
Wallace, R.L., Snell, T.W., 2010. Rotifera, chapter 8. In: Thorp, J.H., Covich, A.P. (Eds.), Ecology and Classification of North American Freshwater Invertebrates. Elsevier, Oxford, pp. 173–235.

II.

Ecotoxicology and Environmental Safety 208 (2021) 111666

Contents lists available at ScienceDirect

Ecotoxicology and Environmental Safety

journal homepage: www.elsevier.com/locate/ecoenv

Research paper

Exogenic production of bioactive filamentous biopolymer by monogonant rotifers

Zsolt Datki [a,*,1], Eva Acs [b,c,1], Evelin Balazs [a], Tamas Sovany [d], Ildiko Csoka [d], Katalin Zsuga [e], Janos Kalman [a], Zita Galik-Olah [a]

[a] Department of Psychiatry, Faculty of Medicine, University of Szeged, Vasas Szent Peter u. 1-3, H-6724 Szeged, Hungary
[b] Danube Research Institute, MTA Centre for Ecological Research, Karolina ut 29-31, H-1113 Budapest, Hungary
[c] National University of Public Service, Faculty of Water Sciences, 6500 Baja, Bajcsy-Zsilinszky utca 12-14., Hungary
[d] Institute of Pharmaceutical Technology and Regulatory Affairs, Faculty of Pharmacology, University of Szeged, Eotvos u. 6, H-6720 Szeged, Hungary
[e] Agrint Kft., Facan sor 56, H-2100 Godollo, Hungary

ARTICLE INFO

Edited by Professor Bing Yan

Keywords:
Monogonant rotifer
Biopolymer
Euchlanis dilatata
SH-SY5Y neuroblastoma cell line
Exudate
Beta-amyloid

Chemical compounds studied in this article:
Acetic acid (PubChem CID: 176)
Beta-amyloid 1-42 (PubChem CID: 57339251)
BSA (PubChem CID: 384256260)
Calcein-AM (PubChem CID: 390986)
Carmine crystals (PubChem CID: 14950)
Collagenase II (PubChem CID: 18680304)
DMSO (PubChem CID: 679)
EDTA (PubChem CID: 6049)
EGTA (PubChem CID: 6207)
Etanol (PubChem CID: 702)
Glycerol (PubChem CID: 753)
HCl (PubChem CID: 313)
KBr (PubChem CID: 253877)
Micro-cellulose (PubChem CID: 16211032)
Methanol (PubChem CID: 887)
$NaHCO_3$ (PubChem CID: 516892)
NaN_3 (PubChem CID: 335587)
NaOH (PubChem CID: 14798)
SDS (PubChem CID: 8778)
Spermidine (PubChem CID: 1102)

ABSTRACT

The chemical ecology of rotifers has been little studied. A yet unknown property is presented within some monogonant rotifers, namely the ability to produce an exogenic filamentous biopolymer, named 'Rotimer'. This rotifer-specific viscoelastic fiber was observed in six different freshwater monogonants (*Euchlanis dilatata, Lecane bulla, Lepadella patella, Itura aurita, Colurella adriatica* and *Trichocerca iernis*) in exception of four species. Induction of Rotimer secretion can only be achieved by mechanically irritating rotifer ciliate with administering different types (yeast cell skeleton, denatured BSA, epoxy, Carmine or urea crystals and micro-cellulose) and sizes (approx. from 2.5 to 50 μm diameter) of inert particles, as inductors or visualization by adhering particles. The thickness of this Rotimer is 33 ± 3 nm, detected by scanning electron microscope. This material has two structural formations (fiber or gluelike) in nano dimension. The existence of the novel adherent natural product becomes visible by forming a 'Rotimer-Inductor Conglomerate' (RIC) web structure within a few minutes. The RIC-producing capacity of animals, depends on viability, is significantly modified according to physiological- (depletion), drug- (toxin or stimulator) and environmental (temperature, salt content and pH) effects. The *E. dilatata*-produced RIC is affected by protein disruptors but is resistant to several chemical influences and its Rotimer component has an overwhelming cell (algae, yeast and human neuroblastoma) motility inhibitory effect, associated with low toxicity. This biopolymer-secretion-capacity is protective of rotifers against human-type beta-amyloid aggregates.

Abbreviations: ASC, Average Size of Conglomerates; ASIP, Average Size of Inductor Particles; Aβ42, Beta-amyloid 1-42; BSA, bovine serum albumin; CA, Covered Area; DW, distilled water; DMSO, dimethyl sulfoxide; EDTA, ethylenediaminetetraacetic acid; EGTA, ethylene glycol-bis(β-aminoethyl ether)-N,N,N′,N′-tetraacetic acid tetrasodium salt; EtOH, etanol; FI, fluorescence intensity; FTIR, Fourier Transform Infrared Spectroscopy; NaN_3, sodium azide; NaOH, sodium hydroxide; NR, Number of Rotifers; MeOH, methanol; RIC, Rotimer-Inductor Conglomerate; RPC, RIC-producing capacity; RPC_i, RPC index; SEM, scanning electron microscope; S.E.M., standard error of the mean; SDS, sodium dodecyl sulfate; TPEN, N,N,N′,N′-Tetrakis(2-pyridylmethyl)ethylenediamine.

* Corresponding author.
E-mail addresses: datki.zsolt@med.u-szeged.hu, datkizsolt@gmail.com (Z. Datki).
[1] First co-authors

https://doi.org/10.1016/j.ecoenv.2020.111666
Received 2 September 2020; Received in revised form 31 October 2020; Accepted 12 November 2020

TPEN (PubChem CID: 5519)
Triton X-100 (PubChem CID: 5590)
Trypsin (PubChem CID: 5311489)
Urea (PubChem CID: 1176)

1. Introduction

Rotifers are multicellular animals of microscopic size, providing a significant part of aquatic biomass (Dahms et al., 2011). Both bdelloids and monogonants are found in marine environment or in freshwater lakes (Snell et al., 2015). Although their bodies consist of approximately 1000 cells, they have complex organ systems, including gastro-intestinal tract, reproductive organs, nervous system or secretory glands. These entities are excellent models of ecotoxicology, aging or pharmaceutical researches (Datki et al., 2018, 2019; Snell et al., 2018; Macsai et al., 2019).

Self-maintenance and the reproductive rate are the two most important factors of these microinvertebrates during their lifespan, and in their natural habitat the general nutrients include degradable organic masses (Fontaneto et al., 2011; Robeson et al., 2011). Rotifers are able to use conglomerates and aggregates as 'food' by their phylogenetically selected ability. Bdelloids, such as *Philodina acuticornis* or *Adineta steineri*, are able to exceedingly catabolize the highly enzyme-resistant human-type neurotoxic aggregates, such as beta-amyloid, alpha-synuclein and scrapie-type prion under certain extreme conditions (e.g. starvation; Datki et al., 2018). Another example for invertebrate adaptive capacity is the secretion of various types of biopolymers, especially in marine species belonging to the phylum of *Mollusca, Echinodermata* or *Arthropoda* (Ganesana et al., 2020).

Biopolymers are produced by living organisms and these chemical substances consist of repetitive units, which form molecular structures of higher order. Based on their chemical properties, several types of natural products can be distinguished: polypeptides, polynucleotides, polysaccharides, peptidoglycans, proteoglycans, glycoproteins and the mixed types of these groups. (Chandra and Rustgi, 1998; Hassan et al., 2019) Their enzyme resistance or sensitivity strongly correlates with their basic structure, for example, polypeptides can be degraded by proteases, such as trypsin or proteinase K (Muhlia-Almazán et al., 2008). The biopolymers, showing specific antimicrobial (Kamiya et al., 2006; Rahman, 2019) or hypoglycemic activities (Ruiz-Torres et al., 2019), are used in multiple fields for pharmaceutical (Yavuz et al., 2019), medical (Humenik et al., 2019) or industrial purposes (Chen and Peng, 2019; Mohamed et al., 2020). The original function of these natural products are various, depending on the lifestyle and environment of relevant animals, e.g. the sessile marine invertebrates (mussels, tubeworm, sea star, limpet, sea cucumber) produce bioadhesives to attach to different surfaces. The adhesive capability depends on the various types of attachment which can be permanent, transitory, temporary and instantaneous. (Hennebert et al., 2018) One of the earliest adhesive biopolymers is described by Aristotle, called *byssus*, which is produced by a marine mollusc, *Pinna nobilis*. This substance is barely studied in the fields of biochemistry, material science, biomedicines and biomimetics. At the southern part of Europe and North Africa this fibrous and shock-absorbing biopolymer was used in textile manufacturing due to its fine, but very resilient structure. There are species-specific differences between the chemical and structural forms of these exudates, but their common characteristics include self-healing, stiffness, bio-renewable- and DOPA-dependent adhesive abilities. Their chemical structures predominantly contain protein with minor amounts of lipids and carbohydrates. These substances are characterized by comprehensive flexibility, ability to fast recovery and high biomimetic potential. Being dissimilar to other typical elastomeric proteins, they provide novel tools for medico-industrial developments. In many cases, the clear chemical definition, the biochemistry and the genomics of these biopolymers remain to be enigmatic. For example, the exact structure of *Gorgonin* (a protein-based polyphenol-containing organic material), which was first described by Pallas (1766), is still unknown (Ehrlich, 2019; Olatunji, 2020).

Since the marine invertebrates adapt to ecological niche, their host defense system is completely different from that of the terrestrial ones. Certain species secrete antibacterial and antitumor factors; furthermore, others produce bioactive factors with the same properties, but with different chemical structures. (Yamazaki et al., 1985, 1989; Kisugi et al., 1992;) No relevant data were found about the biopolymer-secretion of monogonant or bdelloid rotifers. The complex biodiversity of rotifers is dealt with a growing number of studies that intend to reveal the physiology of these invertebrates, still having new properties or phenomena to be explored. A yet unknown capability of monogonants were aimed to describe, understanding how the environmental and chemical factors influence the newly observed rotifer-specific biopolymer secretion, stability and bioactivity. Furthermore, some examples were intended to be shown to demonstrate the potential application of this recently described natural product.

2. Material and methods

2.1. Materials

Materials applied in this work were the followings: yeast (*Saccharomyces cerevisiae*; EU-standard granulated instant form, cat. no.: 2-01-420674/001-Z12180/HU); algae (*Chlorella vulgaris*; BioMenu, Caleido IT-Outsource Kft.; cat. no.:18255); from Sigma-Aldrich: bovine serum albumin (BSA; cat. no.: A-9418); sodium spermidine (cat. no.: S2626), Calcein-AM (cat. no.: 17783), Proteinase K (cat. no.: P-6556), Potassium bromide (cat. no.: 221864), Triton X-100 (cat. no.: X-100), dimethyl sulfoxide (DMSO; cat. no.: D8418), ethylenediaminetetraacetic acid (EDTA; cat. no.: E9884), ethylene glycol-bis(β-aminoethyl ether)-N,N,N′,N′-tetraacetic acid tetrasodium salt (EGTA; cat. no.: E8145), N,N,N′,N′-Tetrakis(2-pyridylmethyl)ethylenediamine (TPEN; cat. no.: P4413), acetic acid (cat. no.: 695092), Whatman filter (pore diameter: 2 μm; cat. no.: 6783-2520), SH-SY5Y human neuroblastoma cell line (cat. no.: 94030304); from Merck: powdered Carmine crystals (Natural Red 4; cat. no.: 2233), sodium azide (NaN_3; cat. no.: 822335), methanol (MeOH; cat. no.: 1.07018.2511), glycerol (cat. no.: 1.04092.1000), hydrochloric acid (HCl; cat. no.: 1.00317.1000), distilled water (DW; Millipore Ultrapure); Dynabeads M-270 epoxy (Life Technologies AS, cat. no.: 14301); from Reanal: sodium dodecyl sulfate (SDS; cat. no.: 24680-1-0833), sodium hydroxide (NaOH; cat. no.: 24578-1-01-38), urea crystals (cat. no.: 08072), micro-cellulose (cat. no.: D-76); from Biochrom HG: trypsin (Seromed, cat. no.: L2103), Collagenase II (Seromed; Worthington, 252 U/mg; cat. no.: L6723); from Corning or Corning-Costar: 24-well plate (cat. no.: 3524), 96-well plate (Nunc; cat. no.: 167008), Petri dish (cat. no.: 430167), flasks (cat. no.: 430168); universal plastic web (pore diameters: 15 and 50 μm); etanol (EtOH; Molar Chemicals Kft.; cat. no.: 02911-481-430); standard medium (mg/L): Ca^{2+} 31.05; Mg^{2+} 17.6; Na^{+} 0.9; K^{+} 0.25; Fe^{2+} 0.001; HCO_3^- 153.097; SO_4^- 3; Cl^- 0.8; F^- 0.02; H_2SiO_3 3.3 (pH = 7.5), elevated salt medium (standard medium supplemented with 790 mg/L $NaHCO_3$). The glass coverslip (diameter: 12 mm, thickness: 0.15 mm; cat. no.: 89167-106) was obtained from VWR International, Houston. The beta-amyloid 1-42 (Aβ42; cat. no.: A14075, human Amyloid b-Peptide 1-42; 107761-42-2) was purchased from AdooQ Bioscience LLC., California.

2.2. Harvesting and identification of different rotifer species

To collect and isolate different monogonant rotifers, the method described by Debortoli et al. (2016) was used with minor modifications. Source of samples was located in the Red Cross Lake (Vértó; 27,000 m^2; GPS coordinates: 46° 16′ 25″ N; 20° 08′ 39″ E; early summer) in Szeged (Southern Great Plain, Hungary). The original media of collected samples were substituted with standard medium in separate Petri dishes. The species collected were *Euchlanis dilatata, Ehrenberg, 1832; Lecane bulla, Gosse, 1851; Lepadella patella, O. F. Muller, 1773; Itura aurita, Ehrenberg, 1830; Colurella adriatica, Ehrenberg, 1831; Trichocerca iernis, Gosse, 1887*; *Cephalodella intuta, Myers, 1924; Brachionus leydigii rotundus, Rousselet, 1907; Brachionus calyciflorus,* Pallas, 1766*; Synchaeta pectinata, Ehrenberg, 1832* which were photographed (Nikon D5100, DSLR, RAW-NEF, 16 MP, ISO 100; Nikon Corp., Kanagawa, Japan) under inverted light microscope (at 63X and 400X magnification; Leitz Labovert, Wetzlar, Germany). Serial images were taken at every 5-μm intervals yielding a total of 5–8 photographic layers per rotifer, which were subsequently merged into one superimposed picture (by using Photoshop CS3 software, Adobe Systems Inc., San Jose) to achieve better resolution. The entities were paralyzed with carboxygenated (5% CO_2) standard medium for 5 min during photo recordings. After the species were identified based on methods described in academic literature (Kertész, 1894; Kutikova, 1970; Koste, 1978; Nogrady and Segers, 2002; Varga, 1966), species-specific information (e.g., body size in relation to age) was applied to collect relatively mature individuals (generally with an egg in their body). Animals were collected and isolated (using a micropipette) to create separated and monoclonal populations. After completing the experiments, *E. dilatata*, *L. bulla* and *C. intuta* were maintained as standard cultures of our laboratory.

2.3. In vivo and in vitro culturing

All investigated rotifers (Fig. 1A-J) were cultured in flasks (25 cm^2 area) filled with standard medium. They were fed every second day by heat-inactivated, homogenized and filtered (plastic web; pore diameter: 15 μm) algae-yeast (in 1:3 ratio) suspension (final dose: 600 μg/mL/case). The live algae- and yeast cell cultures, to carry out viability experiments, were started with rehydration in glucose supplemented (1 mM) standard medium left to rest for 16 h at room temperature.

For in vitro measurements, the popular adrenergic SH-SY5Y human neuroblastoma cell line was applied with the related culturing entirely based on the previous works of Datki et al., (2003, 2018).

2.4. Exudate-inductions and adequate targeted treatments

The experimental animals were isolated by pouring them into Petri dishes (55 cm^2 area). In all rotifer-specific biopolymer (named 'Rotimer') related experiments, 20 mature animals (with an egg inside or with maximal body size) were applied per well in a 24-well plate (1.8 cm^2 area) with 1 mL working volume.

The final (working) concentration of the administered inductors of Rotimer-secretion was 50 μg/mL, diluted from 1 mg/mL stock solution. Every inductor (Table 1) was prepared in line with their own molecular properties: a. yeast: heat inactivated cell skeleton; b. BSA: heat denatured (den-BSA; 20 min, 80 °C, in DW); c. epoxy: metal beads coated with polymers; d. Carmine: mechanically ultra-powdered dye crystals (with classic electric coffee grinder); e. urea: ultra-powdered crystals; f. cellulose: powdered micro-cellulose.

To measure the non-specific adhesion of inductors to well-surface, the medium (without rotifer and Rotimer), containing particles, was decanted from the wells, and the passively covered area was maximum 1% in these blank (rotifers-free) experiments. Secretion of particle-induced biopolymer resulted a 'Rotimer-inductor conglomerate' (RIC) in a high density web form after 20 min incubation time (Fig. 1K-M; with yeast inductor). After carefully removing the well solution, these RIC products were desiccated (dried) at room temperature (25 °C) and at 40% humidity in the dark for 30 min. This preparation method was also administered in high resolution, monitoring the Rotimer fibers and gluelike format (Fig. 1L; with epoxy inductor). The inductor particles were applied under the size of 2 μm (the Carmine inductor was filtered with Whatman filter) or above 50 μm (filtered with plastic web) where they were unable to induce the Rotimer secretion and RIC formation. The RIC patterns, detected by light microscopy, were photographed (Nikon D5100) and the pictures were converted in a black and white graphical format (threshold; 2.04 pixel = 1 μm; 8-bit). These images were analyzed with ImageJ program (Wayne Rasband, USA), extracting data related to the conglomerate-covered area (%) and the average size (μm^2) of this complex. RIC analysis was used to select the higher RIC-producing species using the yeast inductor (Fig. 2A) related to RIC-producing capacity (RPC; **Suppl. Video**); furthermore, the RPC was also applied for screening different Rotimer inductors (Fig. 2B) and

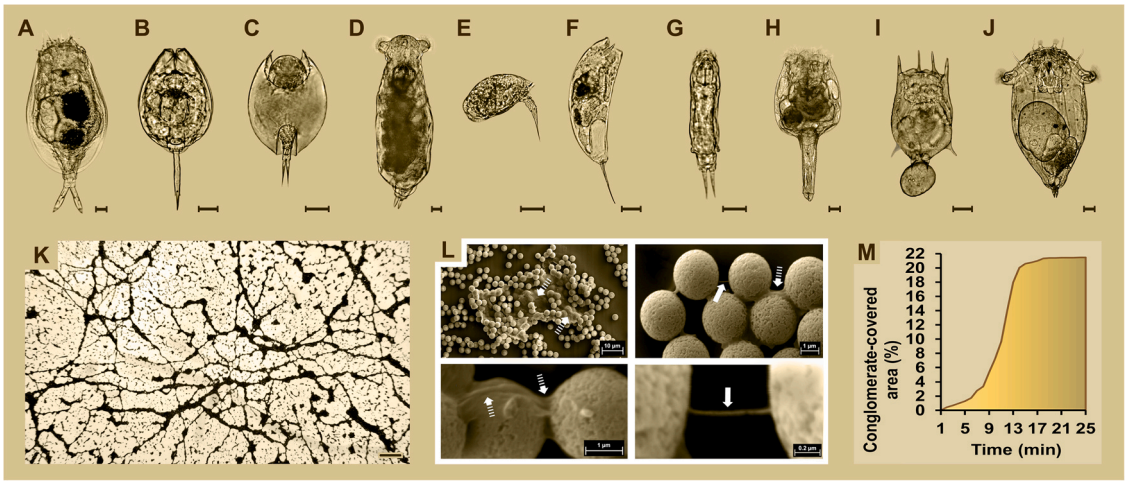

Fig. 1. Presentation of rotifers and their specific biopolymer (Rotimer) by its conglomerates. The representative photos of monogonant rotifer species (A-F) are shown. The monitored species in Rotimer-related experiments (scale bar: 20 μm) are the followings: *Euchlanis dilatata* (A), *Lecane bulla* (B), *Lepadella patella* (C), *Itura aurita* (D), *Colurella adriatica* (E), *Trichocerca iernis* (F), *Cephalodella intuta* (G), *Brachionus leydigii rotundus* (H), *Brachionus calyciflorus* (I), *Synchaeta pectinata* (J). The picture shows the web of 'Rotimer-Inductor Conglomerate' (RIC) which was formed by *E. dilatata* (K; scale bar: 200 μm). The montage of representative photos of SEM (L) show the different types of Rotimer after epoxy induction (scale bars 0.2 and 1 μm). The filamentous form is indicated by arrows and the gluelike structure is presented by dashed arrows. Exponential kinetic of RIC formation (M) was measured by time-dependent (min) saturation of the conglomerate-covered area (%).

Table 1
Outline of basi experimental runs.

Experiments	Monogonant species	Applied inductors	Treatment agents or environment	Test entities, cells or targets	Measured parameters	Visualisation methods
Presentation of rotifers and their specific biopolymer (Rotimer) by its conglomerates. (Fig. 1)	*E. dilatata*	yeast epoxy	standard medium	*E. dilatata*	conglomerate-covered area fiber and gluelike form	light microscopy scanning electron microscopy
Rotifer-specific production of Rotimer-Inductor Conglomerates (RIC) (Fig. 2A)	*E. dilatata* *L. bulla* *L. patella* *I. aurita* *C. adriatica* *T. iernis* *C. intuta* *B. leydigii* *rotondus* *B. calyciflorus* *S. pectinata*	yeast	standard medium	RIC-amount	conglomerate-covered area and average size of conglomerates	light microscopy
Inductor-specific production of Rotimer-Inductor conglomerates (Fig. 2B)	*E. dilatata*	BSA epoxy Carmine urea cellulose	standard medium	*E. dilatata*	conglomerate-covered area and average size of conglomerates	light microscopy
Rotimer producing activity (Fig. 3A)	*E. dilatata*	Carmine	repetitive induction starvation sodium-azide spermidine temperature salt pH	*E. dilatata*	conglomerate-covered area and average size of conglomerates	light microscopy
Rotimer dissolution measurements (Fig. 3B)	*E. dilatata*	Carmine epoxy	rotifer-media trysin proteinase K collagenase II triton X-100 SDS DMSO EDTA EGTA TPEN etanol metanol glycerol HCl acetic acid NaOH	RIC-structure	dissolution time and empirical alterations of the original web quality	light microscopy
Spectroscopic characterization of RIC (Fig. 4)	*E. dilatata*	Carmine	standard medium	*E. dilatata*	infrared wavelength	FTIR
Physiologic effects of the examined RIC in vitro (Fig. 5A)	*E. dilatata*	BSA	standard medium	*C. vulgaris yeast* *SH-SY5Y cells*	motility and intracellular esterase activity	light microscopy and fluorescent plate-reader
The role of Rotimer against beta-amyloid 1-42 (Aβ42) aggregates (Fig. 5B)	*E. dilatata* *L. bulla* *C.intuta* *S. pectinata*	yeast	Aβ42	*E. dilatata* *L. bulla* *C. intuta* *S. pectinata*	motility and intracellular esterase activity	light microscopy and fluorescent plate-reader

rotifer-influencing factors (Fig. 3A; with epoxy inductor). Yeast cell skeleton (as a natural particle) was applied as a common inductor in species-specific RIC production measurements (Fig. 2A). The yeast homogenate, aside from using it as an inductor, compiled two-third of the standard nutrient in the case of all species. The rotifer entities, kept in Petri dish, were treated in populations, during the RIC production-related experiments (Fig. 3A), then they were rinsed twice by standard medium. The investigated animals (20 rotifers/wells) were selected and their RIC production was monitored. There were 10 min breaks between the treatment rounds (20 min/case) under repetitive inductions. After each round, the same rotifers were carefully transported by a micropipette into a new well to start the next cycle. These measurements, together with the starvation experiments, were performed under total nutrient depletion, in order to attenuate the biopolymer synthesis in animals. The NaN_3 (20 μM) and spermidine (50 μM) treatments were carried out after 100× dilutions from stock solutions. During the salt concentration (0 or 1 g/L) and pH (6 or 8) studies, the final concentrations were provided by transferring the supernatant instead of the dilution. Supplemented composition of standard medium to 1 g/L dose was implemented by adding extra $NaHCO_3$. Epoxy beads were applied as an inductor in these experiments, because the RPC index (in statistics) of this agent proved to be the best (Suppl. Fig. 1). In order to assess the sublethal dose of NaN_3, the swimming speed (465 ± 22 μm/s in normal case) of rotifers was monitored as a viability marker to measure its dose-response to NaN_3 (Suppl. Fig. 2). The detailed general outline of the supplemental experiments is presented by Suppl. Table. Before investigating the inductor-cohesive-stability of Rotimer to reveal the structure of RIC (Fig. 3B; Carmine inductor, except of NaOH, where it was Epoxy), the animals were carefully removed by a micropipette. Then, the well-content was supplemented by the 10× concentration of treatment agents (enzymes, solvents, chelators, alcohols and pH-solutions). These RIC-influencing-factors were the followings: normal supernatant media

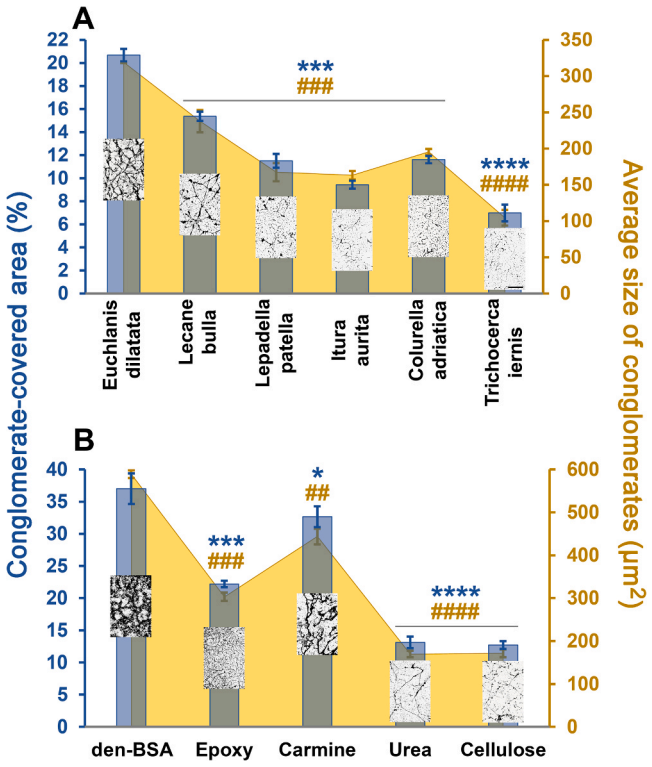

Fig. 2. Rotifer- and inductor-specific production of RIC. Monogonants with different 'Rotimer-Inductor Conglomerate' (RIC) producing capacity (A) and the impacts of various inductors on the web structure (B) are presented by the RIC-covered area (%; blue) and the average size of RIC (μm^2; yellow). The species-specific webs of RIC are shown by the representative photos on each columns (scale bars: 500 μm). Various Rotimer-inductors were measured on the most productive *E. dilatata* (B), where the representative pictures of the different inductor-specific RIC fibers are presented on the columns (scale bars: 500 μm). The investigated agents were denatured bovine serum albumin (den-BSA), epoxy beads, Carmine, urea and cellulose. The error bars represent S.E.M. One-way ANOVA with Bonferroni post hoc test was used for statistical analysis, the levels of significance are p***,### ≤ 0.001 (*, significant difference from *E. dilatata* (A) or from denatured-BSA group (B) in RIC-covered area; # significant difference from *E. dilatata* or from denatured-BSA group (B) in average size of RIC). The black line above the bars means that all these ones show the same level of significance. (For interpretation of the references to colour in this figure legend, the reader is referred to the web version of this article.)

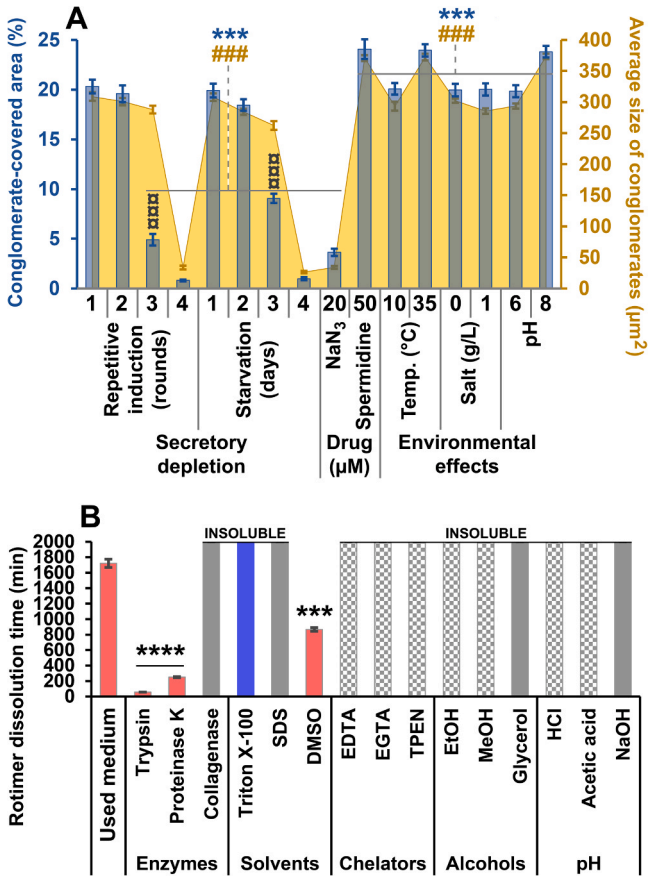

Fig. 3. Rotimer-influencing factors: in vivo secretion and in vitro dissolution. The effects of different conditions on *E. dilatata* Rotimer producing activity (A) were monitored by 'Rotimer-inductor conglomerate' (RIC)-covered area (%; blue) and average size of RIC (μm^2; yellow). The examined conditions were different secretory depletion methods: repeated induction by carmine (rounds) or induction during starvation (days). The applied drugs were the toxic NaN_3 and beneficial spermidine. The investigated environmental conditions were the temperature (4 °C and 30 °C), concentration of salts (0 and 1 g/mL) and various pH (6 and 8). Rotimer dissolution-related experiments were performed by applying various solvents and drug candidate groups (B), which were the followings: medium used by the rotifers (control); enzymes (trypsin, proteinase K, collagenase II); solvents (triton X-100, SDS, DMSO); chelators (EDTA, EGTA, TPEN); alcohols (EtOH; MeOH, glycerol) and pH-related chemical compounds (HCl, acetic acid, NaOH). The columns represent the dissolution time (min) and their colors show the empirical alterations of the original web quality, where the red stands for dissolution; the blue means the conservation in original high quality; the gray shows the insolubility (during 2000 min) and gray square represents the formation of high RIC aggregates. The error bars show S.E.M. One-way ANOVA with Bonferroni post hoc test was used for statistical analysis; the levels of significance are p***,###,¤¤¤ ≤ 0.001 and p**** ≤ 0.0001 (*, significant difference between the columns above or below the upper or the lower gray lines (A) in percentage of RIC-covered area or from the standard environment (B); #, significant difference between the columns above or below the upper or the lower gray lines (A) in average size of the conglomerates; ¤, significant between the percentage of RIC-covered area and percentage of average size of the conglomerates in the relevant conditions). The black line above the bars means that all these ones show the same level of significance. (For interpretation of the references to colour in this figure legend, the reader is referred to the web version of this article.)

of rotifers, trypsin (1%), Proteinase K (0.5 mg/mL), Collagenase II (3 mg/mL), Triton X-100 (1%), SDS (1%), DMSO (70%), EDTA (0.1 M), EGTA (0.1 M), TPEN (0.1 M), EtOH (70%), MeOH (70%), Glycerol (70%), HCl (1 M), acetic acid (70%) and NaOH (1 M). The concentrations were applied at the highest recommended level by manufacturers. All manipulations were performed slowly and carefully to avoid the fluid flow destroying the RIC web. The disruption of the fiber (mechanical resistance against fluid flow) was measured under the microscope (25× magnification) using the removed and transferred micropipettor (at 45° angle, 3 mm from RIC web) of the micro-plate reader (NOVOstar, BMG, Offenburg, Germany). The RIC-stability was provoked by max. 230 μL/s flow velocity (injected volume: 50 μL) where the fibers tore (end of **Suppl. Video**).

Supplementary material related to this article can be found online at doi:10.1016/j.ecoenv.2020.111666.

2.5. The Rotimer and RIC detection with scanning electron microscope

The Rotimer formations (fibers and glues) seemed to be undetectable under inverted light microscope; therefore, analysis with scanning electron microscope (SEM; Fig. 1L) was performed. For these series of experiments, the best and smallest stimulator, epoxy, was used (50 μg/mL) to induce Rotimer secretion and RIC formation in the most productive species, *E. dilatata*. The RIC was produced on a round glass coverslip which was washed with 96% EtOH, DW and finally with standard medium before being experimented in 24-well plates (one coverslip/well/30 mature rotifer). The animals produced RIC for 30 min

on the coverslip under standard conditions, then, they were carefully removed by a micropipette. The glass surface covered by RIC was checked under light microscope, then, it was let dry at room temperature for 1 h. The samples were coated with gold. The selected areas (based on their quality) were subjected to SEM (Zeiss EVO MA 10, Carl Zeiss, Oberkochen, Germany). The sample-carrier coverslip was fixed onto a stub using a double-sided carbon tape. The samples were coated with gold using a Quorum Q150R sputter coater during 120 s. The fine structure of the RIC was observed and photo-documented with the SEM at different magnifications (from 846X to 40.47KX). The detections were operating at 10 kV with an 8-mm working distance, using a secondary electron detector in high vacuum mode. The white balance of SEM photographs was normalized.

2.6. Analysis of Rotimer containing RIC with FTIR spectroscopy

In order to perform FTIR spectroscopy (Kowalczuk and Pitucha, 2019) measurements, Rotimer containing RIC samples were prepared. As a first step, *E. dilatata* (n = 500 ± 30 individuals) populations were harvested into Petri dishes (55 cm^2 area). Then, the inductor (Carmine) was added to the rotifer-containing standard medium for 20 min. The produced RIC was mechanically homogenized by a pipette. The animals were removed by filtration using a plastic web (pore size 50 μm). The animal-free, but RIC-containing solution was then centrifuged by 4000 × *g* for 20 min (in 14 mL volume centrifuge tubes) at room temperature. The supernatant was decanted and the pellet was used for FTIR measurements.

The concentrated RIC solution (15 μL) was dropped onto the surface of potassium bromide pastilles (200 mg, 13 mm diameter) three times, which were compressed with hydraulic press (Specac Inc., UK). The pastilles were then desiccated for 48 h in silica gel filled desiccator. The FTIR spectra of various samples were measured with a Thermo Nicolet Avatar 330 FTIR spectrometer (Thermo Fisher Scientific Ltd., Waltham, MA, USA) using a Transmission E. S. P. accessory applying 128 scans at a resolution of 4 nm. Data were collected with EZ OMNIC software, while spectrum analysis was performed with Spectragryph 1.2.13 (Friedrich Menges, Oberstdorf, Germany) software. A strong shift of baseline was observed due to the beam scattering on the undissolved or recrystallized carmine particles. Furthermore, due to the low signal intensities, resulted by the low sample concentrations, the presence of negative peaks was observed in the 2800–3000 cm^{-1} CH stretching region. It was also resulted by the uncompensated background signal of hydrophobic protective coating on the optical elements of the spectrometer. These artificial distortions and the uncompensated CO_2 signals in the region of 2280–2390 cm^{-1} were cut off from the spectrum prior to baseline correction. To compensate the effect of beam scattering two step baseline correction, simple linear correction, followed by a secondary adaptive correction (coarseness = 10) was applied prior to the analysis.

2.7. Bioactivity-related viability assays

In all viability-related experiments (Table 1), based on Calcein-AM (stock solution: 1 mg/mL in DMSO; final concentration was 5 μM), the labeling interval was 1 h at room temperature in the dark. The viability (cell-fluorescence) and motility (movement of cells) of algae and yeast cells (Fig. 5A) were measured in separate 24-well plates. Confluent cell population (120 ± 11 cells/well) was applied in cytoplasmic calcium detection where the fluorescence intensity (FI) of intracellularly trapped Calcein (ex. 490, em. 520; calibration/gain adjustment was 1% of the maximal relative intensity) was detected. Separate cells (4–5 cells/well) were administered in motility-related investigations. After 24 h treatment with RIC (used inductor: den-BSA) and its reference controls (untreated or only den-BSA treated), the FI of intracellular calcium-specific dye and the moving action in different setups were measured, in the latter case the detection interval of cell motility was 10 min (unit: μm/min).

To test the physiologic effects of the examined RIC (containing Rotimer) in vitro, we applied the SH-SY5Y neuroblastoma cells. The viability (fluorescence) and motility (cell migration) of SH-SY5Y cells were separately measured in 96-well plates. The FI of intracellular Calcein was detected after 24 h treatment with den-BSA or its RIC in a cell culture with confluent monolayer (cell number was 110 ± 8 in one well). Detection interval in cell motility assay (4–5 cells/well) took for 6 h (unit: μm/h) after one-day-treatment.

The potential role of Rotimer against Aβ42 aggregates was investigated in four different species (Fig. 5B; *E. dilatata; L. bulla; C. intuta; S. pectinata*). Concentration of Aβ42 stock solution was 1 mg/mL (DW) with 3 h (25 °C, pH 3.5) aggregation period. Neutralization (to pH 7.5) of this solution was performed with NaOH (1 N). After 10-fold dilution with standard medium, the final (working) concentrations were 100 μg/mL. After harvesting, 30 ± 2 mature rotifers per well (n = 24 well/species in 96 well-plate) were treated in 0.2 mL volume. The treatment period was 5 days in standard conditions (24 °C; 40% air humidity; standard media). The depletion protocol was performed before the Aβ42 was administered and this protocol was in line with the one applied in Fig. 3A-treatment. Every Aβ42-treated group had its own untreated control, which was the reference (100%) in every case. Two parameters of viability were measured, namely the number of rotifers alive and the intracellular esterase activity (indicated by relative fluorescence intensity of Calcein-AM). The populations were observed under light microscope (63X) combined with digital camera (Nikon D5100). The protocol of Calcein-AM measurements were the same with the one applied in Fig. 5A.

2.8. Statistics

The error bars represent the standard error of the mean (S.E.M.). For comparative statistical analysis, the one-way ANOVA was used followed by the Bonferroni post hoc test with SPSS 23.0 (SPSS Inc, Chicago, IL, USA) software for Windows. The homogeneity and normality of the data were checked, and they were found suitable for ANOVA followed by Bonferroni post hoc test. The RPC index (RPC_i) is a relative unit, which was calculated by the following formula: RPC_i = ASC/ASIP * CA/NR; ASC: Average Size of Conglomerates (μm^2); ASIP: Average Size of Inductor Particles (μm^2); CA: Covered Area (%); NR: Number of Rotifers. The different levels of significance are indicated as follows: $p^{*, \#} \leq 0.05$, $p^{**, ¤¤} \leq 0.01$, $p^{***, ###, ¤¤¤} \leq 0.001$ and $p^{****} \leq 0.0001$ (all marks are defined in the given figure legend).

3. Results and discussion

In academic literature, no one has yet described filamentous biopolymer secretion in rotifers, nor in monogonants. The aim of the present study was to describe and characterize a novel rotifer-specific biopolymer, called 'Rotimer' in monogonant rotifers. Biopolymers are scientific hotspots for which researchers have been recently gaining more academic interest (Humenik et al., 2019).

The above mentioned rotifer-specific fiber production was observed in six (Fig. A-F) different freshwater monogonants, which were the followings: *E. dilatata, L. bulla, L. patella, I. aurita, C. adriatica* and *T. iernis*. All investigated animals can be frequently found in lakes or other natural waters; furthermore, they are well-established model organisms of ecotoxicological (Walsh et al., 2009; Suthers et al., 2019;) and pharmaceutical researches (Gutierrez et al., 2020). After permanent laboratory culturing the *E. dilatata* and *L. bulla* proved to have the most intensive RIC production capacity (RPC) out of the six investigated species. Representative photo (Fig. 1K) about RIC formation produced by *E. dilatata* was taken.

Nevertheless, we observed RIC formations in the original medium of wild-type animals collected from their natural habitat, meaning they are able to produce Rotimer in nature. Since, the secreted Rotimer alone could not experientially be detected by light microscope; therefore, its

existence could only be proved with particle adhesion.

No refractions of the Rotimer were detected between two inductor particles at 1000X magnification. In order to try to optically visualize this biopolymer, different types of dyes (Trypan blue, Light green SF, Orange G, Neutral red, Methylene blue, Acridine orange, Ponceau S, Bromophenol blue, Congo red, Fuchsine, Coomassie brilliant blue G-250 or R-250, Luxol fast blue and Methyl red) were tested, diluted in DW or EtOH, but no success was gained in labeling them. Fibers drawn by *E. dilatata* monogonants are very thin (33 ± 3 nm cross section) and they can only be observed by SEM. The produced exogenic Rotimer (Fig. 1L) can either be filamentous (arrow) or gluelike (dashed arrow). Both biopolymer forms are secreted parallelly and attach to the surface of inductors. Secretion of Rotimer could be mechanically induced by approximately 2.5–50 μm diameter particles, respectively in *E. dilatata.* No RIC production above or under this range was observed. Beyond size-specificity, the Rotimer induction does not depend on the qualitative properties (e.g. type of material) of inductors. Percentage of conglomerate-covered area exponentially increased with time, characterizing the kinetics of RIC production in *E. dilatata* (Fig. 1M). The saturation of confluent covering in the measured area took 18–20 min in standard medium. Contrary to monogonants, no fiber-like formations were detected in the case of bdelloids; however, the attachment of their eggs and coating with nutrient particles on the bottom of the flask were observed. Based on these empirical data, bdelloids may likely produce polymer-type secretions. The presence and existence of Rotimer is optically indicated by RIC formation that is fibrous, viscoelastic, floating in fluid (3D formation) and breakable by water jet (**Suppl. Video**; visible at the 56–59 s). Rotifers are able to find the web-formation from a relatively high distance in their dimensions by directional approaching; therefore, it is assumed that the fiber has a specific surface, which can be recognized by them. The longest detected fiber was 1.3 mm (floating in water between two attached ends).

Rotimer was secreted by six different rotifers (Fig. 2A) and this product was investigated to assess which species could be the most effective producers under yeast induction. The representative photos of RIC present which type of rotifers produce it by creating different web structures. Various sizes of Rotimer-inductors were tested on *C. intuta, B. leydigii rotundus, B. calyciflorus* and *S. pectinata*; however, no structured fiber-like polymer production was found. In the quantitative characterization of RIC, the percentage of covered area and the average size of conglomerates were monitored. The *E. dilatata* significantly showed the highest measures in both parameters, thus, this species seemed to be the best producer of RIC formation. The next step was to find out whether there were other non-toxic inductors which might have been more effective than yeast (Fig. 2B). The potential candidates were tested and the average particle size (μm^2; excluding the adhesive Rotimer) were also determined: den-BSA, 165 ± 22; epoxy, 7.5 ± 0.5; Carmine, 50 ± 14; urea, 83 ± 21; cellulose, 75 ± 18 as opposed to the reference yeast, 45 ± 3.

All investigated inductor-types were able to induce Rotimer-secretion, manifested by RIC, that are showed by the representative photos. Accordingly, the process of induction is not specific, but it is exclusively triggered by the size of particles. The RIC composed den-BSA-Rotimer web showed the highest value in the conglomerate-covered area and in the average size of conglomerates. The epoxy and Carmine were also applicable in further experiments. The urea and cellulose were able to induce RIC production; however, their efficiency were much lower than that of the other inductors.

The size-related parameters of particles presented the differences between them, but they were not enough to provide a comprehensive characterization. In order to overcome this problem, the RPC index was developed. This quantified relative index becomes higher, when there are fewer animals the inductor particle size is low and the formed conglomerates are large. According to the RPC index (RPC_i), the epoxy was the most effective inductor, the second one was Carmine and the third one was den-BSA (Suppl. Fig. 1). The most adequate type of inductor was chosen, considering its chemical and biological properties, and RPC_i in the relevant experiments. Based on the universal adhesive property of Rotimer, it may prove to be a useful tool in waste water cleaning. Similarly to other biopolymers (Kalia and Avérous, 2011), it may have a potential industrial use.

As the RIC web seemed to be a very complex formation and it is characteristic to some monogonants, we wanted to test how the different environmental factors influence its production (Fig. 3A). The yeast was applied as an inductor, since it is also a component of the food of rotifers. After repetitive inductions, the depletion of the Rotimer-resources was observed in *E. dilatata*. After the third round of induced stimulation, the average size of conglomerates did not alter, nonetheless, the percentage of conglomerate-covered area significantly decreased. Differences between both of the measured parameters were found in the first-second rounds and third-fourth rounds. Presumably, the animals ran out of the materials needed for secretion and there was probably not enough time for resynthesis. It is supposed that active synthesis of Rotimer is required for RIC production which might be an energetically active process.

After starvation, we observed a second mode of depletion of Rotimer secretion due to the lack of nutrients (Fig. 3A). The size of conglomerates remained the same, after three days without food, but the covered area was significantly reduced. Remarkable alterations of monitored parameters were seen between RIC productions after the first-second day and third-fourth day of starvation. As there was no food available, the rotifers probably used the endogenous Rotimer substrate as energy deposit. The regeneration time of RIC production was 30 ± 4 min applying yeast homogenate or 140 ± 11 min applying den-BSA as inductors as well as foods in starvation-depleted *E. dilatata* entities. In the presence of epoxy, Carmine, urea and cellulose there was no RIC production for more than 6 h incubation time in depleted animals. The systemic production of Rotimer in rotifers is relatively quick and is highly nutrient-dependent.

To measure the properties of the viability marker of Rotimer secretion, the highest sublethal dose of NaN_3 (Suppl. Fig. 2) in *E. dilatata* was determined, which had no toxic effect on them for 6 h. The NaN_3 was applied with the purpose of revealing how the partial mitochondrial dysfunction may influence Rotimer secretion. Based on the current literature, we used the swimming speed as an adequate reference viability marker of monogonants (Dahms et al., 2011; Chen et al., 2014; Guo et al., 2012; Dong et al., 2020). The swimming speed of control animals was 465 ± 22 μm/s in the setup and the RIC production was also manifested by this kind of speed. Deceleration in swimming speed at doses between 50 and 500 μM was observed and thereby, 20 μM was selected for the next experiment. The applied dose of sodium azide had a negative effect on biopolymer formation, presenting the sublethal viability marker properties of Rotimer secretion. This inhibitor of terminal oxidation significantly and parallelly decreased both the percentage of conglomerate-covered area and the average size of conglomerates. Based on pervious results, NaN_3 is a mitochondrial toxin, which reduces the energy synthesis by lowering the efficacy of mitochondrial respiration (Olah et al., 2017). In contrast with that, spermidine had positive effects on all parameters. This is in line with our previous publications where the calorie-mimetic spermidine showed beneficial impact on mitochondrial function and physiology (Datki et al., 2019). These data also supported the assumption that RIC production requires energy. Surprisingly, the lower temperature (10 °C) did not decrease the monitored parameters compared to its controls, while the higher temperature (35 °C) was able to stimulate production. Results found were in line with the publication of Li et al. (2019), who measured different life parameters (trade-offs between egg size and egg number, current reproduction and future survival) of *E. dilatata* at 14 °C, 20 °C and 26 °C. By increasing temperature, the lifespan, pre-mature- and reproductive periods decreased; however, the rate of population growth elevated. Similarly to RIC production, warmer temperature was beneficial for monogonants. Directly using *E. dilatata* entities after isolation,

the elevation (1 g/L) or the reduction (DW) of salt concentration had no effect on RIC production compared to the standard medium (Fig. 3A); however, when these animals were left to rest (washed) in completely ion-free medium for half an hour, the RPC disappeared. The salinization of coastal freshwater raises serious concerns on the protection of their ecosystems (Venâncio et al., 2018). High salinity induces oxidative stress, having a negative impact on lipid metabolism in another monogonant rotifer, *Brachionus koreanus*, demonstrated by Lee et al. (2018). Contrary to these comprehensive data about the salt-sensitivity of monogonants, it was observed that the extreme osmolarity had no negative impact on the monitored parameters. Lower pH (6) did not reduce the above mentioned parameters, while the higher pH (8) was beneficial for RIC production. The pH 6 represented the lower pH range of most natural waters found in the United States and across Europe (Cardwell et al., 2018), where monogonants are found, such as *Brachionus* species which were cultured at different ranges of pH from 6 to 10. The maximum population densities were reached at pH 8. (Gopal et al., 2014).

Furthermore, we were curious to find out how RIC could maintain its integrity in the presence of various chemical agents (Fig. 3B). The structure-preserving stability of particles, adhered by Rotimer, was detected. Although the epoxy seemed to be the best inductor, it could not be applied together with enzymes or ionic molecules due to its superficial specific charges, which may inactivate the applied agents. Carmine was used as inductor in all cases of current experiments, except in the presence of NaOH, because it dissolved these crystals; thus epoxy was added. It was highlighted that RIC lost its integrity in the presence of two-day-old rotifer culture medium, trypsin, proteinase K or DMSO during the time of measurement, suggesting that a protein-type material may fully or partially compose the Rotimer. The RIC preserved its original integrity together with collagenase II, Triton X-100, SDS, glycerol or NaOH. Triton X-100, the nonpolar detergent, showed the highest level of conservation. Moreover, the RIC was extremely aggregated by EDTA, EGTA, TPEN, EtOH, MeOH, HCl or acetic acid without solubilization. It may occur that metal ions and hydration may be necessary for maintaining normal integrity of the Rotimer. Unfortunately, it is very difficult to investigate the Rotimer structure and its components, because right now, we cannot clearly isolate this biopolymer from the relevant inductor. Investigation of this exudate was carried out in the presence of Carmine, a non-proteinous RIC-inductor, with FTIR (Fig. 4).

The FTIR spectrum of the standard medium contains several broad peaks which may be associated with the HCO_3^- and silicic acid content. The spectrum of the Carmine, as inductor molecule, contains two individual peaks in OH stretching region (3732 and 3299 cm^{-1}) belonging to the non-associated and associated OH groups, respectively. The strong right shift of the non-associated peak to 3438 cm^{-1} in the RIC indicates that Rotimer connects to the inductor molecules via the formation of H-bonds of those OH groups which take no part in intramolecular associations. The appearance of a new peak 3250 cm^{-1} could be connected to the N-H stretching of amine groups of the biopolymer. The peaks associated with the C=O stretching appeared in slightly lower wavenumbers than usually. The C=O stretching of aromatic carboxylic acid is visible at 1645 cm^{-1}, while the peak related to the diaromatic keto groups appeared at 1569 cm^{-1}. The relatively unchanged position of these peaks indicates that these groups are not involved in the formation of RIC, possibly due to their partition in intramolecular associations. The appearance of the new peak at the position of 1612 cm^{-1} is related to the amide II vibrations of the Rotimer backbone. The peaks at 1471 cm^{-1} and 1413 cm^{-1} belong to βOH vibrations of carboxylic and phenolic OH groups respectively, while the peak doublet at 1292 cm^{-1} and 1259 cm^{-1} may be associated with the βOH vibration of secondary alcoholic groups. The peak quadruplet in the 980–1080 cm^{-1} region belongs to the C-O stretching of various molecular parts. Considerable differences of the pure carmine and carmine-Rotimer complex may be observed in this region, but due to the low signal intensity and strong overlapping peaks the cause of the change may not be clearly identified.

The results of FTIR analysis indicate strong H-bond-based interactions between the inductor Carmine crystals and the Rotimer, which exhibits peptide like nature. However, the separation of Rotimer peaks was impossible due to the strong overlapping of the Carmine and Rotimer signals. The clear molecular identification of the Rotimer structure will require further investigations.

Finally, the intention was to demonstrate the representative bioactivity of monogonants-secreted Rotimer. The physiological effects (viability and motility) of *E. dilatata*-derived RIC with Rotimer content on three different cell types (Fig. 5A) were investigated. Den-BSA was applied as inductor, which can be found in standard medium of human cell culturing; therefore, it had no extra physiologic impact on the cells in the setup. The average movement of cells were properly measurable (algae: 87 ± 18 μm/min; yeast: 150 ± 39 μm/min; neuroblastoma: 64 ± 19 μm/h) in untreated controls. Passive (diffusion-based floating) and active (cell-movement) motility can occur in algae and yeast, while only an active one was detectable in the human neuroblastoma line. The RIC slightly decreased the viability of algae or neuroblastoma, where the toxicity did not reach the LD50; furthermore, it ceased their motility in all types of cells. Based on our previous work (Datki et al., 2018), we were interested in Aβ-related toxicity in the presence of Rotimer (Fig. 5B). The natural nutrient of rotifers includes aggregated and conglomerated organic masses in their native habitat. Investigation of the harmful Aβ42 on rotifers is an interdisciplinary approach in toxicology-related life sciences. Four species were treated with Aβ42 aggregates; only two of them secreted Rotimer (*E. dilatata; L. bulla*). In

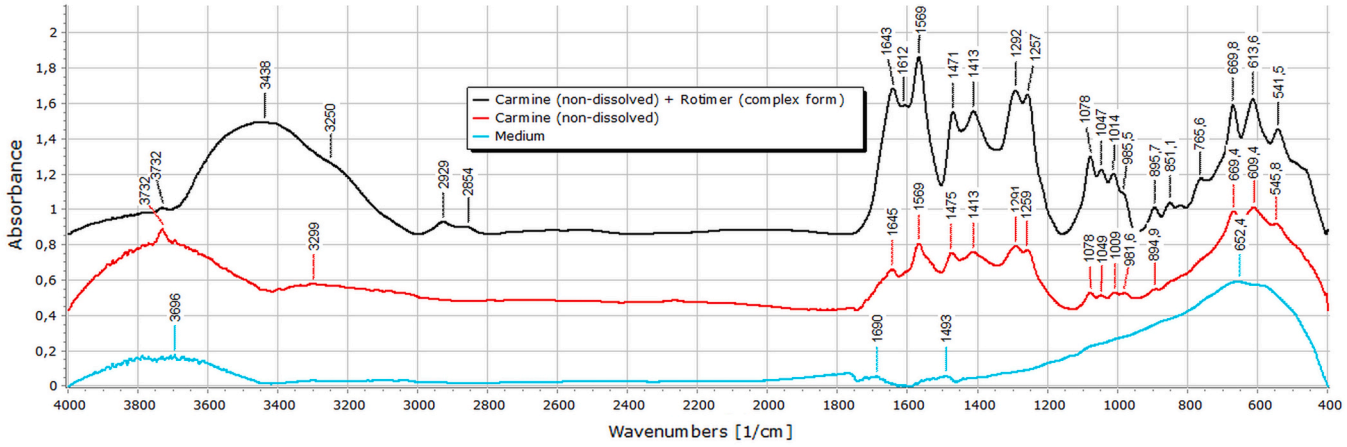

Fig. 4. FTIR spectra of the medium (blue), the Carmine crystals (red) and the Carmine-Rotimer complexes (black). (For interpretation of the references to colour in this figure legend, the reader is referred to the web version of this article.)

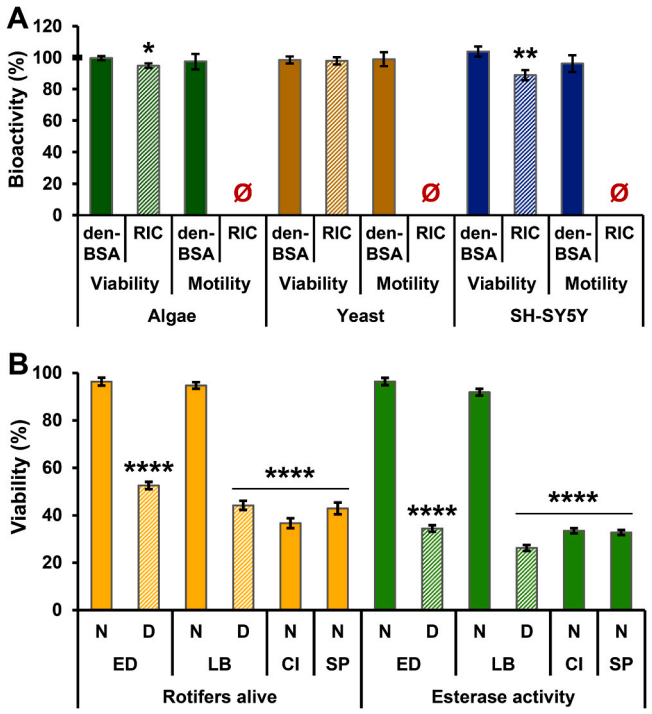

Fig. 5. Bioactivities of monogonant-secreted Rotimer. The special effect of *E. dilatata*-secreted RIC on different types of cell viability and motility (A) is presented. The percentage of bioactivity on viability and motility of algae (*Chlorella vulgaris;* green), yeast (*Saccharomyces cerevisiae;* yellow) and human neuroblastoma cells (SH-SY5Y; blue) was monitored in the presence of untreated control (100%) and denatured bovine serum albumin (den-BSA; full columns; reference control) or 'Rotimer-inductor conglomerate' (RIC; stripped columns). The untreated control was 100% marked with bold line on the *y-axis*. The error bars represent S.E.M. One-way ANOVA with Bonferroni post hoc test was used for statistical analysis; the levels of significance are $p^* \leq 0.05$ and $p^{**} \leq 0.01$ (*, significant difference from untreated control group). The impacts of monogonant-secreted Rotimer on viability in beta-amyloid 1–42 (Aβ42)-treated populations (B) are shown. Four species were investigated: *Euchlanis dilatata* (ED); *Lecane bulla* (LB); *Cephalodella intuta* (CI) and *Synchaeta pectinata* (SP). The number of rotifers alive (orange) and the relative fluorescence intensity of esterase activity (green) were measured and their percentages are presented. The species-specific untreated control was the reference 100% (data not shown). The full columns represent the Aβ42-treated normal (N) populations, while the stripped ones indicate the Aβ42-administered and Rotimer-depleted (D) ones. The error bars represent S.E.M. One-way ANOVA with Bonferroni post hoc test was used for statistical analysis; the level of significance is $p^{****} \leq 0.0001$ (*, significant difference from untreated species-specific control group). The black line above the bars means of treatments with the same level of significance. (For interpretation of the references to colour in this figure legend, the reader is referred to the web version of this article.)

secretion capable animals the Rotimer depletion was applied to investigate the role of this biopolymer in Aβ-sensitivity/toxicity. It was found that *E. dilatata* and *L. bulla* are not sensitive to Aβ42 aggregates in their normal state, where the number of rotifers alive and esterase activity was the same as in the case of species-specific untreated controls (100%). After in vivo biopolymer-depletion the animals lost their resistance against neurotoxic aggregates; and the measured parameters were significantly reduced, compared to their controls. The same phenomenon (significant decrease) was observed in those animals *(C. intuta; S. pectinata)*, which did not secrete exogenic filamentous biopolymer. The number of rotifers alive refers to the in vivo characteristics of the investigated populations, while the esterase activity indicates the cellular membrane integrity of the individuals. These results suggest that Rotimer can play an essential protective role against Aβ aggregate-toxicity in some monogonant rotifers. Although the molecular structure and the holistic biological/biotechnological significance of this proteinous-nature polymer is yet unknown, it will need further physical-chemical analysis.

4. Conclusion

The current study presents a novel and bioactive rotifer-specific biopolymer (having filamentous and gluelike forms), called Rotimer, derived from certain monogonants. In the presence of this exudate, its motility-inhibition effects in different cell types and its protective impacts in rotifers against neurotoxic aggregates were observed. This viscoelastic and chemically fairly resistant product might be a promising active molecule and drug candidate for ecotoxicological protection (e.g. water-clearing) or in researches related to cancer- and neurodegenerative diseases. The specific molecular structure and the holistic biological/biotechnological significance of this proteinous natural polymer is yet unknown.

Funding

The authors received no specific funding for this work.

Supplementary text

Methods

The empirical presentation of Rotimer secretion and RIC production can be seen in the video (**Suppl. Video**; MOV, full HD resolution, 16:9 ratio, 30 frame/s). The RIC producing capacity index (RPC_i) was calculated by the formula described in the statistics (Suppl. Fig. 1). The doses of NaN3 were applied in 100x dilutions (Suppl. Fig. 2).

CRediT authorship contribution statement

Conceptualization, Zs.D. and Z.G.O.; Methodology, Zs.D., Z.G.O., E. A., E.B., T.S. and I.Cs.; Validation, Zs.D., Z.G.O., and K.Zs.; Formal analysis, Zs.D., Z.G.O. and E.B.; Investigation, Zs.D., Z.G.O., E.B., E.A. and T.S; Resources, Zs.D., J.K.; Data curation, Zs.D., Z.G.O., E.A. and T. S.; Writing-original draft preparation, Zs.D. and Z.G.O.; Writing-review and editing, Zs.D., Z.G.O., E.B. and J.K.; Visualization, Zs.D.; Supervision, Zs.D., Z.G.O., I.Cs. and J.K.; Project administration, Zs.D., Z.G.O.; Funding acquisition, Zs.D. and J.K.

Acknowledgments

The authors wish to thank to Anna Szentgyorgyi MA, a professional in English Foreign Language Teaching for proofreading the manuscript.

Conflicts of interest

No conflicts of interests declared.

Appendix A. Supporting information

Supplementary data associated with this article can be found in the online version at doi:10.1016/j.ecoenv.2020.111666.

References

Cardwell, A.S., Adams, W.J., Gensemer, R.W., Nordheim, E., Santore, R.C., Ryan, A.C., Stubblefield, W.A., 2018. Chronic toxicity of aluminum, at a pH of 6, to freshwater organisms: empirical data for the development of international regulatory standards/criteria. Environ. Toxicol. Chem. 37, 36–48. https://doi.org/10.1002/etc.3901.

Chandra, R., Rustgi, R., 1998. Biodegradable polymers. Prog. Polym. Sci. 23, 1273–1335.

Chen, Q., Peng, D., 2019. Nematode chitin and application. Adv. Exp. Med. Biol. 11421, 209–219. https://doi.org/10.1007/978-981-13-7318-3_10.

Chen, J., Wang, Z., Li, G., Guo, R., 2014. The swimming speed alteration of two freshwater rotifers Brachionus calyciflorus and Asplanchna brightwelli under dimethoate stress. Chemosphere 95, 256–260. https://doi.org/10.1016/j.chemosphere.2013.08.086.

Dahms, H.U., Hagiwara, A., Lee, J.S., 2011. Ecotoxicology, ecophysiology, and mechanistic studies with rotifers. Aquat. Toxicol. 101, 1–12. https://doi.org/10.1016/j.aquatox.2010.09.006.

Datki, Z., Galik-Olah, Z., Bohar, Z., Zadori, D., Fulop, F., Szatmari, I., Galik, B., Kalman, J., Vecsei, L., 2019. Kynurenic acid and its analogs are beneficial physiologic attenuators in bdelloid rotifers. Molecules 24, 2171. https://doi.org/10.3390/molecules24112171.

Datki, Z., Juhász, A., Gálfi, M., Soós, K., Papp, R., Zádori, D., Penke, B., 2003. Method for measuring neurotoxicity of aggregating polypeptides with the MTT assay on differentiated neuroblastoma cells. Brain Res. Bull. 62, 223–229. https://doi.org/10.1016/j.brainresbull.2003.09.011.

Datki, Z., Olah, Z., Hortobagyi, T., Macsai, L., Zsuga, K., Fulop, L., Bozso, Z., Galik, B., Acs, E., Foldi, A., Szarvas, A., Kalman, J., 2018. Exceptional in vivo catabolism of neurodegeneration-related aggregates. Acta Neuropathol. Commun. 6, 6. https://doi.org/10.1186/s40478-018-0507-3.

Debortoli, N., Li, X., Eyres, I., Fontaneto, D., Hespeels, B., Tang, C.Q., Flot, J.F., Van Doninck, K., 2016. Genetic exchange among bdelloid rotifers is more likely due to horizontal gene transfer than to meiotic sex. Curr. Biol. 26, 723–732. https://doi.org/10.1016/j.cub.2016.01.031.

Dong, L.L., Wang, H.X., Ding, T., Li, W., Zhang, G., 2020. Effects of TiO2 nanoparticles on the life-table parameters, antioxidant indices, and swimming speed of the freshwater rotifer Brachionus calyciflorus. J. Exp. Zool. Ecol. Integr. Physiol. 333, 230–239. https://doi.org/10.1002/jez.2343.

Ehrlich, H., 2019. Marine Biological Materials of Invertebrate Origin. Springer International Publishing AG. https://doi.org/10.1007/978-3-319-92483-0 part of Springer Nature 2019.

Fontaneto, D., Westberg, M., Hortal, J., 2011. Evidence of weak habitat specialisation in microscopic animals. PLoS One 6, e23969. https://doi.org/10.1371/journal.pone.0023969.

Ganesana, A.R., Guru, M.S., Balasubramanian, B., Mohan, K., Liu, W.C., Arasu, M.V., Al-Dhabi, N.A., Duraipandiyan, V., Ignacimuthu, S., Sudhakar, M.P., Seedevi, P., 2020. Biopolymer from edible marine invertebrates: a potential functional food. J. King Saud. Univ. Sci. 32, 1772–1777. https://doi.org/10.1016/j.jksus.2020.01.015.

Gopal, P., Citarasu, T., Punitha, S.M.J., Selvaraj, T., Albindas, S., Sindhu, A.S., Babu, M. M., 2014. Influence of physical and nutritive parameters on population and size variation in two species of rotifers. J. Aqua Trop. 29, 121–134.

Guo, R., Ren, X., Ren, H., 2012. A new method for analysis of the toxicity of organophosphorus pesticide, dimethoate on rotifer based on response surface methodology. J. Hazard. Mater. 237, 270–276. https://doi.org/10.1016/j.jhazmat.2012.08.041.

Gutierrez, M.F., Molina, F.R., Frau, D., Mayora, G., Battauz, Y., 2020. Interactive effects of fish predation and sublethal insecticide concentrations on freshwater zooplankton communities. Ecotoxicol. Environ. Saf. 196, 110497 https://doi.org/10.1016/j.ecoenv.2020.110497.

Hassan, M.E., Bai, J., Dou, D.Q., 2019. Biopolymers; definition, classification and applications. Egypt. J. Chem. 62, 1725–1737. https://doi.org/10.21608/EJCHEM.2019.6967.1580.

Hennebert, E., Gregorowicz, E., Flammang, P., 2018. Involvement of sulfated biopolymers in adhesive secretions produced by marine invertebrates. Biol. Open 7, bio037358. https://doi.org/10.1242/bio.037358.

Humenik, M., Pawar, K., Scheibel, T., 2019. Nanostructured, self-assembled spider silk materials for biomedical applications. Adv. Exp. Med. Biol. 1174, 187–221. https://doi.org/10.1007/978-981-13-9791-2_6.

Kalia, S., Avérous, L., 2011. Biopolymers: Biomedical and Environmental Applications, First ed. John Wiley and Sons Inc, Hoboken, New Jersey.

Kamiya, H., Sakai, R., Jimbo, M., 2006. Bioactive molecules from sea hares. Prog. Mol. Subcell. Biol. 43, 215–239. https://doi.org/10.1007/978-3-540-30880-5_10.

Kertész, K., 1894. Budapest és környékének Rotatoria-Faunája. Rózsa Kálmán és Neje Print,, Budapest.

Kisugi, J., Kamiya, H., Yamazaki, M., 1992. Biopolymers from marine invertebrates. XII. A novel cytolytic factor from a hermit crab, Clibanarius longitarsus. Chem. Pharm. Bull. 40, 1641–1643. https://doi.org/10.1248/cpb.40.1641.

Koste, W., 1978. Rotatoria - Die Radertiere Mitteleuropas. Ein Bestimmunsgwerk, begründet von Max Voigt. Überornung Monogononta,, Berlin - Stuttgart, pp. 285–289. https://doi.org/10.1002/iroh.19800650226.

Kowalczuk, Dorota, Pitucha, Monika, 2019. Application of FTIR method for the assessment of immobilization of active substances in the matrix of biomedical materials. Materials 12, 2972. https://doi.org/10.3390/ma12182972.

Kutikova, L.A., 1970. Kolovratki fauna SSSR. Fauna SSSR, vol. 4. Akademia Nauk Leningrad, pp. 362–367.

Lee, M.C., Park, J.C., Yoon, D.S., Han, J., Kang, S., Kamizono, S., Om, A.S., Shin, K.H., Hagiwara, A., Lee, J.S., 2018. Aging extension and modifications of lipid metabolism in the monogonont rotifer Brachionus koreanus under chronic caloric restriction. Sci. Rep. 8, 1741. https://doi.org/10.1038/s41598-018-20108-7.

Li, W., Lian, B., Niu, C., 2019. Effects of temperature on life history strategy of the rotifer Euchlanis dilatata. Zool. Sci. 36, 52–57. https://doi.org/10.2108/zs170096.

Macsai, L., Olah, Z., Bush, A.I., Galik, B., Onody, R., Kalman, J., Datki, Z., 2019. Redox modulating factors affect longevity regulation in rotifers. J. Gerontol. Biol. Sci. Med. Sci. 74, 811–814. https://doi.org/10.1093/gerona/gly193.

Mohamed, S., El-Sakhawy, M., El-Sakhawy, M.A., 2020. Polysaccharides, protein and lipid -based natural edible films in food packaging: a review. Carbohydr. Polym. 238, 116178 https://doi.org/10.1016/j.carbpol.2020.116178.

Muhlia-Almazán, A., Sánchez-Paz, A., García-Carreño, F.L., 2008. Invertebrate trypsins: a review. J. Comp. Physiol. B 178, 655–672. https://doi.org/10.1007/s00360-008-0263-y.

Nogrady, T., Segers, H., 2002. Rotifera Vol. 6: Asplanchnidae, Gastropodidae, Lindiidae, Microcodidae, Synchaetidae, Trocoshphaeridae and Filinia. In: Dumont, H.J. (Ed.), Guides to the Identification of the Microinvertebrates of the Continental Waters of the World. Leiden, pp. 59–79.

Olah, Z., Bush, A.I., Aleksza, D., Galik, B., Ivitz, E., Macsai, L., Janka, Z., Karman, Z., Kalman, J., Datki, Z., 2017. Novel in vivo experimental viability assays with high sensitivity and throughput capacity using a bdelloid rotifer. Ecotoxicol. Environ. Saf. 144, 115–122. https://doi.org/10.1016/j.ecoenv.2017.06.005.

Olatunji, O., 2020. Aquatic Biopolymers, Understanding their Industrial Significance and Environmental Implications. Springer International Publishing. https://doi.org/10.1007/978-3-030-34709-3.

Pallas, P.S., 1766. Elenchus zoophytorum systems generum adumbrations generaliores et specierum cognitarum succinactas descriptions cum selectis auctorum synonymis. Hagae Comitum 451pp.

Rahman, M.A., 2019. Collagen of extracellular matrix from marine invertebrates and its medical applications. Mar. Drugs 17, 118. https://doi.org/10.3390/md17020118.

Robeson, M.S., King, A.J., Freeman, K.R., Birky Jr., C.W., Martin, A.P., Schmidt, S.K., 2011. Soil rotifer communities are extremely diverse globally but spatially autocorrelated locally. Proc. Natl. Acad. Sci. USA 108, 4406–4410. https://doi.org/10.1073/pnas.1012678108.

Ruiz-Torres, V., Rodríguez-Pérez, C., Herranz-López, M., Martín-García, B., Gómez-Caravaca, A.M., Arráez-Román, D., Segura-Carretero, A., Barrajón-Catalán, E., Micol, V., 2019. Marine invertebrate extracts induce colon cancer cell death via ROS-mediated DNA oxidative damage and mitochondrial impairment. Biomolecules 9, 771. https://doi.org/10.3390/biom9120771.

Snell, T.W., Johnston, R.K., Gribble, K.E., Mark Welch, D.B., 2015. Rotifers as experimental tools for investigating aging. Invertebr. Reprod. Dev. 59, 5–10. https://doi.org/10.1080/07924259.2014.925516.

Snell, T.W., Johnston, R.K., Matthews, A.B., Zhou, H., Gao, M., Skolnick, J., 2018. Repurposed FDA-approved drugs targeting genes influencing aging can extend lifespan and healthspan in rotifers. Biogerontology 19, 145–157. https://doi.org/10.1007/s10522-018-9745-9.

Suthers, I.M., Rissik, D., Richardson, A.J., 2019. Plankton. A Guide to Their Ecology and Monitoring for Water Quality, Second ed. CRC Press, Florida.

Varga L., 1966. Rotifers I. Hungarian Academy of Sciences, Budapest.

Venâncio, C., Castro, B.B., Ribeiro, R., Antunes, S.C., Abrantes, N., Soares, A., Lopes, I., 2018. Sensitivity of freshwater species under single and multigenerational exposure to seawater intrusion. Philos. Trans. R. Soc. B 374, 20180252. https://doi.org/10.1098/rstb.2018.0252.

Walsh, E.J., Schröder, T., Wallace, R.L., Rico-Martinez, R. 2009. Cryptic speciation in Lecane bulla (Monogononta: Rotifera) in Chihuahuan Desert waters. S.I.L. Proceedings, 30, 1046–1050. doi:10.1080/03680770.2009.11902298.

Yamazaki, M., Kisugi, J., Kimura, K., Kamiya, H., Mizuno, D., 1985. Purification of antineoplastic factor from eggs of a sea hare. FEBS Lett. 185, 295–298. https://doi.org/10.1016/0014-5793(85)80926-1.

Yamazaki, M., Tansho, S., Kisugi, J., Muramoto, K., Kamiya, H., 1989. Purification and characterization of a cytolytic protein from purple fluid of the sea hare, Dolabella auricularia. Chem. Pharm. Bull. 37, 2179–2182. https://doi.org/10.1248/cpb.37.2179.

Yavuz, B., Chambre, L., Kaplan, D.L., 2019. Extended release formulations using silk proteins for controlled delivery of therapeutics. Expert. Opin. Drug Deliv. 16, 741–756. https://doi.org/10.1080/17425247.2019.1635116.

Experiments	Monogonant species	Applied inductors	Treatment agents or environment	Test entities, cells or targets	Measured parameters	Visualisation methods
Rotimer-Inductor Conglomerate (RIC) production (Suppl. Video)	*E. dilatata*	yeast	standard medium	*E. dilatata*	Rotimer production and behavior of rotifers	light microscopy
RIC-producing capacity index calculation (Suppl. Fig. 1)		yeast BSA epoxy Carmine urea cellulose	standard medium		RIC producing capacity index	light microscopy
Dose-dependecy of NaN_3 toxicity (Suppl. Fig. 2)		-	sodium-azide		swimming speed	light microscopy

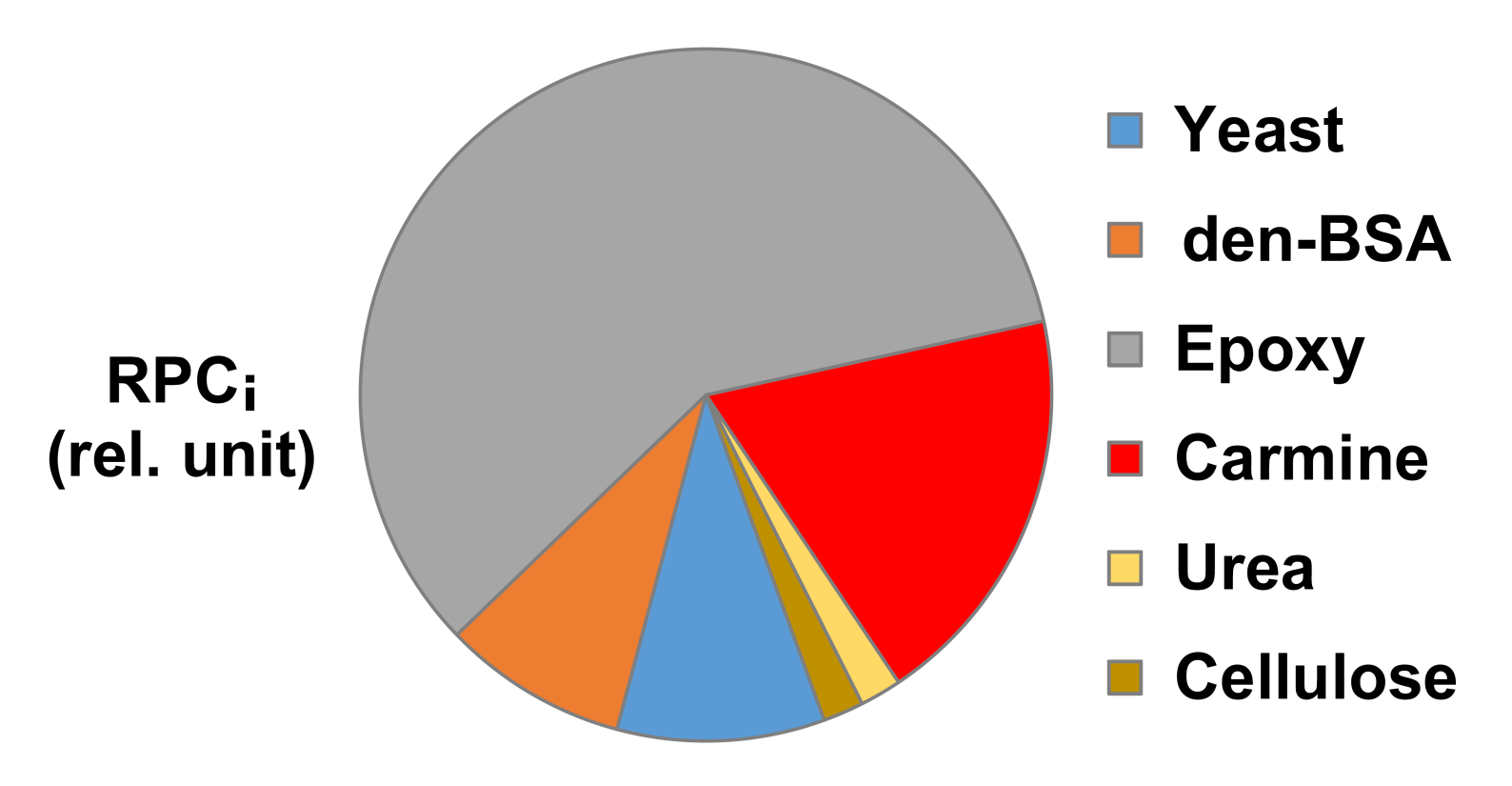
RPCi
(rel. unit)
Yeast
den-BSA
Epoxy
Carmine
Urea
Cellulose

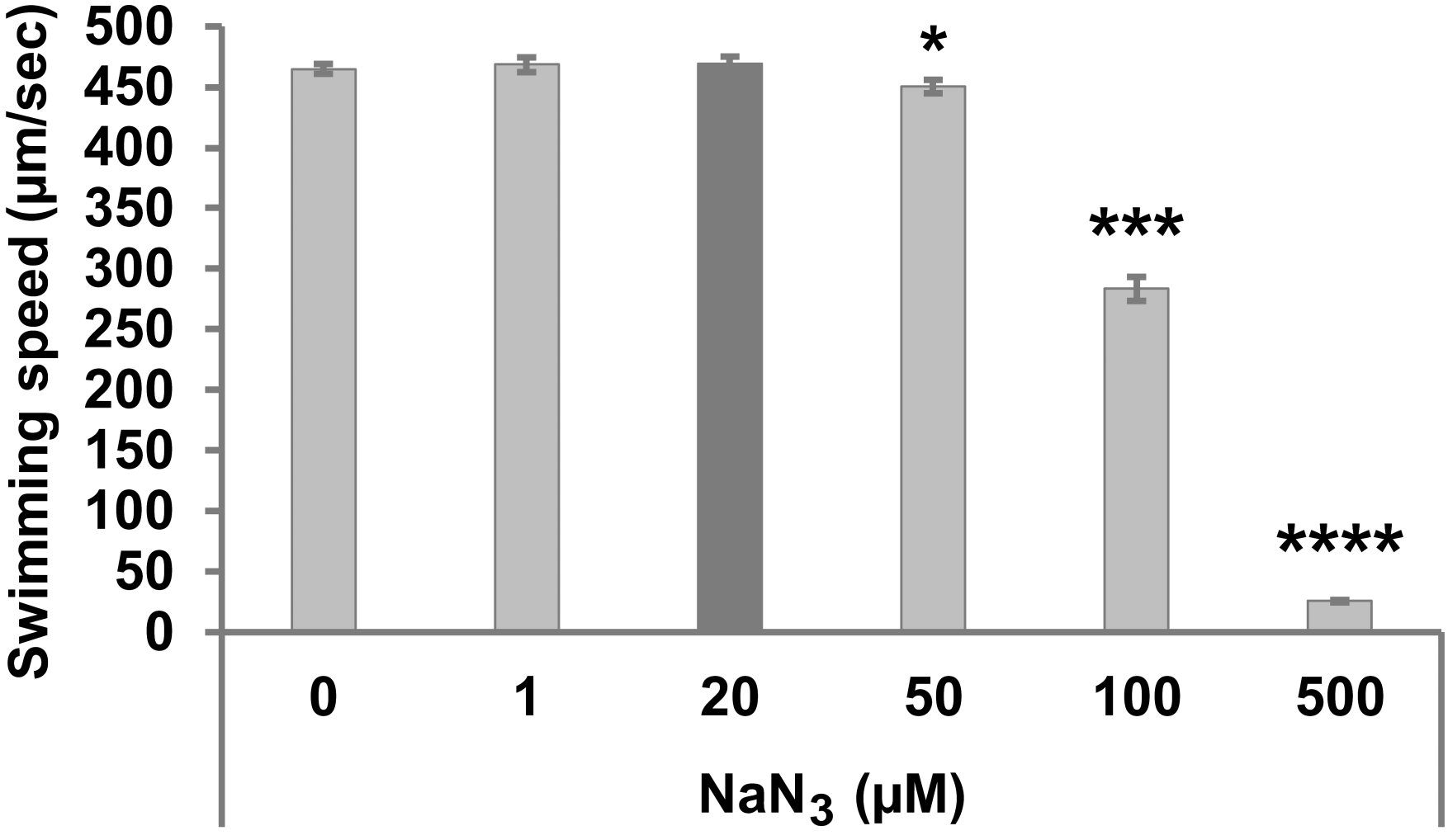
Swimming speed (µm/sec)
500
450
400
350
300
250
200
150
100
50
0
*
***
****
0
1
20
50
100
500
NaN3 (µM)

III.

Ecotoxicology and Environmental Safety 220 (2021) 112399

Contents lists available at ScienceDirect

Ecotoxicology and Environmental Safety

journal homepage: www.elsevier.com/locate/ecoenv

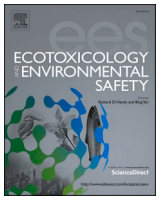

External modulation of Rotimer exudate secretion in monogonant rotifers

Evelin Balazs [a], Zita Galik-Olah [a], Bence Galik [b,c], Ferenc Somogyvari [d], Janos Kalman [a], Zsolt Datki [a,*]

[a] Department of Psychiatry, Faculty of Medicine, University of Szeged, Vasas Szent Peter u. 1–3, H-6724 Szeged, Hungary
[b] Bioinformatics Research Group, Bioinformatics and Sequencing Core Facility, Szentágothai Research Centre, University of Pécs, Ifjusag u. 20, H-7624 Pécs, Hungary
[c] Department of Clinical Molecular Biology, Medical University of Bialystok, ul.Jana Kilinskiego 1, 15-089 Bialystok, Poland
[d] Department of Medical Microbiology and Immunobiology, Faculty of Medicine, University of Szeged, Dóm square 10, H-6720 Szeged, Hungary

ARTICLE INFO

Edited by: Dr Yong Liang

Keywords:
Monogonant rotifer
Biopolymer
Euchlanis dilatata
Lecane bulla
Exudate
Rotimer

Chemical compounds studied in this article:
Ascorbic acid (PubChem CID: 54670067)
$CaCl_2$ (PubChem CID: 24844)
cAMP (PubChem CID: 6076)
Carmine crystals (PubChem CID: 14950)
Catechin (PubChem CID: 9064)
Choline chloride (PubChem CID: 6209)
DMSO (PubChem CID: 679)
EDTA (PubChem CID: 6049)
Ethyl nicotinate (PubChem CID: 69188)
Glucose (PubChem CID: 5793)
Glycerol (PubChem CID: 753)
Isoguvacine (PubChem CID: 3765)
KCl (PubChem CID: 4873)
LiCl (PubChem CID: 23681138)
Meclofenoxate hydrochloride (PubChem CID: 19379)
$MgCl_2$ (PubChem CID: 24644)
NaCl (PubChem CID: 5234)
Selegiline (PubChem CID: 26757)
Spermidine (PubChem CID: 1102)
$SrCl_2$ (PubChem CID: 6101868)
Taurine (PubChem CID: 1123)

ABSTRACT

The Rotimer, a rotifer-specific biopolymer, is an exogenic bioactive exudate secreted by different monogonant species (e.g. *Euchlanis dilatata* or *Lecane bulla*). The production of this viscoelastic biomolecule is induced by different micro-particles, thereby forming a special Rotimer-Inductor Conglomerate (RIC) in a web format. In this case, the water insoluble Carmine crystals, filtered to size (max. diameter was 50 μm), functioned as an inductor. The RIC production is an adequate empirical indicator to follow up this filamentous biopolymer secretion experientially; moreover, this procedure is very sensitive to the environmental factors (temperature, pH, metals and possible natural pollutant agents). The above mentioned species show completely different reactions to these factors, except to the presence of calcium and to the modulating effects of different drugs. One of the novelties of this work is that the Rotimer secretion and consequently, the RIC-formation is a mutually obligatory and evolutionary calcium-dependent process in the concerned monogonants. This *in vivo* procedure needs calcium, both for the physiology of animals and for fiber formation, particularly in the latter case. The conglomerate covered area (%) and the detection of the longest filament (mm) of the given RIC were the generally and simultaneously applied methods in the current modulating experiments. Exploring the regulatory (e.g. calcium-dependency) and stimulating (e.g. Lucidril effect) possibilities of biopolymer secretion are the basis for optimizing the RIC-production capacities of these micro-metazoans.

Abbreviations: cAMP, cyclic adenosine monophosphate; CCA, conglomerate covered area; DMSO, dimethyl sulfoxide; DW, distilled water; ED, *Euchlanis dilatata*; EDTA, ethylenediaminetetraacetic acid; LB, *Lecane bulla*; LFC, longest filament of conglomerate; NIH, National Institutes of Health; RIC, Rotimer-Inductor Conglomerate; SEM, standard error of the mean.

* Corresponding author.
E-mail address: datki.zsolt@med.u-szeged.hu (Z. Datki).

https://doi.org/10.1016/j.ecoenv.2021.112399
Received 22 February 2021; Received in revised form 10 May 2021; Accepted 30 May 2021

1. Introduction

Nowadays, molecular investigations are dominant parts of biological research. Despite of this, the renaissance of supramolecular and experiential biology is manifested in the various applications of their numerous advantages. The metazoan-based '*micro-in vivo*' systems are inevitable in all types of fundamental researches (e.g. longevity; Macsai et al., 2018) and for high throughput screening (e.g. viability; Olah et al., 2017; Rico-Martínez et al., 2016).

One of the scientific profiles of the rotifer-type-models is the complex description and characterization of different environmental (temperature, pH and salinity) or biological (toxicity, modulation, abnormalities, biomolecule productions, etc.) effects. Rotifers highly tolerate natural environmental changes; moreover, they are able to survive life-incompatible conditions by halting activities, such as reducing metabolism by suspending active life or egg production (Jönsson and Wojcik, 2017; Kanazawa et al., 2017; Shain et al., 2016). Benefiting from these evolutionally developed anatomic and physiologic abilities (Gilbert, 2017), rotifers respond to external challenges by producing different types of biomolecules (e.g. biopolymers; Datki et al., 2021) applying optimized phenotypic plasticity.

Biopolymers are produced by living organisms from specific monomers; therefore, they can be classified based on their basic chemical structures: polypeptides, polysaccharides, polynucleotides and combined forms (Mohan et al., 2016). The structural formation of polymers always requires cross-linkers, such as metal ions, e.g. calcium (Silva et al., 2009). These biomolecules (e.g. cellulose, chitin, spider silk, casein, collagen, albumin in Plant or Animal kingdoms) have been deeply investigated and their multilevel applications are unquestionable (Niaounakis, 2015). However, their properties are very diverse according to how the producing species adapt to the environment.

As the eco-friendly approach becomes dominant in industrial developments, the relevance of biopolymers gains more importance due to their biodegradable, renewable and environmentally friendly nature (Lalit et al., 2018). These natural agents are applied in environmental protection, agriculture, food-, pharmaco- and energetic industries (Yavuz et al., 2019). The producer, living organisms are in tight connection with their endemic microenvironment, which has crucial regulatory role in the relevant biopolymer production. (Ibrahim et al., 2018).

It is a widely-known evolutionary theory that the rhizomes of life are derived from water; therefore, the first biopolymers were produced by ancient marine species, such as ammonites, sea urchins, snails, etc. (Frenkel-Pinter et al., 2021). These biocomposites were 'soft', 'hard' or a mix of them, protecting the unicellular organisms or metazoans from thermal, chemical, and ultraviolet stresses (Ehrlich, 2019). As a consequence of diverse natural habitat (e.g. oceans, seas, lakes, rivers, ponds, wetlands, puddles, streams, canals and thermal springs), aquatic organisms have developed different versions of polymers having a wide range of properties such as energy preservatives, structural and metabolic ones, or functions related to cell renewal and water repellence. These complex biomolecules can be found in the extracellular spaces, cell walls, inner tissues and exoskeletons or in exudate form in water and land. Various factors can environmentally influence secretion and formation of biopolymers, including salinity, depth, light intensity, temperature, pressure, density, pH, prey/predator presence, nutrients, dissolved gases, water flow rate, flora and fauna. (Olatunji, 2020).

Water-based ecological niches are extremely sensitive to industrial or chemical pollution; thus, the investigation of concerned aquatic microinvertebrates is a current scientific issue. The evolutionary ancient rotifers are ideal models for ecotoxicological measurements (Dahms et al., 2011), but they had not been studied in the context of biopolymer secretion. The team of Datki et al. (2021) was first to describe a novel phenomenon in this theme; namely that these animals are capable of secreting filamentous or glue-type exudates following particle-based mechanic irritation. This previously described rotifer-specific bioactive biopolymer, named Rotimer, is a universally functional molecule of these micro-metazoans. The Rotimer, produced among other things by some monogonant species (e.g. *Euchlanis dilatata* or *Lecane bulla*), is an exogenic and viscoelastic biopolymer having fibrous or gluelike forms. This exudate, in complex formation with particle-type mechanic stimulator (e.g. insoluble Carmine crystals or epoxy-metal beads), forms the Rotimer-Indictor Conglomerate (RIC) in a web structure (Datki et al., 2021). In this RIC formation, the above mentioned biopolymer has a proteinous nature; its exact chemical composition and structure is yet unknown. Based on academic literature it has been proved that numerous species can secrete biopolymers, similarly to rotifers; however, the regulation of this novel Rotimer is yet undescribed.

The aim of this study is to investigate selected environmental factors and possible pollutant agents on Rotimer secretion, experientially monitored by RIC formation. Those chemicals were chosen which might be released to natural waters by certain industries or urban sources. This work intends to shed light on their impacts on the amount and quality of Rotimer, rather than elaborating on their secretion-dependent mechanism of actions.

2. Material and methods

2.1. Materials

Materials applied in this work were the following: yeast (*Saccharomyces cerevisiae*; EU-standard granulated instant form, cat. no.: 2-01-420674/001-Z12180/HU); algae (*Chlorella vulgaris*; BioMenu, Caleido IT-Outsource Kft.; cat. no.:18255); from Sigma-Aldrich: spermidine (cat. no.: S2626), dimethyl sulfoxide (DMSO; cat. no.: D8418), ethylenediaminetetraacetic acid (EDTA; cat. no.: E9884), ascorbic acid (cat. no.: A1300000), catechin (cat. no.: C-1788), glucose (cat. no.: 47829), taurine (cat. no.: T0625), cyclic adenosine monophosphate (cAMP; cat. no.: A9501), ethyl nicotinate (cat. no.: E40609); from Merck: powdered Carmine crystals (Natural Red 4; cat. no.: 2233), glycerol (cat. no.: 1.04092.1000); distilled water (DW; Millipore SAS, Direct-Q 3 UV, ultrapure; type 1; Molsheim, France); different pH-calibrated media (Mettler Toledo SevenEasy pH meter, Switzerland, InLab 413; cat. no.: Z654272); from Reanal: NaCl (cat. no.: 14064–1–38), KCl (cat. no.: 30080), LiCl (cat. no.: 12033), $CaCl_2$ (cat. no.:11024), $MgCl_2$ (cat. no.: 232-094-6), $SrCl_2$ (cat. no.: 19066), ethylenediaminetetraacetic acid (EDTA; cat. no.: 9884), choline chloride (cat. no.: 11222); from KRKA Novo Mestro: Lucidril (meclofenoxate hydrochloride; cat. no.: 5812-67/721/1-63); from Other Pharmacy: Selegiline (cat. no.: 903871-2G); from Cambridge Research Biochemicals: isoguvacine (cat. no.: PE7097); from Molecular Probes: Fluo-3 (cell impermeable calcium-specific fluorescent dye; cat. no.: F3715); from Corning or Corning-Costar: 24-well plate (cat. no.: 3524), from Greiner Bio-One GmbH: microplate 96 well plate (clear, half area, cat. no.: 675101); Petri dish (cat. no.: 430167), flasks (cat. no.: 430168); universal plastic web (pore diameter: 50 μm); Acrodisc 13 filter, Low Protein Binding (pore diameter: 0.2 μm; cat. no.: 4454) from Gelman Sciences; standard medium (mg/L): Ca^{2+} 31.05; Mg^{2+} 17.6; Na^{+} 0.9; K^{+} 0.25; Fe^{2+} 0.001; HCO_3^- 153.097; SO_4^- 3; Cl^- 0.8; F^- 0.02; H_2SiO_3 3.3 (pH = 7.5).

2.2. Animals

The measurements were carried out on invertebrate monogonant rotifers *Euchlanis dilatata* and *Lecane bulla*; thus, according to the current international regulations, no specific ethical permission was needed. The animals were obtained from Red Cross Lake (GPS coordinates: 46° 16′ 25″ N; 20° 08′ 39″ E; early summer) in Szeged (Southern Great Plain, Hungary). They have been maintained in a standard laboratory environment for 4 years. The experiments were performed in accordance with globally accepted norms: Animals (Scientific Procedures) Act, 1986, associated guidelines, EU Directive 2010/63/EU for animal experiments, and the National Institutes of Health guide for the care and

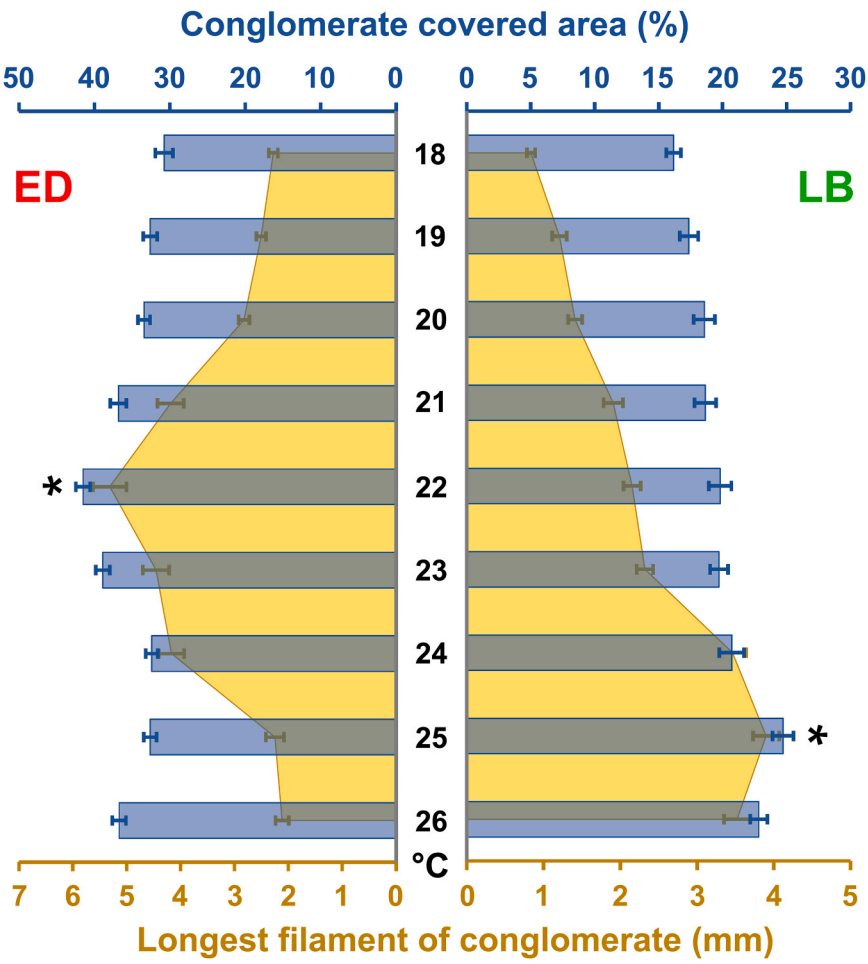

Fig. 1. The effect of temperature on RIC formation. The impacts of temperature on 'Rotimer-Inductor Conglomerate' (RIC) produced by *Euchlanis dilatata* (ED; red) and *Lecane bulla* (LB; green) are presented by the RIC-covered area (%; blue) and the longest filament of conglomerate (mm; yellow). The error bars represent SEM. One-way ANOVA with Bonferroni *post hoc* test was used for statistical analysis, the levels of significance are $p^* \leq 0.05$ (*, significant difference from all the other measured data, indicating the optimum, the significance is higher than or equal to 95% in both measured parameters).

use of Laboratory animals (NIH Publications No. 8023, revised 1978). Animal studies comply with the ARRIVE guidelines. The rotifers were cultured based on the methods previously published by Datki et al. (2021), using flasks (25 cm^2 area), filled with standard medium. They were fed every second day by heat-inactivated, homogenized and filtered (plastic web; pore diameter: 15 μm) algae-yeast (in 1:3 ratio) suspension (final dose: 600 μg/mL/case). The *E. dilatata* and *L. bulla* are maintained as standard cultures in our *micro-in vivo* laboratory.

2.3. Treatment of rotifers

Every measurement was performed in standard environment (24 °C, pH = 7.5, 40% air humidity, in standard media and 12:12 h dark-light), except for the actual parameter of interest or the optimized experiments (for *E. dilatata*: 22 °C, pH = 7.8; for *L. bulla* 25 °C, pH = 7.2). The experimentally applied animals were isolated by pouring them into Petri dishes (55 cm^2 area). In all experiments (n = 24, well; in all groups) related to rotifer-specific biopolymer (named Rotimer), 20–22 mature (with maximal body size or with an egg inside) entities were applied in a 24-well plate (1.8 cm^2 well-area) with 1 mL working volume per well.

The influence of changing environmental parameters (temperature and pH) and the treatment with various agents (20 μM) lasted for 10 h with a constant number of unfed animals. These RIC-influencing chemicals were the follows: DMSO, ascorbic acid, Lucidril, catechin, glycerol, glucose, taurine, selegiline, cAMP, spermidine, ethyl nicotinate, isoguvacine and choline. The various media with different pH values (from 6.6 to 8.4) were made freshly before all relevant treatments.

The animals were let to rest (washed) in DW for 30 min before being applied in metal salts (100 mg/L) related experiments. These salts were the follows: NaCl, KCl, LiCl, $CaCl_2$, $MgCl_2$ and $SrCl_2$. These measurements, with constant number of unfed rotifers, were carried out after making 10x dilutions from stock solutions. The RIC induction was initiated with mechanically ultra-powdered water insoluble Carmine crystal particles after 5 min treatment with different metal-salts.

2.4. RIC-analysis

The RIC-analysis is a slightly modified adaptation of the method applied by Datki et al. (2021). The final (working) concentration of the administered inductor (Carmine) of Rotimer-secretion was 50 μg/mL which was diluted from 2 mg/mL stock solution. The Carmine-induced biopolymer formed RIC in a high density web structure after 30 min incubation time. After removing the well solution by pipette, these RIC products were desiccated (dried) at room temperature (24 °C) and at 40% humidity in darkness for 60 min. The inductor particles were applied above the size of 50 μm (filtered with plastic web). All manipulations were performed slowly and carefully to avoid fluid flow destroying the exudate web.

The amount and pattern of RIC was detected by light microscopy (Labovert FS; 63x magnification). The photos (Nikon D5100, 16 MP RAW and ISO 100) were converted in a black and white graphical format (threshold, 2.04 pixel = 1 μm, 408 pixel = 0.2 mm and 8-bit). These images were analyzed with ImageJ program (Wayne Rasband, USA), extracting data related to the conglomerate-covered area (%) of this crystal-biomolecule complex.

Detection of the longest filament of RIC was performed under light microscope with 25x magnification applying Bürker-type square grid in

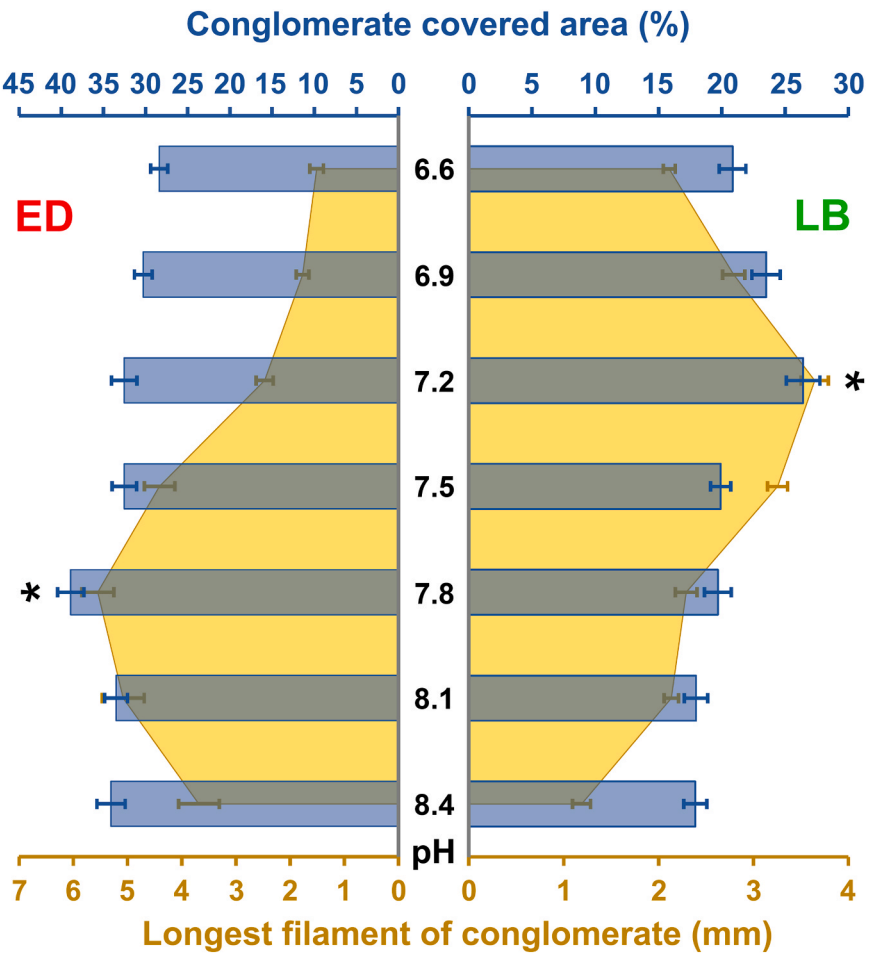

Fig. 2. The effect of pH on RIC formation. The impacts of pH on 'Rotimer-Inductor Conglomerate' (RIC) produced by *Euchlanis dilatata* (ED; red) and *Lecane bulla* (LB; green) are presented by the RIC-covered area (%; blue) and the longest filament of conglomerate (mm; yellow). The error bars represent SEM. One-way ANOVA with Bonferroni *post hoc* test was used for statistical analysis, the levels of significance are $p^* \leq 0.05$ (*, significant difference from all the other measured data, indicating the optimum, the significance is higher than or equal to 95% in both measured parameters).

parallel layering with plate-wells. In the web of RIC (in every relevant well) the longest straight filament with two attachment points was measured (in mm).

2.5. Fluorescent detection of calcium level in rotifer-medium

Detecting the relative changes of calcium ion level in rotifer-media was carried out with a plate-reader-based fluorescent method. The external $CaCl_2$ concentration in the current media was 5 mg/L (45 μM), supplemented with 205 mg/L NaCl; therefore, the total salt concentration was equivalent with the standard medium. In these experiments, calcium-specific and cell-impermeant Fluo-3 (stock solution: 1 mg/mL; final concentration: 50 μM) was applied. Low $CaCl_2$ concentration provided 0.9:1 calcium: dye ratio, since without free dye surplus the potential alterations cannot be detected precisely.

The rotifer-free samples (0.15 mL) were filtered with Acrodisc 13 filter (pore diameter 0.2 μm) from the respective well-media (1 mL) of applied 24-well plates. The maximal calcium-specific signal did not decrease in the presence of Carmine in this animal-free setup. The labeling interval with Fluo-3 was 10 min at room temperature in the dark. The readings were carried out in a 96-well (clear) half-area plate, using NOVO star plate-reader (BMG Labtech, Germany). The volume of wells was 95 μL medium supplemented with 5 μL Fluo-3 (from 1 mM stock solution). The extinction/emission was set at 500/530 nm and the number of flash/well/cycle was 30. Before the first turn, orbital shaking was applied where the shaking time was set at 3 s and the plate-rounds were 600/min. The readings and the gain adjustment were normalized to the background of the free-dye. This blank was 650 relative unit, 1% of the maximum fluorescence intensity with dye and without calcium (210 mg/L NaCl). Fluorescence intensity of the Fluo-3 increased about 14–15-fold after calcium binding (reference samples: 100% relative unit, without animals and Carmine). Optimized conditions (except for the calcium amount) were applied to both rotifer species in photometric experiments.

2.6. Statistics

The error bars represent the standard error of the mean (SEM). For comparative statistical analysis, the one-way ANOVA was used followed by the Bonferroni *post hoc* test with SPSS 23.0 (SPSS Inc, Chicago, IL, USA) software for Windows. The homogeneity and normality of the data were checked, and they were found suitable for ANOVA followed by Bonferroni *post hoc* test. The different levels of significance are indicated as follows: $p^* \leq 0.05$, $p^{***,\#\#\#} \leq 0.001$ (all marks are defined in the given figure legend).

3. Results and discussion

The rotifers are validated models of toxicity screening related to environmental parameters and chemical agents (Rico-Martínez et al., 2016). The biopolymer producing capacity of these micro-metazoans has just recently been discovered (Datki et al., 2021). The Rotimer is such a biomolecule, which is essential for the survival of the animals (food-trapping, gluing the eggs and water purification) that produce it. Secretion of the above mentioned multifunctional product largely depends on the environmental factors. These influencing factors have various impacts on rotifers according to their degree; however, every species has its own optimum. The *E. dilatata* preferred lower

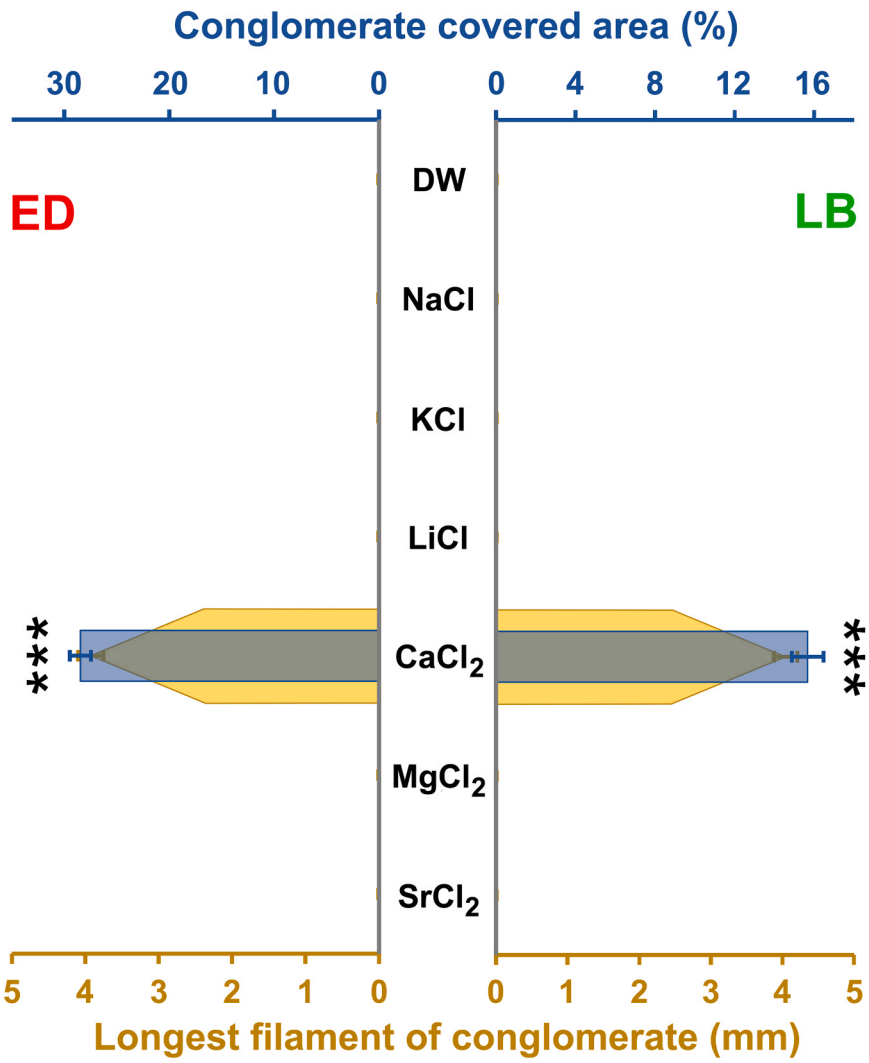

Fig. 3. The effect of different metal ions on RIC formation, The impacts of various metal ions on 'Rotimer-Inductor Conglomerate' (RIC) produced by *Euchlanis dilatata* (ED; red) and *Lecane bulla* (LB; green) are presented by the RIC-covered area (%; blue) and the longest filament of conglomerate (mm; yellow). The error bars represent SEM. One-way ANOVA with Bonferroni *post hoc* test was used for statistical analysis, the levels of significance are $p^{***} \leq 0.001$ (*, significant difference from all the other measured data, indicating the optimum, the significance is higher than or equal to 99.1% in both measured parameters).

temperature (22 °C; Fig. 1) and higher pH (pH=7.8; Fig. 2) than *L. bulla* (25 °C and pH=7.2) did in our laboratory conditions. In case of the species-specific optimum, both RIC markers (conglomerate covered area and longest fiber of conglomerate) showed similarly high values; while distancing from that optimum, parameters decreased, especially in fiber length. In the case of *E. dilatata*, these markers produced approximately 2-fold change in average, compared to *L. bulla*.

Natural waters contain various metal ions which implicitly influence the flora and fauna (Armour, 2016). Applying natural salts (Fig. 3) in artificial conditions revealed that only calcium ion is inevitable for exudate secretion. There is no RIC production in its absence. A similar phenomenon was described related to mucin biopolymers, where the sol-gel transition is pH- and also calcium dependent (Curnutt et al., 2020). It is true to the fact that the freshly harvested rotifers can produce Rotimer in a fully demineralized environment, but the animals washed and let to rest for minimum half an hour in DW cannot secrete the biopolymer (Datki et al., 2021). These micro-metazoans presumably have some amount of stocked metal ions; however, the exudate secretion capacity disappears without natural replacement of the essential minerals. Comparing the ion content of standard culture media (210 mg/L), a lower dose (100 mg/L) was applied, since this concentration level was acceptable in terms of osmolarity, yet neither ion proved to be toxic. The one-component treatment solutions showed significant differences compared to both standard and only calcium-containing media. Surprisingly, neither the magnesium, nor the strontium was able to replace the calcium, unlike in the case of some physiological process (Saris et al., 2000; Hendrych et al., 2016). These facts prove that the calcium sensors or receptors of rotifers are very specific to this particular ion.

The abiotic factors, such as temperature (Wenjie et al., 2019) and minerals (Hernández-Flores et al., 2020), have significant modulating effects on the global aquatic environment. Rotifers are particularly sensitive to all these factors, thus forming a natural regulating-, viability- and toxicity indicator systems (Pérez-Legaspi and Rico-Martínez, 2001).

To precisely evaluate the calcium-dependency of RIC production, dose-efficacy was measured (Fig. 4). As it turned out, the sodium has no impact on exudate production, the different calcium doses were supplemented with this, equaling the amount of metal ions, similarly to that of the standard media. Assuring constant osmolarity in artificial environment is essential to assess dose-dependency. Regarding biopolymer production, optimums of the two investigated species differ from each other, since 50 mg/L is the most optimal level for the *E. dilatata*, while 100 mg/L is the most favorable for *L. bulla*. Moreover, the first one produces twice as much Rotimer as the latter one. Results suggest that 10–20% of conglomerate formation already starts in the presence of a relatively low dose (0.1 mg/L) of calcium. In the case of both species sudden increase in activity was observed at 5 mg/L dose; moreover, it was found that the production of exudate dramatically reduces in the presence of calcium (50 mg/L) together with EDTA (100 mg/L). The EDTA is a well-known chelator of different metal ions (e.g. calcium,

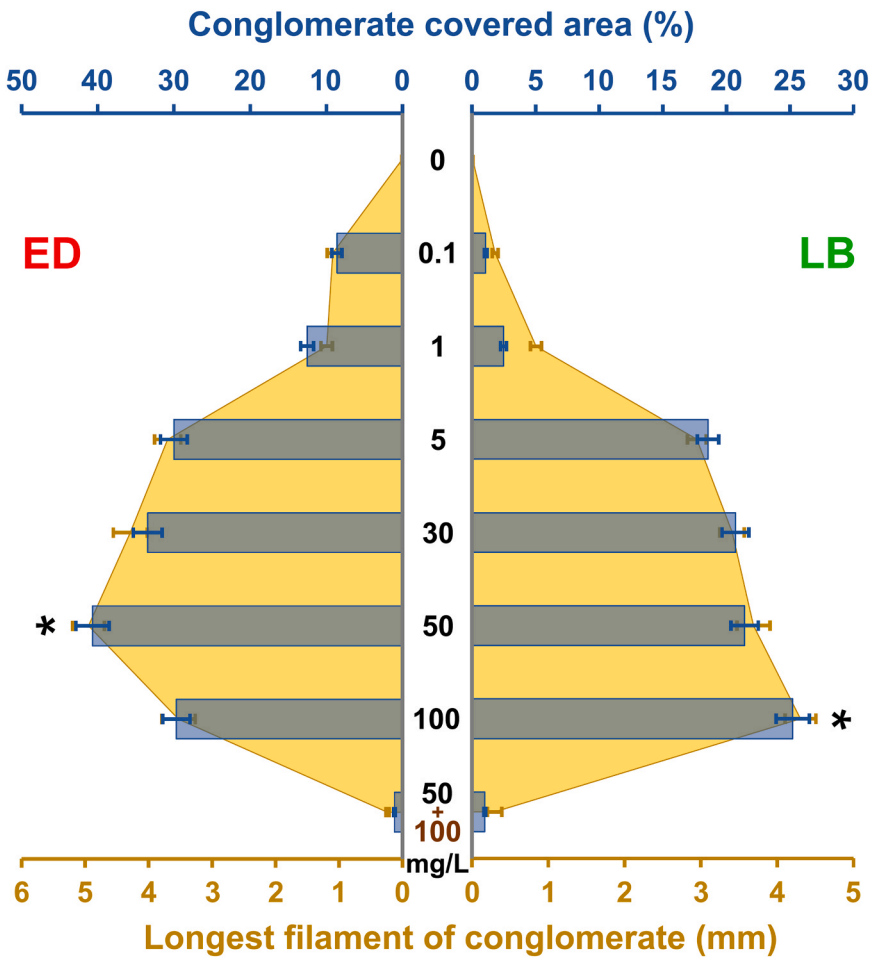

Fig. 4. Dose-dependent effect of calcium on RIC formation, The impacts of various doses of calcium on 'Rotimer-Inductor Conglomerate' (RIC) produced by *Euchlanis dilatata* (ED; red) and *Lecane bulla* (LB; green) are presented by the RIC-covered area (%; blue) and the longest filament of conglomerate (mm; yellow). EDTA (100 mg/L; brown) was used against calcium (50 mg/L; black) in the control measurement (bottom column). The error bars represent SEM. One-way ANOVA with Bonferroni *post hoc* test was used for statistical analysis, the levels of significance are $p^* \leq 0.05$ (*, significant difference from all the other measured data, indicating the optimum, the significance is higher than or equal to 95% in both measured parameters).

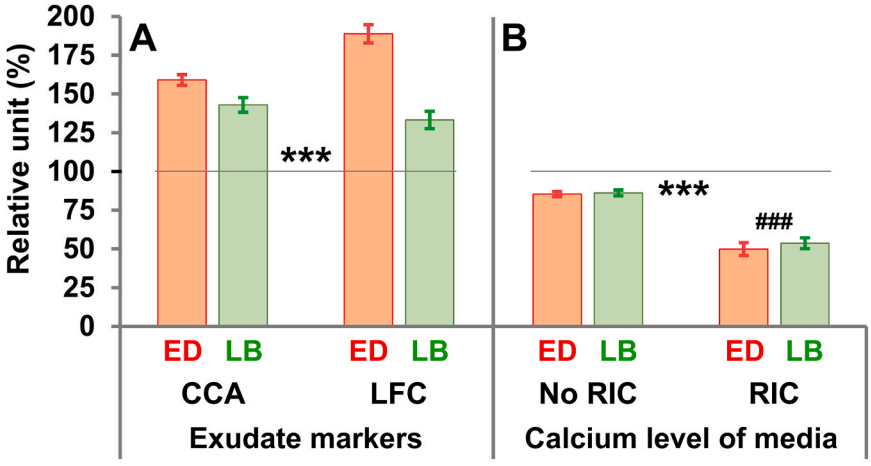

Fig. 5. RIC formation (A) and use of calcium (B) under species-specific optimized conditions. The influencing factors were optimized in species-specific manner in *Euchlanis dilatata* (ED; red) and *Lecane bulla* (LB; green) populations. The percentage of relative units of exudate markers (A) was presented as conglomerate covered area (CCA) and longest filament of conglomerate (LFC). The changes in species-specific calcium uptake from the media (B) were measured in the presence or absence of 'Rotimer-Inductor Conglomerate' (RIC). The error bars represent SEM. One-way ANOVA with Bonferroni *post hoc* test was used for statistical analysis, the levels of significance are $p^{***,\#\#\#} \leq 0.001$ (*, significant difference from the standard culturing, which was the 100% indicated by the black line; #, significant difference from the 'No RIC' columns).

magnesium, copper or zinc; Zaitoun and Lin, 1997) and it had no negative effect on the viability of the animals up to the level of 200 mg/L dose, which was measured by swimming speed (μm/sec; Suppl. Fig.). The inhibitory effect of non-membrane permeable calcium-specific chelator (George and Brady, 2020) on RIC production proves that this process happens extracellularly, presumably at the inlet of the intestinal tract. The calcium dependency of biopolymer-secretion and formation is not a rare phenomenon in the animal kingdom, especially in aquatic invertebrates (Wang et al., 2003; Ehrlich, 2019).

In the case when the exudate secretion was induced in species-specific optimal circumstances in modified medium (*E. dilatata*: 22 °C, pH=7.8, calcium 50 mg/L; *L. bulla*: 25 °C, pH=7.2, calcium 100 mg/L), both species showed significantly higher activity (Fig. 5**A**) compared to their controls (100%; standard environmental factors and media). The RIC amount and the length of filaments show that *E. dilatata* can be better stimulated than *L. bulla*. In another experiment, but also in an optimized environment (except for calcium concentration, which was only 5 mg/L), the rotifers used calcium both for their physiological needs and for RIC production (Fig. 5**B**). It was shown by non-cell permeable Fluo-3 fluorescent dye (Zhang et al., 2014) that

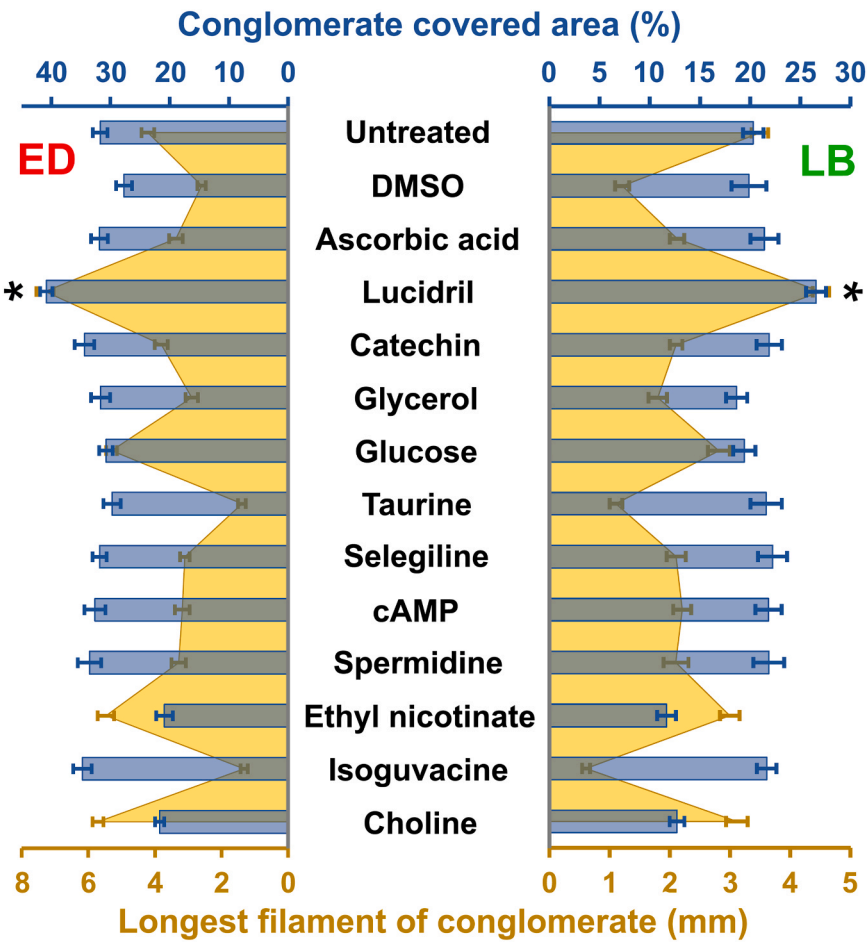

Fig. 6. The effect of different chemical agents on RIC formation. The impacts of various chemicals on 'Rotimer-Inductor Conglomerate' (RIC) produced by *Euchlanis dilatata* (ED; red) and *Lecane bulla* (LB; green) are presented by the RIC-covered area (%; blue) and the longest filament of conglomerate (mm; yellow). The error bars represent SEM. One-way ANOVA with Bonferroni *post hoc* test was used for statistical analysis, the levels of significance are $p^* \leq 0.05$ (*, significant difference from all the other measured data, indicating the optimum, the significance is higher than or equal to 95% in both measured parameters).

significantly more calcium was used by the animals during RIC production than without its induction. The control measurements were carried out in the same media (with also reduced calcium content) lacking animals and the inductor. The reason for it was to enhance the molarity ratio of the detectable dye. These data suggest that rotifers extract and bind metal ions from their environment. The same process can be observed in the case of marine corals (Mitterer, 1978; Howard and Brown, 1984).

Rotimer as a biomaterial can likely absorb calcium during its formation which may even take part in the global level processes of freshwater and marine sediments. Our present and previous studies show that biopolymer production is essential for the rotifers to live and survive.

Numerous environmental pollutant chemicals may come from industrial sources or inadequately handled communal waste in human habitat (Bieber et al., 2018). The short-term (a few hours) effects of the investigated agents (DMSO, ascorbic acid, Lucidril, cathecin, glycerol, glucose, taurine, selegiline, cAMP, spermidine, ethyl nicotinate, isoguvacine and choline) were very different; however, both species reacted with the same tendency (Fig. 6). There were a few cases in which the amount of conglomerate remained average; however, the length of the fibers significantly shortened (glycerol, taurine and isoguvacine) compared to the control. Among the investigated group of agents there were two chemicals (ethyl nicotinate and choline) which effects resulted a decreased amount of RIC with relatively long fibers. In the last variation of the exudate marker related pattern (Lucidril and glucose), high ratio of the covered area was detected with longer fibers than that of the control. Lucidril (Lazarova-Bakarova and Genkova-Papasova, 1989; Verma and Nehru, 2009) may be highlighted for its holistic stimulating effect as a conclusion. Based on the previously described results, concerning the pollutant agents, it is unequivocal that the activity or sensitivity of *E. dilatata* is higher than that of the *L. bulla* related to the exudate secretion. Here, the goal was not to explore the agents' mechanism of action on the rotifers, but to demonstrate the various and holistic effects of these chemicals on the external secretion of micro-metazoans.

Although both investigated rotifers are monogonants, their numerous phenotypic differences and physiological variations can be explained by their ancient phylogenetic divergence. These species show similarity only in calcium-dependent biopolymer production, suggesting that it is an evolutionarily ancient capability. The fact that rotifers have preserved this ability indicates that this product is a multifunctional bioactive molecule with a highly pronounced bioindicator role. Further investigation of the Rotimer has high potential for future applications. The phenomenon that the natural or artificial molecules influence the microscopic fauna, such as rotifers in the current case, in a relatively quick and different manner, raises the concern of preserving the natural environmental balance.

4. Conclusion

Examination of the conglomerate-covered area and the longest fiber of conglomerate markers revealed that the *E. dilatata* and *L. bulla* rotifer species react differently to all these parameters except for drug effects and calcium dependency of exudate secretion. Identical and opposite trends were also observed in the changes of the two examined RIC markers. The amount of conglomerate rarely correlated with the length of its fibers. The greatest novelty of this work lies in the fact that the production of Rotimer proved to be obligatorily calcium-dependent; moreover, this special exudate is a promising bioindicator of the

natural aquatic environment. Species-specific and simultaneous optimization of natural influencing factors significantly increased the RIC formation. Regulation and stimulation of biopolymer production may yield further investigations and possible industrial production of this substance in the future.

Funding

This research was conducted within the project which has received funding from the European Union's Horizon 2020 research and innovation programme under the Marie Skłodowska-Curie grant agreement, Nr. 754432 and the Polish Ministry of Science and Higher Education and Developing scientific workshops of medical-, health sciences and pharmaceutical training (grant number: EFOP 3.6.3-VEKOP-16-2017-00009).

CRediT authorship contribution statement

Zs.D. and Z.G.O.: Conceptualization. Zs.D., E.B. and Z.G.O: Methodology. Zs.D., Z.G.O. and F.S.: Validation. Zs.D., Z.G.O., F.S. and E.B.: Formal analysis. Zs.D., E.B. and Z.G.O: Investigation. Zs.D., J.K.: Resources. Zs.D., Z.G.O., E.B. and B.G.: Data curation. Zs.D. and Z.G.O.: Writing - original draft. Zs.D., Z.G.O., and B.G.: Writing - review & editing. Zs.D.: Visualization. Zs.D., Z.G.O. and J.K.: Supervision. Zs.D., Z. G.O. and E.B.: Project administration. Zs.D. and J.K.: Funding acquisition.

Declaration of Competing Interest

The authors declare that they have no known competing financial interests or personal relationships that could have appeared to influence the work reported in this paper.

Acknowledgments

The authors wish to thank to Anna Szentgyorgyi MA, a professional in English Foreign Language Teaching for proofreading the manuscript.

Appendix A. Supporting information

Supplementary data associated with this article can be found in the online version at doi:10.1016/j.ecoenv.2021.112399.

References

Armour, M.-A., 2016. Protecting health from metal exposures in drinking water. Rev. Environ. Health 31 (1), 29–31. https://doi.org/10.1515/reveh-2015-0079.

Bieber, S., Snyder, S.A., Dagnino, S., Rauch-Williams, T., Drewes, J.E., 2018. Management strategies for trace organic chemicals in water. A review of international approaches. Chemosphere 195, 410–426. https://doi.org/10.1016/j.chemosphere.2017.12.10.

Curnutt, A., Smith, K., Darrow, E., Walters, K.B., 2020. Chemical and microstructural characterization of pH and [Ca2+] dependent sol-gel transitions in mucin biopolymer. Sci. Rep. 10 (1), 8760. https://doi.org/10.1038/s41598-020-65392-4.

Dahms, H.U., Hagiwara, A., Lee, J.S., 2011. Ecotoxicology, ecophysiology, and mechanistic studies with rotifers. Aquat. Toxicol. 101, 1–12. https://doi.org/10.1016/j.aquatox.2010.09.006.

Datki, Zs, Acs, E., Balazs, E., Sovany, T., Csoka, I., Zsuga, K., Kalman, J., Galik-Olah, Z., 2021. Exogenic production of bioactive filamentous biopolymer by monogonant rotifers. Ecotoxicol. Environ. Saf. 208, 111666 https://doi.org/10.1016/j.ecoenv.2020.111666.

Ehrlich, H., 2019. Marine Biological Materials of Invertebrate Origin. Springer International Publishing AG. https://doi.org/10.1007/978-3-319-92483-0 part of Springer Nature 2019.

Frenkel-Pinter, M., Rajaei, V., Glass, J.B., Hud, N.V., Williams, L.D., 2021. Water and life: the medium is the message. J. Mol. Evol. 89, 2–11. https://doi.org/10.1007/s00239-020-09978-6.

George, T., Brady, M.F., 2020. Ethylenediaminetetraacetic Acid (EDTA). StatPearls [Internet]. Treasure Island (FL). StatPearls Publishing,. Bookshelf ID: NBK565883.

Gilbert, J.J., 2017. Non-genetic polymorphisms in rotifers: environmental and endogenous controls, development, and features for predictable or unpredictable environments. Biol. Rev. Camb. Philos. Soc. 92, 964–992. https://doi.org/10.1111/brv.12264.

Hendrych, M., Olejnickova, V., Novakova, M., 2016. Calcium versus strontium handling by the heart muscle Gen. Physiol. Biophys. 35 (1), 13–23. https://doi.org/10.4149/gpb_2015026.

Hernández-Flores, S., Santos-Medrano, G.E., Rubio-Franchini, I., Rico-Martínez, 2020. Evaluation of bioconcentration and toxicity of five metals in the freshwater rotifer Euchlanis dilatata Ehrenberg, 1832. R. Environ. Sci. Pollut. Res. Int. 27 (12), 14058–14069. https://doi.org/10.1007/s11356-020-07958-3.

Howard, L.S., Brown, B.E., 1984. Heavy metals and coral reefs. Oceanogr. Mar. Biol. Ann. Rev. 22, 195–210.

Ibrahim, M.S., Sani, N., Adamu, M., Abubakar, M.K., 2018. Biodegradable polymers for sustainable environmental and economic development. MOJ. Biorg. Org. Chem. 2 (4), 192–194. https://doi.org/10.15406/mojboc.2018.02.00080.

Jönsson, K., Wojcik A., I., 2017. Tolerance to X-rays and heavy ions (Fe, He) in the Tardigrade Richtersius coronifer and the Bdelloid Rotifer Mniobia russeola. Astrobiology 17, 163–167. https://doi.org/10.1089/ast.2015.1462.

Kanazawa, M., Nanri, T., Saigusa, M., 2017. Anhydrobiosis affects thermal habituation in the Bdelloid Rotifer, Adineta sp. Zool. Sci. 34, 81–85. https://doi.org/10.2108/zs160057.

Lalit, R., Mayank, P., Ankur, K., 2018. Natural fibers and biopolymers characterization: a future potential composite material. Stroj. Cas. J. Mech. Eng. 68 (1), 33–50. https://doi.org/10.2478/scjme-2018-0004.

Lazarova-Bakarova, M.B., Genkova-Papasova, M.G., 1989. Influence of nootropic drugs on the memory-impairing effect of clonidine in albino rats. Methods Find. Exp. Clin. Pharmacol. 11 (4), 235–239.

Macsai, L., Datki, Z.L., Csupor, D., Horváth, A., Zomborszki, Z.P., 2018. Biological activities of four adaptogenic plant extracts and their active substances on a Rotifer model. Evid. Based Complement. Altern. Med. 2018, 1–4. https://doi.org/10.1155/2018/3690683.

Mitterer, R.M., 1978. Amino acid composition and metal binding capability of the skeletal protein of corals. Bull. Mar. Sci. 28 (1), 173–180 (8).

Mohan, S., Oluwafemi, O.S., Kalarikkal, N., Thomas, S., Songca, S.P., 2016. Biopolymers Appl. Nanosci. Nanotechnol. Rec. Adv. Biopol. ⟨10.5772/62225⟩.

Niaounakis, M., 2015. Biopolymers: Application and Trends. Published by Elsevier Inc.

Olah, Z., Bush, A.I., Aleksza, D., Galik, B., Ivitz, E., Macsai, L., Janka, Z., Karman, Z., Kalman, J., Datki, Z., 2017. Novel in vivo experimental viability assays with high sensitivity and throughput capacity using a bdelloid rotifer. Ecotoxicol. Environ. Saf. 144, 115–122. https://doi.org/10.1016/j.ecoenv.2017.06.005.

Olatunji, O., 2020. Aquatic biopolymers, understanding their industrial significance and environmental implications. Springer International Publishing. https://doi.org/10.1007/978-3-030-34709-3.

Pérez-Legaspi, I.A., Rico-Martínez, R., 2001. Acute toxicity tests on three species of the genus Lecane (Rotifera: Monogononta). Hydrobiologia 446, 375–381. https://doi.org/10.1023/A:1017531712808.

Rico-Martínez, R., Arzate-Cárdenas, M.A., Robles-Vargas, D., Pérez-Legaspi, I.A., Alvarado-Flores, J., Santos-Medrano, G.E., 1975. Fluorescence polarization studies of squid giant axons stained with N-methylanilinonaphthalenesulfonates. Biophys. Struct. Mech. 1, 221–237. https://doi.org/10.5772/61771.

Saris, N.-E.L., Mervaala, E., Karppanen, H., Khawaja, J.A., Lewenstam, A., 2000. Magnesium. Clin. Chim. Acta 294 (1–2), 1–26. https://doi.org/10.1016/s0009-8981(99)00258-2.

Shain, D.H., Halldórsdóttir, K., Pálsson, F., Aðalgeirsdóttir, G., Gunnarsson, A., Jónsson, Þ, Lang, S.A., Pálsson, H.S., Steinþórssson, S., Arnason, E., 2016. Colonization of maritime glacier ice by bdelloid Rotifera. Mol. Phylogenet. Evol. 98, 280–287. https://doi.org/10.1016/j.ympev.2016.02.020.

Silva, M.A., da, Bierhalz, A.C.K., Kieckbusch, T.G., 2009. Alginate and pectin composite films crosslinked with Ca2+ ions: Effect of the plasticizer concentration. Carbohyd. Polym. 77 (4), 736–742. https://doi.org/10.1016/j.carbpol.2009.02.014.

Verma, R., Nehru, B., 2009. Effect of centrophenoxine against rotenone-induced oxidative stress in an animal model of Parkinson's disease. Neurochem. Int. 55 (6), 369–375. https://doi.org/10.1016/j.neuint.2009.04.001.

Wang, L., Shelton, R.M., Cooper, P.R., Lawson, M., Triffitt, J.T., Barralet, J.E., 2003. Evaluation of sodium alginate for bone marrow cell tissue engineering. Biomaterials 24 (20), 3475–3481 doi: 10.1016/s0142-9612(03)00167-4.

Wenjie, L., Binxia, L., Cuijuan, 2019. Effects of temperature on life history strategy of the Rotifer Euchlanis dilatata. Feb 1 N. Zool. Sci. 36 (1), 52–57. https://doi.org/10.2108/zs170096.

Yavuz, B., Chambre, L., Kaplan, D.L., 2019. Extended release formulations using silk proteins for controlled delivery of therapeutics. Expert Opin. Drug Deliv. 16, 741–756. https://doi.org/10.1080/17425247.2019.1635116.

Zaitoun, M.A., Lin, C.T., 1997. Chelating Behavior between Metal Ions and EDTA in Sol−Gel Matrix. J. Phys. Chem. B 101 (10), 1857–1860. https://doi.org/10.1021/jp963102d.

Zhang, S., Li, C., Gao, J., Qiu, X., Cui, Z., 2014. Application of the Ca2+ indicator fluo-3 and fluo-4 in the process of H2O2 induced apoptosis of A549 cell. Zhongguo Fei Ai Za Zhi 17 (3), 197–202. https://doi.org/10.3779/j.issn.1009-3419.2014.03.03.

IV.

International Journal of Biological Macromolecules 201 (2022) 262–269

Contents lists available at ScienceDirect

International Journal of Biological Macromolecules

journal homepage: www.elsevier.com/locate/ijbiomac

The interacting rotifer-biopolymers are anti- and disaggregating agents for human-type beta-amyloid *in vitro*

Zsolt Datki [a,*], Evelin Balazs [a], Bence Galik [b,c], Rita Sinka [d], Lavinia Zeitler [a], Zsolt Bozso [e], Janos Kalman [a], Tibor Hortobagyi [f,g,1], Zita Galik-Olah [a,1]

[a] Department of Psychiatry, Albert Szent-Györgyi Medical School, University of Szeged, Korányi fasor 8-10, H-6725 Szeged, Hungary
[b] Bioinformatics Research Group, Bioinformatics and Sequencing Core Facility, Szentágothai Research Centre, University of Pécs, Ifjúság u. 20, H-7624 Pécs, Hungary
[c] Department of Clinical Molecular Biology, Medical University of Bialystok, ul.Jana Kilinskiego 1, 15-089 Bialystok, Poland
[d] Department of Genetics, Faculty of Science and Informatics, University of Szeged, Közép fasor 52, H-6726, Hungary
[e] Department of Medical Chemistry, Albert Szent-Györgyi Medical School, University of Szeged, Semmelweis u. 6, H-6725 Szeged, Hungary
[f] Department of Pathology, Albert Szent-Györgyi Medical Center, University of Szeged, Állomás u. 1., H-6725 Szeged, Hungary
[g] Department of Old Age Psychiatry, Institute of Psychiatry Psychology & Neuroscience, King's College London, Box PO70, De Crespigny Park, Denmark Hill, SE5 8AF London, UK

ARTICLE INFO

Keywords:
Monogonant
Rotifer
Biopolymer
beta-amyloid
Aggregation
Euchlanis dilatata

ABSTRACT

Neurodegeneration-related human-type beta-amyloid 1-42 aggregates (H-Aβ) are one of the biochemical markers and executive molecules in Alzheimer's disease. The exogenic rotifer-specific biopolymer, namely Rotimer, has a protective effect against H-Aβ toxicity on *Euchlanis dilatata* and *Lecane bulla* monogonant rotifers. Due to the external particle-dependent secreting activity of these animals, this natural exudate exists in a bound form on the surface of epoxy-metal beads, named as Rotimer Inductor Conglomerate (RIC). In this current work the experiential *in vitro* molecular interactions between Rotimer and Aβs are presented. The RIC form was uniformly used against H-Aβ aggregation processes in stagogram- and fluorescent-based experiments. These well-known cell-toxic aggregates stably and quickly (only taking a few minutes) bind to RIC. The epoxy beads (as carriers) alone or the scrambled version of H-Aβ (with random amino acid sequence) were the ineffective and inactive negative controls of this experimental system. The RIC has significant interacting, anti-aggregating and disaggregating effects on H-Aβ. To detect these experiments, Bis-ANS and Thioflavin T were applied during amyloid binding, two aggregation-specific functional fluorescent dyes with different molecular characteristics. This newly described empirical interaction of Rotimer with H-Aβ is a potential starting point and source of innovation concerning targeted human- and pharmaceutical applications.

1. Introduction

Various neurotoxic peptides (*e.g.*, beta-amyloids) or proteins (*e.g.*, alpha-synuclein, huntingtin and prion) are involved in the development of neurodegenerative diseases, where the aggregation is caused by an abnormal conformational change in related molecules [1]. These dysfunctions occur either extra- or intracellularly [2,3]. Several types of cell-toxic aggregates are known depending on different cognitive diseases [4], such as Alzheimer's disease (AD), characterized by human-type beta-amyloid 1-42 (H-Aβ) deposits in the brain [5].

The aggregating-mechanism of Aβs is influenced by different agents, which may have anti-aggregating and/or disaggregating effects. Numerous studies have shown [6] that natural compounds (*e.g.*, *Ginkgo biloba* extracts) have high pharmacological potentials and attenuating effects against the AD. Curcumin, besides its widespread positive effects, is another natural molecule that can also block the aggregation and is able to dissociate an existing one [7]. Various active substances with herbal origin show antagonistic effects against amyloid genesis activity and they may even have preventive and therapeutic relevance in dementias [8]. Some molecules (*e.g.*, polyphenols or chaperones), in addition to inhibiting aggregation, can stabilize the native protein conformation [9]. Moreover, some anti-inflammatory small molecules (*e.g.*, Aspirin) can also inhibit the aggregation processes, and significantly reverse the conformation of beta-sheet structures to alpha helix

* Corresponding author.
E-mail address: datki.zsolt@med.u-szeged.hu (Z. Datki).
[1] The authors contributed equally to this work (co-last authors).

https://doi.org/10.1016/j.ijbiomac.2021.12.184
Received 13 November 2021; Received in revised form 17 December 2021; Accepted 29 December 2021
Available online 7 January 2022

[10].

Various biopolymers emerged as new scientific possibilities in the research field and in the pragmatic application of natural agents. Based on their multifunctional roles in the living world, the question arises as to what impact they may have on aggregation processes. The answer can be investigated in an interdisciplinary approach connecting biotechnology with neurobiology. Since biopolymers are also involved in degradation processes in the natural habitat [11]; therefore, they may influence the conglomeration and aggregation processes. Several biopolymers affect the polymerization or precipitation of different types of organic materials and molecules [12]. Thus, preventing/inhibiting peptide or protein aggregation processes are also worth studying.

The secreting exudates had primarily been investigated with an industrial purpose; nevertheless, their beneficial effects have also been studied in medicine. A representative example for this technical translation is the gold nanoparticles, coated with dextrin or chitosan, which are able to inhibit insulin amyloid fibrillation in a complex form [13]. These biopolymer-coated particles interact with the insulin monomers and prevent the formation of its oligomers. The polysaccharide β-D-glucan and carboxylmethylated derivatives were also able to block platelet aggregation [14]. In addition to various compounds, numerous proteins complexes (*e.g.*, heat shock types) attenuate the aggregation of different monomers [15]. Because biopolymers are biocompatible, biodegradable and have low immunogenicity, they are promising theoretical sources in biomedicine [16], even in neurobiology. There are several natural molecules (*e.g.*, collagen, gelatin, heparin or chitosan) that are the bases of artificial products available in clinical application [17]. Furthermore, many plant-based polymers (*e.g.*, cellulose) can also be used as medical engineering constructs due to their good physical properties. These agents are suitable as therapeutic molecules in drug and gene delivery [18].

Based on basic- and preclinical research, Ow et al. [19] asserts that biomolecules play an increasing role in neuromedicine, related to the modulation of aggregation processes *in vitro*.

Some micrometazoans are able to produce exogenous biopolymers [20]. Of these phylogenetically conservative beings, the rotifers form large portion of natural water biomass; moreover, their possible application as modern *micro-in vivo* models have been demonstrated in several interdisciplinary areas, *e.g.*, in pharmacotoxicology, neurobiology and especially in neurobiochemistry. Their exceptional ability for survival in neurotoxic aggregates-supplemented environment has been recently revealed [21]. This fact brings the rotifers into the attention of researchers committed to amyloid-related science. These animals are outstanding candidates for holistic and experiential studies investigating neurotoxic aggregates. Rotifer-specific biopolymer (namely Rotimer) was recently discovered and first described by Datki et al., [22] in academic literature. The production of *Euchlanis dilatata*- and *Lecane bulla*-specific Rotimers, as monogonant bioproducts, can be induced by mechanically stimulating these animals with various types of microparticles (*e.g.*, carmine or urea crystals, epoxy beads and microcellulose). The multiple *in vitro* bioactivities of these biomolecules were proved by applying three different cell types: alga, yeast and human SH-SY5Y neuroblastoma. The exudates had no negative effect on the cells; however, they completely inhibited the motility and the proliferation of neuroblastoma cultures.

The effect of the Rotimer was further investigated on rotifers in terms of their viability, where the animals were treated with aggregated H-Aβ. The H-Aβ was non toxic to those native entities which were able to produce fiber webs; however, it proved to be harmful for Rotimer-depleted ones. In these experiments, the relations between biopolymer and H-Aβ were indirectly tested *in vivo*. The potential interaction of Rotimer and H-Aβ is directly investigated *in vitro* in animal-free conditions in this current study. Two different methods were applied to examine the potential Rotimer-Aβs connections: stagogram pattern analysis (interaction measurements) parallelly with fluorescence-based methods such as anti- and disaggregation monitoring. Stagogram analysis is an adequate tool for quick and holistic evaluation of the possible reactions between rotifer-type biopolymers and human-type aggregates. This optical imaging-based method has a history in biomarker research [23], but this is the first time, that it was applied for investigating the interacting effect of biopolymers.

The H-Aβ containing deposits or plaques can be detected by various absorbent (*e.g.*, Congo red) or fluorescent dyes (*e.g.*, Thioflavin S, Thioflavin T/ThT/, ANS or Bis-ANS). Among methods (*e.g.*, mass spectrometry or infrared spectroscopy), analyzing molecular interaction, the efficacy of the anti-amyloid compounds *in vitro* can be semi-quantified by detecting the relative fluorescence intensity of the above-mentioned dyes [24] in targeted biochemical samples. Functional fluorophores with different specificity can be selected depending on the type of Aβs and the aim of the related experiments. The aggregates, as targets with various size and profiles, bind to dyes in diverse extents. The Bis-ANS is better able to detect the oligomer-type of H-Aβ then the fibrils with a larger conformational spectrum. The ThT binds with higher affinity to H-Aβ fibrils than to oligomers, based on the beta-sheet structure preference [24,25].

Based on the previously published facts [21,22] as well as on the novelties of the current research, the Rotimer has a high potential of becoming a promising drug candidate for human application in pharmacology and clinical medicine.

2. Materials and methods

2.1. Materials

Materials applied in this work were the following: yeast (*Saccharomyces cerevisiae*; EU-standard granulated instant form, cat. no.: 2-01-420674/001-Z12180/HU); algae (*Chlorella vulgaris*; BioMenu, Caleido IT-Outsource Kft.; cat. no.:18255); the applied fluorescent dyes were obtained from Sigma-Aldrich: 4,4′-dianilino-1,1′-binaphthyl-5,5′-disulfonic acid dipotassium salt (Bis-ANS, cat. no.: D4162) and Thioflavin T (ThT; cat. no.: T3516); from Merck: distilled water (DW; Millipore Ultrapure); from Life Technologies AS: DynaMag-2 magnet (cat. no.: 12321D); Dynabeads M-270 superparamagnetic epoxy beads (cat. no.: 14301); from Greiner: 96-well microplate with half-area (cat. no.: 675101, Greiner Bio-One International); from Corning: treated (cat. no.: 430293) and non-treated (cat. no.: 430591) Petri dishes, culture flasks (cat. no.: 430168); Whatman filter with 10 μm diameter pore (cat. no.: 6728-5100); universal plastic web (pore diameter: 50 μm); the amount of diluted cations and anions in standard medium (mg/L): Ca^{2+} 30; Mg^{2+} 15; Na^{+} 3.2; K^{+} 0.5; HCO_3^{-} 150; SO_4^{-} 2.5; Cl^{-} 1.4; NO_3^{-} 4.5; F^{-} 0.01; SiO_2 8; pH = 7.5; conductibility (20 °C): 428 μS/cm. Human-type beta-amyloid 1-42 (H-Aβ; cat. no.: A14075, human Amyloid b-Peptide 1-42; cat. no.: 107761-42-2) was purchased from AdooQ Bioscience LLC., California. The scrambled Aβ (S-Aβ) (LKAFDIGVEYNKVGEGFAISHG-VAHLDVSMFGEIGRVDVHQA) were prepared at the Department of Medical Chemistry, University of Szeged, Szeged, Hungary. The peptides were synthesized on an Fmoc-Ala-Wang resin using Nα-Fmoc-protected amino acids with a CEM Liberty microwave peptide synthesizer (Mathews, NC, USA).

2.2. Preparation of the amyloid aggregates

The concentrations of the various beta-amyloid (H-Aβ and S-Aβ) stock solutions were 1 mg/mL in DW. The aggregation time was 3 h (3 h) or 3 days (3d) alone or together with Rotimer Inductor Conglomerate (RIC) at 24 °C (pH 3.5). The neutralization (to pH 7.5) was performed with NaOH (1 N) [26]. At the end of the aggregation process the samples were vortexed (5 min; 600 rpm) and before using theirs stock solutions, they were ultrasonicated (Emmi-40 HC, EMAG AG, Mörfelden-Walldorf, Germany) for 10 min at 45 kHz to achieve semi-sterilization and homogenization. After 20-fold dilution with standard medium, the final concentration of Aβs were 50 μg/mL.

2.3. Animal culture

The experiments were performed on *E. dilatata* and *L. bulla* monogonant rotifer species; therefore, no specific ethical permission was needed according to the current international regulations. The species have been maintained and cultured at standard laboratory conditions for several years. These parameters and the origin of the above-mentioned rotifers were precisely described previously by Datki et al. [22]. For standard food of cultures, a mixture of homogenized baker's yeast and alga was used after heat-inactivation and filtration (diameter of particles ranged 8–10 μm).

2.4. Rotimer induction, RIC production and harvesting

As a first step, monogonant populations (1200 ± 85 individuals) were harvested from the culturing flasks by selective accumulation of animals with a plastic web (pore size 50 μm) into surface-treated Petri dishes (55 cm^2 area). The animals were currently unfed, their stomachs were empty by the second day following feeding. This precaution was necessary to avoid contamination of RIC-solution with their faeces.

The inductor (epoxy-metal beads; 200 μL vortexed stock solution with a dose of 6 mg/mL concentration) of Rotimer secretion was added to the rotifer-containing standard medium (30 mL in Petri dishes) for 2 h. Based on the manufacturer's product description of the Dynabeads M-270, 1 mg of these beads can bind approximately 10 ± 2 μg of ligands (in this case the Rotimer); however, 6 mg of beads from one induction can theoretically bind about 50–60 μg Rotimer onto their surfaces if they are widely covered. Calculating with this amount of biopolymer, the working concentration of Aβs was determined to be 50 μg/mL. The RIC productions by rotifers were monitored under light microscope (at 63× magnification; Leitz Labovert FS, Wetzlar, Germany). The attachment of Rotimer onto the epoxy beads was validated by scanning electron microscopy which was presented in our previous publication [22].

In order to perform all types of measurements in this work, RIC samples were prepared in a newly modified version compared to previous studies. The medium, including animals in Petri dishes, was removed repetitively and carefully by a pipette (5 mL working volume) then, the Rotimer-containing RIC were mechanically recovered and homogenized in 5 mL DW. The remaining rotifers were removed by filtration using the above-mentioned plastic web. The animal-free, but RIC-containing solution was then prepared at room temperature, applying DynaMag-2 magnet to fix the exudate-coated beads temporarily and reversibly. The supernatant was removed by a pipette and the RIC-pellet was washed once with DW and finally resuspended in 150 μL DW. This conglomerate material solution was used for all types of measurements.

2.5. RIC-Aβ interaction protocols

2.5.1. Stagogram-based optical assay

After a short time (5 min) of incubation, the interaction between mixed monogonant-specific RIC (6 mg Rotimer-coated epoxy beads per mL) and 3 h or 3d Aβ aggregates were investigated. The beads were isolated with a magnet in the previously described way. After discarding

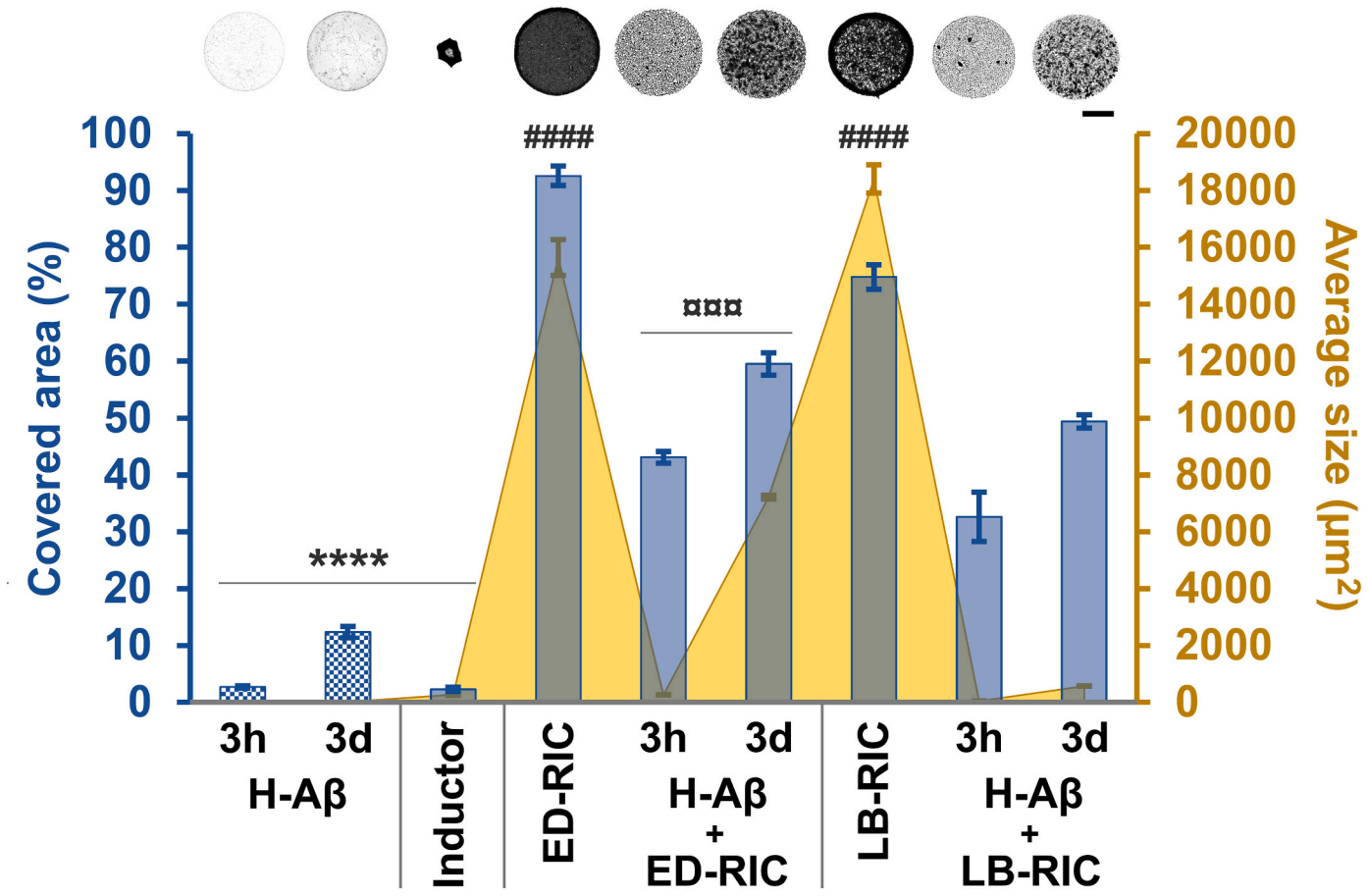

Fig. 1. Stagogram-based optical imaging and analysis of RIC and aggregated H-Aβ interactions. ED: *Euchlanis dilatata*; LB: *Lecane bulla*; RIC: Rotimer Inductor Conglomerate; H-Aβ: human-type beta-amyloid 1-42; Scale bar represents 0.5 mm. The error bars represent SEM. One-way ANOVA with Bonferroni *post hoc* test was used for statistical analysis, the levels of significance are $p^{¤¤¤¤} \leq 0.001$ or $p^{****,\#\#\#\#} \leq 0.0001$ (*, significant difference from all other groups; $^{\#}$, significant difference from those treated with the same ED-RIC; $^{¤}$, significant difference from LB-RIC belonging to the same group).

the supernatant, the pellet was washed and resuspended in 150 μL DW. Drops ($n = 10$) with 1 μL volume were put onto non-treated hydrophobic plastic surface of Petri dish, then, they were dried for 1 h at 40% humidity.

The formed stagograms of the drops (Fig. 1) were detected by light microscopy and were photographed (Nikon D5600, 25 MP, RAW/NEF, 14 bit; Nikon Corp., Kanagawa, Japan). The digital pictures were converted into a black and white graphical format with greyscale (threshold; 2.46 pixel = 1 μm; 8-bit). Maximum measured area of the drops was 1.68 mm^2. These images (total area of this complex) were analyzed with ImageJ program (Wayne Rasband, USA) and the related extracting data of the conglomerate-covered area (%) and the average size (μm^2) were presented.

2.5.2. *Bis-ANS- and ThT-based fluorescent assays*

The amyloid-sensitive Bis-ANS and ThT dyes were applied in fluorescent-based *in vitro* (animal-free) experiments ($n = 12$ wells/sample type) including investigations on: quick molecular interaction (Fig. 2) and on anti-aggregation (Fig. 3A) or disaggregation (Fig. 3B). The final dose of the dyes was 50 μM.

In these interaction-specific experiments, the 3 h or 3d Aβ aggregates (final concentration 50 μg/mL) were mixed with RIC (6 mg epoxy beads/mL), similarly to the stagogram protocol, where the incubation time was only 5 min. The free Aβ-containing supernatants and the RIC-Aβ pellets were measured separately. Bis-ANS was used for 3 h samples, while ThT was preferred in the case of 3d ones. In the anti-aggregation study, the H-Aβ-stock solution (1 mg/mL) and the concentrated RIC (120 mg epoxy/mL) were incubated together during the whole aggregating period (3d). The H-Aβ and RIC stock solutions were also incubated together for 12 h and the measurements were also performed in the case of disaggregation experiments. In these cases, the Rotimer containing RIC-Aβ mixes were not separated to pellet and supernatant, their fluorescent intensity was recorded together by applying the fluorescent dyes alternately. The dose ratio of Aβs and the theoretically calculated Rotimer was 1:1 in each study.

Samples containing the investigated molecules were measured with a BMG NOVOstar micro-plate reader (BMG Labtech, Ortenberg, Germany) at ex/em: 405/520 nm on Bis-ANS and 450/480 nm on ThT, using a 96-well plate with half well area (100 μL/well). The number of laser flashes per well was 30 and orbital shaking (3 s and 600 rpm) was applied before each detection. Calibration/gain adjustment was 1% of the maximal relative intensity, where the blank of the relevant

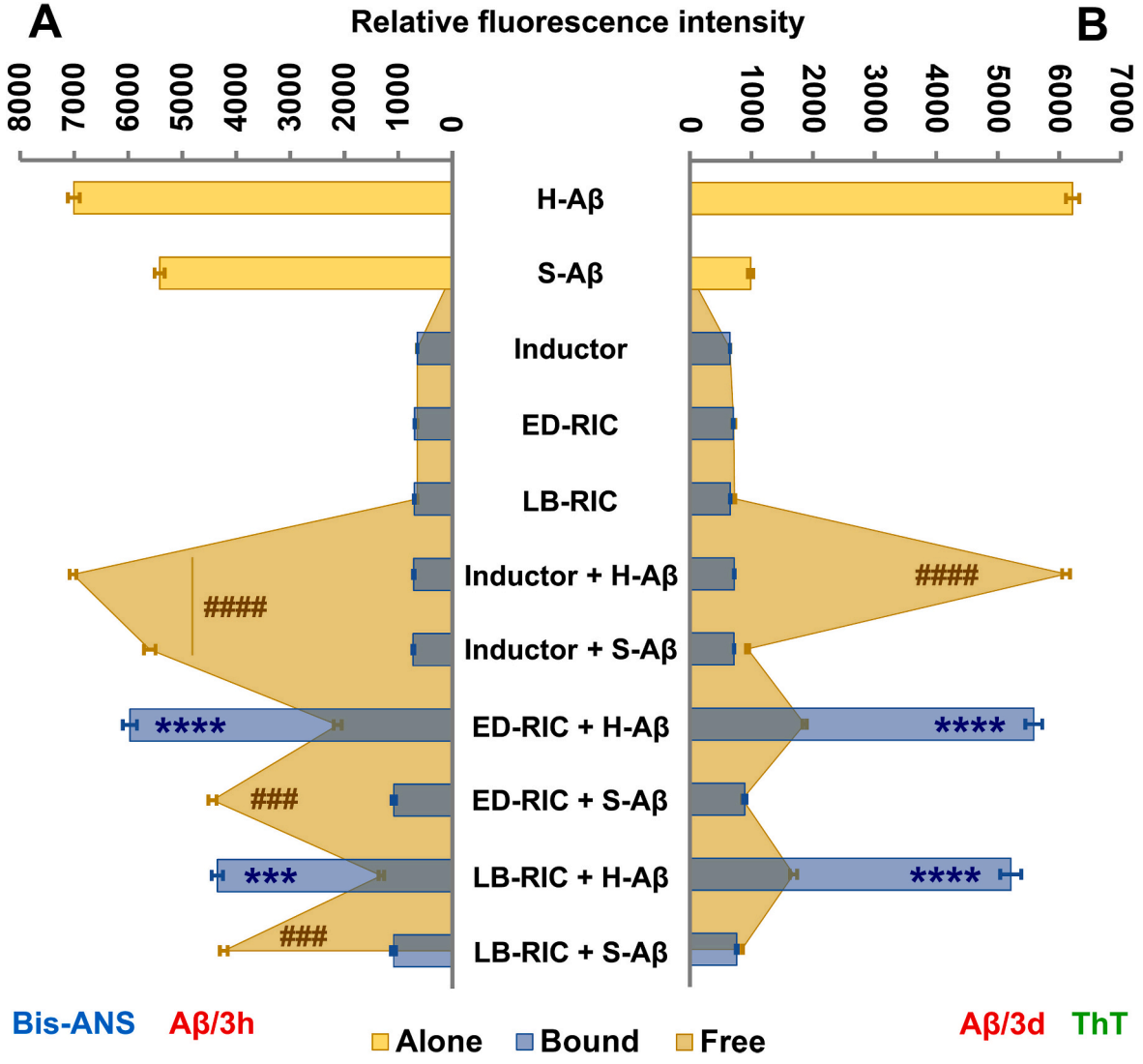

Fig. 2. Quick and sequence-based interaction of *E. dilatata*- and *L. bulla*-specific RIC with H-Aβ aggregates (3 h and 3d). ED: *Euchlanis dilatata*; LB: *Lecane bulla*; RIC: Rotimer Inductor Conglomerate; H-Aβ: human-type beta-amyloid 1-42. The error bars represent SEM. One-way ANOVA with Bonferroni *post hoc* test was used for statistical analysis, the levels of significance are $p^{***,\#\#\#} \leq 0.001$ or $p^{****,\#\#\#\#} \leq 0.0001$ (*, significant difference from all other bound-type groups; #, significant difference from all other free-type inductor, RIC and RIC + H-Aβ groups).

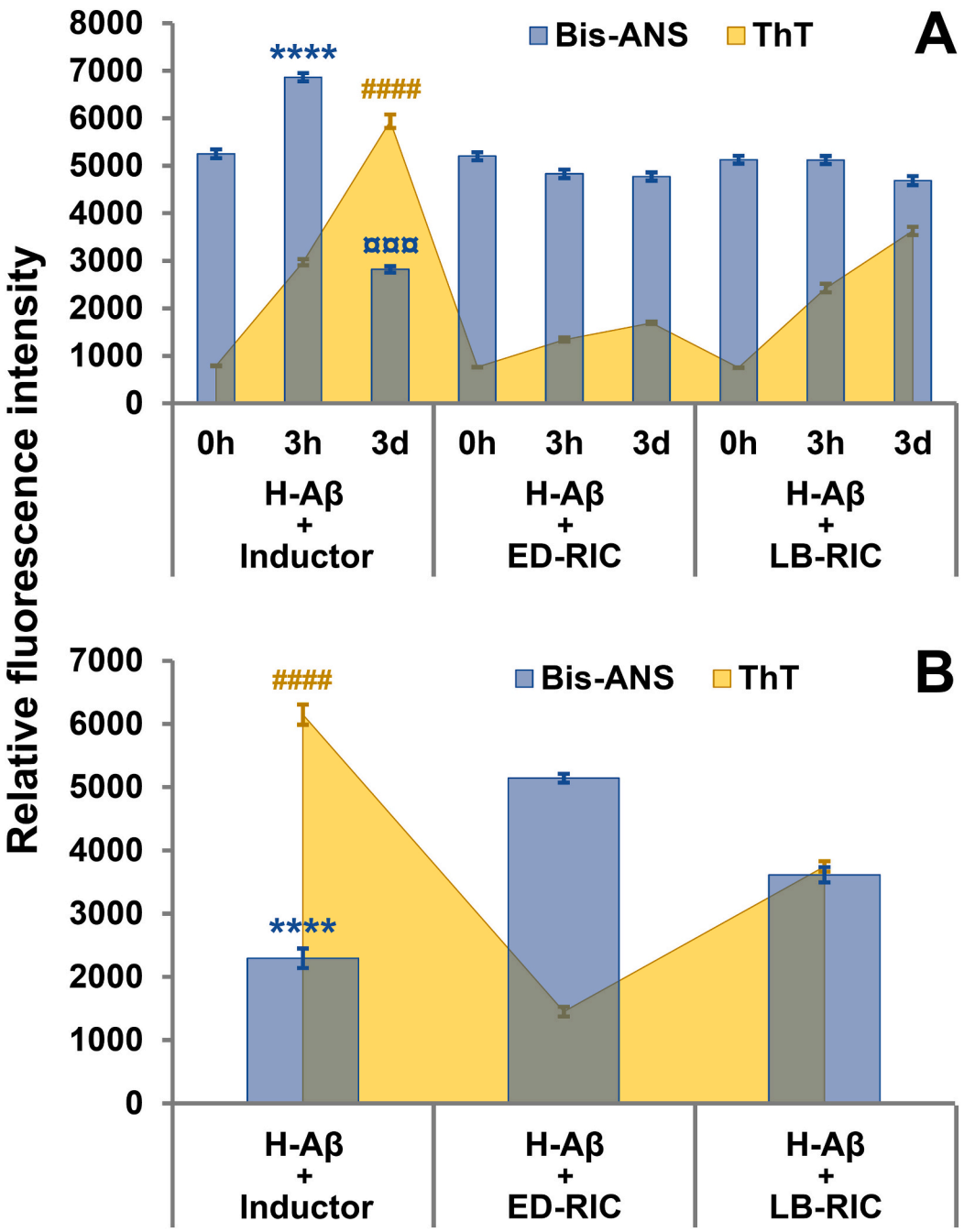

Fig. 3. Anti-aggregation (A) and disaggregation (B) effects of *E. dilatata*- and *L. bulla*-specific RIC against H-Aβ aggregates (3 h and 3d). ED: *Euchlanis dilatata*; LB: *Lecane bulla*; RIC: Rotimer Inductor Conglomerate; H-Aβ: human-type beta-amyloid 1-42. The error bars represent SEM. One-way ANOVA with Bonferroni *post hoc* test was used for statistical analysis, the levels of significance are $p^{¤¤¤¤} \leq 0.001$ or $p^{****, ####} \leq 0.0001$ (*, significant difference from all other Bis-ANS groups; #, significant difference from all other ThT groups; ¤, significant difference from RIC-containing 3d Bis-ANS group).

fluorescent dye was about 650. The labelling time of the samples with the dyes took 5 min before starting detection.

2.6. Statistics

Statistical analysis was performed with SPSS 23.0 (SPSS Inc., USA) using one-way ANOVA with Bonferroni *post hoc* test. The error bars represent the standard error of the mean (SEM). The homogeneity and normality of the data were checked, and they were found suitable for ANOVA followed by Bonferroni *post hoc* test. Using the above-mentioned statistical test, 99% confidence level (1-aplha, alpha = 0.01) was applied and 1% error was handled in this analysis. The different levels of significance are indicated as follows: $p^{***, ###, ¤¤¤} \leq 0.001$ and $p^{****, ####} \leq 0.0001$. All relations and comparisons between the presented groups are defined in the given figure legend.

3. Results and discussion

The investigation of function, nature and applicability of biopolymers is a significant branch of biology nowadays [27]. The list of these natural and multifunctional materials is long; moreover, all of them have unique characteristics, making it necessary to study them individually. Such a relevant material is the recently published rotifer-specific biopolimer, namely Rotimer [22]. This biomolecule is a species-specific exudate of the relevant micrometazoa. *E. dilatata* and *L. bulla* monogonants are prominent representatives of the exogenic fiber-producing animals.

This current study has two objectives: on one hand to investigate the binding between the biopolymer-containing conglomerates and H-Aβ neurotoxic aggregates and, on the other hand, to reveal the effects of RIC complex on H-Aβ aggregation itself. The measurements could not be

carried out with Rotimer lacking an inductor material (epoxy-metal beads), because according to our current knowledge and empirical experience, there is no method available to remove the mentioned biomolecule from the inductor without any structural changes (*e.g.*, a chemical one, such as racemization in alkaline solution). The organizing conditions and the binding of aggregates were monitored directly and indirectly with optical imaging methods; however, the detailed investigation of physicochemical properties was beyond the scope of this paper. RIC is the only possible form used for empirical characterization [28] and treatment studies at the time of this current publication.

Presumably, the Rotimer plays an outstanding role in the neurotoxic aggregates-catabolism caused by rotifers [21]; therefore, it is reasonable to study this exceptional phenomenon. As a first step, the quick interaction (taking a few minutes) between the natural polymers of rotifers and the artificially made H-Aβ was investigated, applying two different methods. The binding between H-Aβ and *E. dilatata*- or *L. bulla*-RIC (ED/LB-RIC) was measured by the so-called stagogram analysis (Fig. 1), which is a simple, but widely accepted method to visualize, for instance, the aggregation capacity of the different molecular composition of samples, based on their optical diversity [23,29]. This technique is a sensitive crystallizing process using the covered (%) area and average size (μm^2) parameters of particles. These indicators can be adequately applied during the image analysis, based on the number and size of the conglomerate unit; moreover, the dried drops can be qualitatively differentiated. Differently treated groups were investigated and compared with the adequate controls. The effective agent in the present case was the RIC (epoxy beads with Rotimer).

The Aβs were aggregated for 3 h (3 h) or for three days (3d) before mixing them with the respective RIC. Then, we measured the inductor itself, H-Aβ and ED/LB-RIC alone, and the conglomerates of H-Aβ with the ED/LB-RIC respectively, using the stagogram based optical assay (Fig. 1). The solutions of fresh (0 min) H-Aβ and S-Aβ (with a random sequence of amino acids) were not presented on the stagogram figure, because they showed transparent crystallizing patterns; therefore, the borders of the dried samples could not be identified.

The crystallized drops of the groups were different both in their density and structure phenotype (Fig. 1). This is a closed and precisely defined chemical environment with few components; however, it is a well controllable *in vitro* system. The profiles of the different samples represent the interactions between the components during crystallization. The presence, absence, or variations in the amounts of determining factors is the quintessence of this drying process. According to the optical stagogram markers, the parameters of H-Aβ, the inductor and the conglomerates significantly differed from each other. The more aggregated (3d) H-Aβ showed a denser pattern compared to the ones incubated for a few hours (3 h). Both RIC groups of the two tested rotifers presented outstanding density in the empiric analysis of stagograms; therefore, they provided maximal reference to further analyze other samples. After removing the unbound/free H-Aβ, it can be noted that the biopolymers of the two species bind to aggregates; furthermore, the optical density of relevant stagograms, derived from RIC alone, decreased in the presence of H-Aβ in the conglomerate. We observed a higher level of density of the ED-RIC/H-Aβ conglomerate compared to the LB-RIC/H-Aβ ones. Based on the results, it can be stated that there are possible molecular interactions between the Rotimer and Aβs, particularly with the H-Aβ form. The relations between RIC and H-Aβ of both rotifer species showed similar tendencies; however, we also noticed that the pictures were significantly brighter of the samples originating from *L. bulla*.

Besides and parallel with the optical analysis, the quick interactions between the molecules of interest were investigated by fluorescent methods. To measure the fluorescent indicator signals, two adequate dyes were applied, the Bis-ANS and the ThT. According to literature, these molecules have different binding affinities to various aggregates [30]. These functional sensors can mark the oligomeric and fibrillar forms of Aβs, labeling the whole conformational spectrum of H-Aβs. The Bis-ANS is more sensitive to the oligomers [24], while the ThT is more adequate for the fibrils [25,31]. Based on the previous Aβ characterizations [21,32–34], it can be stated that the 3 h and 3d aggregating periods are well-reflected for the larger quantity of the oligomers or fibrils in the relevant samples. The H-Aβ (3 h) with lower organization contains oligomers in higher proportions, and they were measured by Bis-ANS, while the considered fibrillar ones with longer incubation time (3d) were detected by ThT (Fig. 2). All samples were monitored with both fluorophores in anti- (Fig. 3A) and disaggregating (Fig. 3B) measurements.

The results of the interaction studies (Fig. 2) can be classified into three units: 1. H-Aβ-types alone; 2. inductor, various RIC-versions and the inductor-Aβ interactions as appropriate controls; 3. the connections between the species-specific RIC and the various H-Aβs (according to amino acid sequence and levels of aggregation). Based on the applied aggregates, three categories can be identified: 1. Aβs alone; 2. free Aβs in the supernatant; 3. binding Aβs to the RIC-types.

The given forms of H-Aβ aggregates showed elevated fluorescence intensities in the presence of both Bis-ANS and ThT, in contrast with S-Aβ, which shows higher signal intensity rather together with Bis-ANS. The S-Aβ with random sequence presented decreased aggregating organization. Measurements of the Aβs alone were the reference points for further experiments. The relevant fluorescence intensities of the inductor and ED/LB-RIC combinations were also measured and used as a background control to the aspecific binding. Based on the achieved results it can be concluded that they show a minimal binding between the above-mentioned reference controls and the applied fluorescent dyes during the relatively short incubation time. Besides these cutoff values, the binding of Aβs to biopolymer-containing RIC was significantly measurable. Here, the inductor alone was not a disturbing factor either. After removing the non-bound (free) Aβs with supernatant, the binding of aggregates to RIC were labeled. The H-Aβ interacted with the conglomerates of both rotifer species, and a relatively high fluorescent signal was shown, while the S-Aβ had a lower value similarly to the background control. The data derived from this reference amyloid type led us conclude sequence specificity in H-Aβ-binding to biopolymers. In our previous publication [35], the sequence-specific effect of H-Aβ was proved in the autocatabolism-related processes of rotifers compared to S-Aβ. The H-Aβ samples with lower (3 h) or higher (3d) conformational organization were significantly bound to both tested Rotimer coatings, but they showed higher affinity to the biopolymer secreted by *E. dilatata* than the one produced by *L. bulla*.

After proving the particular interaction between Rotimer and H-Aβ, the effects of the investigated biopolymer on aggregation processes were tested using Bis-ANS and ThT measurements, which were able to indirectly detect the approximate aggregation status of Aβs. The controls showed similar fluorescence intensity to the previously measured ones (Fig. 2); therefore, they were not presented again in this case. To measure the anti-aggregating effects of RIC-types (Fig. 3A), H-Aβ was applied with various aggregation times (0 h, 3 h and 3d). During co-incubation, the inductor alone did not inhibit the aggregation of H-Aβ; however, the initial signal of Bis-ANS significantly decreased in the 3d sample, while the ThT signal increased. These results refer to the time-dependent high aggregation level of H-Aβ; moreover, these processes are in line with the relevant literature [36,37]. In contrast with the above mentioned, the H-Aβ (3 h and 3d) + RIC related ThT signals decreased in samples of both relevant species, while the Bis-ANS fluorescence remained on the reference (0 min) level. The materials from *E. dilatata* proved to be more effective in anti-aggregation processes than the ones derived from *L. bulla* applying the same experimental period of time. The 3d group showed the less efficiency. In the LB-RIC and H-Aβ/3d combination, the ThT resulted an elevated level; thus, unlike in the other samples, there was no clear conclusion about the aggregation changes of H-Aβ.

The following experiments revealed that the presence of the inductor alone during a further 12 h had no impact on the condition of 3d-pre-

aggregated H-Aβ (Fig. 3B). In these cases, the Bis-ANS and ThT signal ranges are alike the previously presented data (Fig. 3A). In contrast, the control Bis-ANS and ThT values significantly differed from the RIC-containing ones from the same category at the end of disaggregating processes. During the co-incubation time, the RIC of both monogonant species increased the level of Bis-ANS sensitive oligomers, and they decreased the concentration of ThT-specific fibrillar forms. Based on the characteristics of the two fluorophores it may be assumed that the presence of Rotimer in the samples has a disaggregating effect against the H-Aβ. Such as in the previous measurements, the biopolymer of *E. dilatata* was more efficient, and it gave more comprehensible results about the condition of the neurotoxic aggregates.

Different behavior of RIC-types on H-Aβ-binding and aggregating processes, derived from the two different species, can be further explained. One interpretation may be that *L. bulla* originally secreted less biopolymer to the epoxy beads than *E. dilatata*. Another possibility is that the biopolymers may differ in the various rotifer species in terms of structure, functionality, and efficacy. The anti-aggregation effect of LB-RIC did not increase when the number of animals was higher during longer secretion time (4 h) of Rotimer, or a two-fold dose of RIC was tested in the presence of standard H-Aβ amount (data not shown).

Altogether, the results show that the ED/LB-RIC, with proteinous exudate on their surface, explicitly binds the H-Aβ. It is an efficient influencing factor in aggregation kinetics; moreover, the activity of the species-specific biopolymers may differ from each other. Further proteomic experiments (*e.g.*, mass spectrometry) are needed to investigate the interaction between the Rotimer and the neurotoxic protein aggregates (*e.g.*, alpha-synuclein and prions). It is well-known that during the Rotimer secretion, the calcium is built-in [28], and it may provide different ionic characteristics to this biomaterial; therefore, the metal ion content of the biopolymer may enhance these molecular relations. The mechanism of anti- and disaggregating ability may be similar to the action of beta-sheet-breaker molecules or that of some natural (LPFFD, [38]; RIIGL, [39–41]) or artificial (LPYFD, [32,42]) peptide sequences. The spectroscopic analysis of Rotimer may give the proper answer to these questions, which will be part of the following projects.

In summary, it is essential to highlight that the direct molecular effects of natural polymers [43,44] on neurodegeneration-related amyloids have been barely investigated, resulting only a few cases [13]. Based on the results obtained, Rotimer is assumed to have a structure-breaking capability, dissociating H-Aβ aggregates. The current rotifer-specific biomaterials, namely Rotimers, were used for that purpose for the first time. Concerning the protective role of Rotimer against H-Aβ, indirect *in vivo* measurements were carried out [22]; however, *in vitro* binding, anti- and disaggregating experiments have never been previously performed. Moreover, this interdisciplinary approach may also open novel perspectives in pharmacological research against Alzheimer's disease.

4. Conclusion

Various interactions were discovered between human-type amyloids and other biological and synthetic drugs, *e.g.*, antibodies, hormones, polymers, or small molecules. The present work aimed to measure the binding interaction between the Rotimer-containing conglomerate (formed by rotifers) and neurotoxic H-Aβ peptide aggregates; moreover, to investigate the effect of this RIC on Aβ aggregation processes. To prove these, two test methods were used, namely optical stagogram and fluorescence intensity measurement. The obtained results reflect the relationship between RIC and H-Aβ, in addition, the stable interaction shows Aβ sequence specificity. There was minimal binding between RIC and S-Aβ. The conglomerate of both monogonant rotifer species (*E. dilatata* and *L. bulla*) interacted with H-Aβ considered as oligomer and/or fibril type; however, ED-RIC was more effective in binding and aggregation processes. The novelty of this work is the first demonstration of the *in vitro* interaction between Rotimer and H-Aβ by presenting the anti- and disaggregating effects of this biopolymer against the neurotoxic agents of AD. Due to its properties mentioned above, this natural material needs further study in the future; moreover, this biopolymer can be a relevant molecular specimen for developing drug candidates in neurodegeneration-related research.

Ethical approval

All applicable international, national, and/or institutional guidelines for the care and use of animals were followed. Our experiments were performed on rotifers; therefore, according to the current ethical regulations, no specific ethical permission was needed. The investigations were carried out in accordance with globally accepted norms: Animals (Scientific Procedures) Act, 1986, associated guidelines, EU Directive 2010/63/EU for animal experiments and the National Institutes of Health guide for the care and use of Laboratory animals (NIH Publications No. 8023, revised 1978). Our animal studies comply with the ARRIVE guidelines.

Availability of data and material

The datasets used and/or analyzed during the current study available from the corresponding author on reasonable request.

Funding

This project was supported by the János Bolyai Research Scholarship of the Hungarian Academy of Sciences; by the UNKP-21-5-SZTE-555 New National Excellence Program of the Ministry for Innovation and Technology from the source of the National Research, Development and Innovation Found; by the European Union's Horizon 2020 research and innovation programme under the Marie Skłodowska-Curie grant agreement, Nr. 754432; by the Polish Ministry of Science and Higher Education; by the SZTE ÁOK-KKA No. 5S 567 (A202) and by the Developing Scientific Workshops of Medical-, Health Sciences and Pharmaceutical Training (grant number: EFOP 3.6.3-VEKOP-16-2017-00009; Hungary).

CRediT authorship contribution statement

Zsolt Datki: Investigation, Formal analysis, Writing- Original draft preparation, Visualization, Funding acquisition, Project administration. Evelin Balazs: Visualization, Writing- Original draft preparation, Funding acquisition. Bence Galik: Software, Data Curation, Funding acquisition. Lavinia Zeitler: Methodology, Visualization. Janos Kalman: Conceptualization, Resources. Rita Sinka: Resources, Writing-Reviewing and Editing. Zsolt Bozso: Methodology, Resources. Tibor Hortobagyi: Resources, Writing - Review & Editing, Funding acquisition. Zita Galik-Olah: Validation, Writing - Review & Editing, Project administration.

Declaration of competing interest

The authors declare that they have no competing interests.

Acknowledgements

The authors wish to thank to Anna Szentgyorgyi MA, a professional in English Foreign Language Teaching for proofreading the manuscript.

References

[1] H. Chi, H.Y. Chang, T.K. Sang, Neuronal cell death mechanisms in major neurodegenerative diseases, Int. J. Mol. Sci. 19 (2018) 1–18, https://doi.org/10.3390/ijms19103082.

[2] J.R. Backstrom, G.P. Lim, M.J. Cullen, Z.A. Tökés, Matrix Metalloproteinase-9 (MMP-9) is synthesized in neurons of the human hippocampus and is capable of

degrading the amyloid-peptide (1–40), J. Neurosci. 16 (24) (1996) 7910–7919, https://doi.org/10.1523/JNEUROSCI.16-24-07910.1996.
[3] C.A. Ross, M.A. Poirier, Protein aggregation and neurodegenerative disease, Nat. Med. 10 (2004) S10–S17, https://doi.org/10.1038/nm1066.
[4] R.J. Baranello, K.L. Bharani, V. Padmaraju, N. Chopra, D.K. Lahiri, N.H. Greig, M. A. Pappolla, K. Sambamurti, Amyloid-Beta protein clearance and degradation (ABCD) pathways and their role in Alzheimer's disease, Curr. Alzheimer Res. 12 (2015) 32–46, https://doi.org/10.2174/1567205012666141218140953.
[5] V. Kumar, N. Sami, T. Kashav, A. Islam, F. Ahmad, M.I. Hassan, Protein aggregation and neurodegenerative diseases: from theory to therapy, Eur. J. Med. Chem. 124 (2016) 1105–1120, https://doi.org/10.1016/j.ejmech.2016.07.054.
[6] B. Vellas, N. Coley, P.J. Ousset, G. Berrut, J.F. Dartigues, B. Dubois, H. Grandjean, F. Pasquier, F. Piette, P. Robert, J. Touchon, P. Garnier, H. Mathiex-Fortunet, S. Andrieu, Long-term use of standardised ginkgo biloba extract for the prevention of Alzheimer's disease (GuidAge): a randomised placebo-controlled trial, Lancet Neurol. 11 (2012) 851–859, https://doi.org/10.1016/S1474-4422(12)70206-5.
[7] F. Yang, G.P. Lim, A.N. Begum, O.J. Ubeda, M.R. Simmons, S.S. Ambegaokar, P. Chen, R. Kayed, C.G. Glabe, S.A. Frautschy, G.M. Cole, Curcumin inhibits formation of amyloid β oligomers and fibrils, binds plaques, and reduces amyloid in vivo, J. Biol. Chem. 280 (2005) 5892–5901, https://doi.org/10.1074/jbc.M404751200.
[8] X. Le Bu, P.P.N. Rao, Y.J. Wang, Anti-amyloid aggregation activity of natural compounds: implications for Alzheimer's drug discovery, Mol. Neurobiol. 53 (2016) 3565–3575, https://doi.org/10.1007/s12035-015-9301-4.
[9] R.H.K.M.K. Siddiqi, P. Alam, S.K. Chaturvedi, Y.E. Shahein, Mechanisms of protein aggregation and inhibition, Front. Biosci. (Elite Ed.) 9 (2017) 1–20, https://doi.org/10.2741/e781.
[10] T. Thomas, T.G. Nadackal, K. Thomas, Aspirin and non-steroidal anti-inflammatory drugs inhibit amyloid-β aggregation, Neuroreport. 12 (2001) 959–4965, https://doi.org/10.1097/00001756-200110290-00024.
[11] A. George, M.R. Sanjay, R. Srisuk, J. Parameswaranpillai, S. Siengchin, A comprehensive review on chemical properties and applications of biopolymers and their composites, Int. J. Biol. Macromol. 154 (2020) 329–338, https://doi.org/10.1016/j.ijbiomac.2020.03.120.
[12] K.J. Wilkinson, A. Joz-Roland, J. Bufjee, Different roles of pedogenic fulvic acids and aquagenic biopolymers on colloid aggregation and stability in freshwaters, Limnol. Oceanogr. 42 (1997) 7–14, https://doi.org/10.4319/lo.1997.42.8.1714.
[13] B. Meesaragandla, S. Karanth, U. Janke, M. Delcea, Biopolymer-coated gold nanoparticles inhibit human insulin amyloid fibrillation, Sci. Rep. 10 (2020) 1–14, https://doi.org/10.1038/s41598-020-64010-7.
[14] L.S. Bezerra, M. Magnani, R.J.H. Castro-Gomez, H.C. Cavalcante, T.A.F. da Silva, R. L.P. Vieira, I.A. de Medeiros, R.C. Veras, Modulation of vascular function and anti-aggregation effect induced by (1 → 3) (1 → 6)-β-D-glucan of Saccharomyces cerevisiae and its carboxymethylated derivative in rats, Pharmacol. Rep. 69 (2017) 448–455, https://doi.org/10.1016/j.pharep.2017.01.002.
[15] S.G. Roman, N.A. Chebotareva, B.I. Kurganov, Anti-aggregation activity of small heat shock proteins under crowded conditions, Int. J. Biol. Macromol. 100 (2017) 97–103, https://doi.org/10.1016/j.ijbiomac.2016.05.080.
[16] S. Nagarajan, S. Radhakrishnan, S.N. Kalkura, S. Balme, P. Miele, M. Bechelany, Overview of protein-based biopolymers for biomedical application, Macromol. Chem. Phys. 220 (2019) 1–16, https://doi.org/10.1002/macp.201900126.
[17] A.O. Elzoghby, W.M. Samy, N.A. Elgindy, Protein-based nanocarriers as promising drug and gene delivery systems, J. Control. Release 161 (2012) 38–49, https://doi.org/10.1016/j.jconrel.2012.04.036.
[18] S.K. Nitta, K. Numata, Biopolymer-based nanoparticles for drug/gene delivery and tissue engineering, Int. J. Mol. Sci. 14 (2013) 1629–1654, https://doi.org/10.3390/ijms14011629.
[19] S.Y. Ow, I. Bekard, D.E. Dunstan, Effect of natural biopolymers on amyloid fibril formation and morphology, Int. J. Biol. Macromol. 106 (2018) 30–38, https://doi.org/10.1016/j.ijbiomac.2017.07.171.
[20] B. Lengerer, R. Pjeta, J. Wunderer, M. Rodrigues, R. Arbore, L. Schärer, E. Berezikov, M.W. Hess, K. Pfaller, B. Egger, S. Obwegeser, W. Salvenmoser, P. Ladurner, Biological adhesion of the flatworm macrostomum lignano relies on a duo-gland system and is mediated by a cell type-specific intermediate filament protein, Front. Zool. 11 (2014) 1–15, https://doi.org/10.1186/1742-9994-11-12.
[21] Z. Datki, Z. Olah, T. Hortobagyi, L. Macsai, K. Zsuga, L. Fulop, Z. Bozso, B. Galik, E. Acs, A. Foldi, A. Szarvas, J. Kalman, Exceptional in vivo catabolism of neurodegeneration-related aggregates, Zool. Lett. 4 (2018) 1–12, https://doi.org/10.1186/s40478-018-0507-3.
[22] Z. Datki, E. Acs, E. Balazs, T. Sovany, I. Csoka, K. Zsuga, J. Kalman, Z. Galik-Olah, Exogenic production of bioactive filamentous biopolymer by monogonant rotifers, Ecotoxicol. Environ. Saf. 208 (2021) 1–10, https://doi.org/10.1016/j.ecoenv.2020.111666.
[23] J. Murube, Tear crystallization test: two centuries of history, Ocul. Surf. 2 (2004) 7–9, https://doi.org/10.1016/S1542-0124(12)70019-8.
[24] M. Yu, T.M. Ryan, S. Ellis, A.I. Bush, J.A. Triccas, P.J. Rutledge, M.H. Todd, Neuroprotective peptide-macrocycle conjugates reveal complex structure-activity relationships in their interactions with amyloid β, Metallomics 6 (2014) 1931–1940, https://doi.org/10.1039/c4mt00122b.
[25] C. Xue, T.Y. Lin, D. Chang, Z. Guo, Thioflavin T as an amyloid dye: fibril quantification, optimal concentration and effect on aggregation, R. Soc. Open Sci. 4 (2017) 1–12, https://doi.org/10.1098/rsos.160696.
[26] A.N. Kalweit, H. Yang, J. Colitti-Klausnitzer, L. Fulóp, Z. Bozsó, B. Penke, D. Manahan-Vaughan, Acute intracerebral treatment with amyloid-beta (1–42) alters the profile of neuronal oscillations that accompany LTP induction and results in impaired LTP in freely behaving rats, Front. Behav. Neurosci. 9 (2015) 1–16, https://doi.org/10.3389/fnbeh.2015.00103.
[27] S. Mohan, O.S. Oluwafemi, N. Kalarikkal, S. Thomas, S.P. Songca, Biopolymers – application in nanoscience and nanotechnology, recent advBiopolym. (2016) 47–72, https://doi.org/10.5772/62225.
[28] E. Balazs, Z. Galik-Olah, B. Galik, F. Somogyvari, J. Kalman, Z. Datki, External modulation of rotimer exudate secretion in monogonant rotifers, Ecotoxicol. Environ. Saf. 220 (2021) 1–8, https://doi.org/10.1016/j.ecoenv.2021.112399.
[29] A. Solé, Untersuchung über die bewegung der teilchen im stagogramm und influenzstagogramm, Kolloid-Zeitschrift. 151 (1957) 55–62, https://doi.org/10.1007/BF01502258.
[30] N.D. Younan, J.H. Viles, A comparison of three fluorophores for the detection of amyloid fibers and prefibrillar oligomeric assemblies. ThT (Thioflavin T); ANS (1-Anilinonaphthalene-8-sulfonic Acid); and bisANS (4,4′-Dianilino-1,1′-binaphthyl-5,5′-disulfonic Acid), Biochemistry 54 (2015) 4297–4306, https://doi.org/10.1021/acs.biochem.5b00309.
[31] H. Levine, Thioflavine T interaction with synthetic Alzheimer's disease beta-amyloid peptides: detection of amyloid aggregation in solution, Protein Sci. 2 (1993) 404–410, https://doi.org/10.1002/pro.5560020312.
[32] Z. Datki, R. Papp, D. Zádori, K. Soós, L. Fülöp, A. Juhász, G. Laskay, C. Hetényi, E. Mihalik, M. Zarándi, B. Penke, In vitro model of neurotoxicity of Aβ 1–42 and neuroprotection by a pentapeptide: irreversible events during the first hour, Neurobiol. Dis. 17 (2004) 507–515, https://doi.org/10.1016/j.nbd.2004.08.007.
[33] Z. Bozso, B. Penke, D. Simon, I. Laczkó, G. Juhász, V. Szegedi, Á. Kasza, K. Soós, A. Hetényi, E. Wéber, H. Tóháti, M. Csete, M. Zarándi, L. Fülöp, Controlled in situ preparation of Aβ(1–42) oligomers from the isopeptide "iso-Aβ(1–42)", physicochemical and biological characterization, Peptides 31 (2010) 248–256, https://doi.org/10.1016/j.peptides.2009.12.001.
[34] L. Fülöp, M. Zarándi, K. Soós, B. Penke, Self-assembly of Alzheimer's disease-related amyloid peptides into highly ordered nanostructures, Nanopages 1 (2006) 69–83, https://doi.org/10.1556/nano.1.2006.1.3.
[35] E. Balazs, Z. Galik-Olah, B. Galik, Z. Bozso, J. Kalman, Z. Datki, Neurodegeneration-related beta-amyloid as autocatabolism-attenuator in a micro-in vivo system, in: IBRO Reports 9, 2020, pp. 319–323, https://doi.org/10.1016/j.ibror.2020.10.002.
[36] R. Pellarin, A. Caflisch, Interpreting the aggregation kinetics of amyloid peptides, J. Mol. Biol. 360 (2006) 882–892, https://doi.org/10.1016/j.jmb.2006.05.033.
[37] A. Sharma, M.A. McDonald, H.B. Rose, Y.O. Chernoff, S.H. Behrens, A. S. Bommarius, Modeling amyloid aggregation kinetics: a case study with Sup35NM, J. Phys. Chem. B 125 (2021) 4955–4963, https://doi.org/10.1021/acs.jpcb.0c11250.
[38] B.F.C. Soto, E.M. Sigurdsson, L. Morelli, R.A. Kumar, E.M. Castaño, Beta-sheet breaker peptides inhibit fibrillogenesis in a rat brain model of amyloidosis: implications for Alzheimer's therapy, Nat. Med. (1998) 822–826, https://doi.org/10.1038/nm0798-822.
[39] L. Fülöp, M. Zarándi, Z. Datki, K. Soós, B. Penke, β-amyloid-derived pentapeptide RIIGL a inhibits Aβ 1–42 aggregation and toxicity, Biochem. Biophys. Res. Commun. 324 (2004) 64–69, https://doi.org/10.1016/j.bbrc.2004.09.024.
[40] Ü. Murvai, K. Soós, B. Penke, M.S.Z. Kellermayer, Effect of the beta-sheet-breaker peptide LPFFD on oriented network of amyloid β25-35 fibrils, J. Mol. Recognit. 24 (2011) 453–460, https://doi.org/10.1002/jmr.1113.
[41] M.H. Viet, S.T. Ngo, N.S. Lam, M.S. Li, Inhibition of aggregation of amyloid peptides by beta-sheet breaker peptides and their binding affinity, J. Phys. Chem. B 115 (2011) 7433–7446, https://doi.org/10.1021/jp1116728.
[42] I. Laczkó, E. Vass, K. Soós, L. FüLöp, M. Zarándi, B. Penke, Aggregation of Aβ(1–42) in the presence of short peptides: conformational studies, J. Pept. Sci. 14 (2008) 731–741, https://doi.org/10.1002/psc.990.
[43] R. Balart, D. Garcia-Garcia, V. Fombuena, L. Quiles-Carrillo, M.P. Arrieta, Biopolymers from natural resources, Polymers (Basel). 13 (2021) 1–9, https://doi.org/10.3390/polym13152532.
[44] L.I. Atanase, Micellar drug delivery systems based on natural biopolymers, Polymers (Basel). 13 (2021) 1–33, https://doi.org/10.3390/polym13030477.